RegMedNet

fsg

eBook: electroporation

CONTENTS

Foreword

We are pleased to present you with this eBook on electroporation.

Electroporation is a powerful transfection tool that utilizes an electrical pulse to transiently increase the permeability of the cell membrane, allowing nucleic acids or proteins to enter the cells. Having the ability to introduce molecules into cells is beneficial in many applications, including the study of gene function and protein expression and the engineering of cells for cell and gene therapy applications.

Unfortunately, many of the cell types that are typically used for cell therapies, such as primary T cells, natural killer cells, or hematopoietic stem cells, cannot be efficiently transfected using traditional electroporation methods.

In this eBook, we delve further into the applications of electroporation for cell therapies and investigate how advanced electroporation technologies, such as nucleofection, can overcome challenges when working with difficult-to-transfect cell types.

We hope you enjoy reading these expert insights into electroporation with us.

Megan Giboney
Editor, RegMedNet
m.giboney@future-science-group.com

Beyond the barrier: an interview about non-viral transfection

Ludger Altrogge
Head of Cell Engineering
Research & Development
Lonza
(Cologne, Germany)

Theodore Roth
Resident, Stanford Pathology;
Co-Founder, Arsenal
Biosciences
(CA, USA)

Ludger Altrogge is the Head of Cell Engineering Research & Development at Lonza Cologne. He is a trained biochemist with a Diploma Thesis completed at the Max-Planck-Institute for Developmental Biology (Tübingen, Germany) and a PhD from the University of Basel (Basel, Switzerland), both in Neurobiology. He started his career as senior scientist at amaxa (now Lonza). In his role he is driving product development of complex laboratory instruments and related consumables for biology or medical research applications. During his career, he gained profound knowledge in non-viral gene editing.

Theo Roth was the founding Chief Scientific Officer and is a scientific co-founder of Arsenal Biosciences (CA, USA). He completed his undergraduate and Masters work at Stanford University (CA, USA) and the National Institutes of Health (MD, USA) in biomedical informatics and systems biology. During his MD-PhD at University of California, San Francisco (CA, USA), he developed non-viral genome targeting and pooled knock-in screening, new methods for large scale genetic engineering of primary human immune cells. He is currently completing his residency in clinical pathology at Stanford University.

1 **Ludger, where do you see advantages of non-viral methods, such as electroporation, for gene modification?**

Non-viral methods provide flexibility with regards to the type of cargo/substrate used. For instance, it cannot only deliver nucleic acids (DNA, mRNA) but also proteins such as Cas9 RNPs for CRISPR-based gene editing. Non-viral methods are suitable for both transient expression e.g., of a therapeutic gene, or stable genetic engineering of cells. The first can be achieved by delivering mRNA or DNA (plasmids,

minicircles or nanocircles), while transposase systems (e.g., Sleeping Beauty or PiggyBac), as well as engineered nucleases for targeted integrations (e.g., CRISPR) lead to stable genetic engineering of cells. With the latter, a safer and precisely controlled modification can be achieved. Viral- and transposase-based modifications are generally more efficient, but are less controllable as integration occurs randomly in the genome. Delivering the engineered nucleases as preassembled RNPs allows for a better dosage control of the modification.

2 Theo, how are you using electroporation in your lab?

We use Lonza electroporators for a wide variety of gene editing applications. We are able to flexibly edit different cell types, cell lines and primary cells, small and large numbers of cells, arrayed and pooled editing format, different macromolecule payloads – the flexibility to do all of these types of experiments with a single system enables us to think about the ideal experiment for whatever we are testing and know that we'll be able to use our existing system to accomplish it.

3 Ludger, can you give more insight to the non-viral gene transfer technology that Lonza offers?

The key for a successful implementation of a non-viral technology is to combine high transfection efficiencies that can be achieved by viruses with the flexibility of a non-viral technology. Our solution is an improved electroporation technology, the Nucleofector® Technology. Optimized electrical parameters combined with cell-type-specific solutions enable the transfer of a molecule directly into the cell's nucleus. It has been optimized for highly efficient transfection of primary cells, including those relevant for ex-vivo cell therapy. Since it does not rely on proliferation, it can even transfect non-dividing cells, like resting T cells.

It is based on three key components: Firstly, a Nucleofector Device, as mentioned by Theo, that generates unique electrical pulses. Secondly, specified Nucleofection vessels used in combination with cell-type specific Nucleofector Solutions acting as a supportive environment for high transfection efficiency, cell viability and functionality. And thirdly, optimized protocols offering comprehensive guidance for optimal Nucleofection conditions along with tips for cell sourcing, passage, growth conditions and media and post-transfection culture.

There are different platforms available ranging from small-scale, higher throughput (96-well or 384-well) for drug discovery phases to larger- scale for preclinical and manufacturing phases.

4 Theo, in your opinion, what are the advantages to use Nucleofector Technology for CRISPR/Cas9 mediated genome editing?

We really take advantage of the 96-well electroporation capacity of the Nucleofector. The ability to make genetic edits in high throughput within the 96-well format enables editing, screening and validation experiments across scales to be accomplished simply and using the same instrument.

5 Theo, do you also perform CRISPR Screens?

Yes, we perform both arrayed and pooled screens on the Lonza system. We can make 96 different gene edits all on one plate – or we can make hundreds of millions of cells all edited with a single pooled library. This flexibility, while using the same editing technology, lets us bounce around experiment types, running exactly the right type of experiment for each question we are asking.

6 Theo, where do you see the use of Nucleofector Technology for therapeutic approaches and drug development?

By lowering the cost of screening new genetically edited cellular medicines, we are able to test more potential therapies earlier in the development cycle. This means that by the time a drug enters a patient, it wasn't just the best out of say five options, it was the best out of five hundred or five thousand. More effective drugs going into trials from the start will hopefully lead to faster drug development and most importantly faster approved, effective and safe drugs being offered to patients.

Disclaimer: The opinions expressed by Theodore Roth are his own and do not necessarily reflect the view of Stanford University.

Theo Roth was a speaker in Lonza's virtual live event "Genome Editing of Immune Cells" in September 2022. Please register here to watch the video on demand.

Lonza

New 4D-Nucleofector® Platform

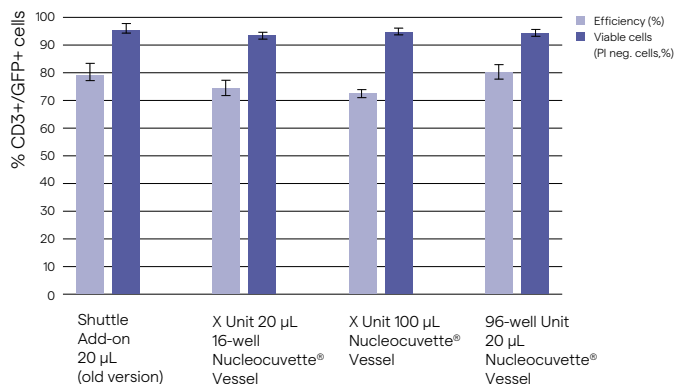## Efficient and Reproducible Results for Your Transfection Applications

The modular design of the Nucleofector® Platform with units for small, medium or large scale, adherent cells or cells in suspension, allows you to configure the 4D-Nucleofector® System to fit your specific research needs. Up to 3 functional units can be added to the 4D-Nucleofector® Core Unit and each is suited for different applications:

X Unit: Nucleofection® of various cell numbers in different formats (16-well Nucleocuvette® Strips or 100 μL Nucleocuvette® Vessels)

Y Unit: Enabling adherent Nucleofection® in 24-well culture plates

LV Unit: Large-scale transfection of up to 1×10⁹ cells in a single run

96-well Unit: Higher throughput Nucleofection® Experiments in 96-well Nucleocuvette® Plates

Cell type-specific Optimized Protocols or recommendations are available in our Knowledge Center. In these Optimized Protocols we share our recommended Nucleofection® Conditions as well as our experience and knowledge for treatment of individual cell types.

lonza.com/New-4D-Nucleofector

Transferability of Nucleofection® Conditions Between Units and Vessels

Transfection of human T cells with plasmid DNA (pMax-GFP® Plasmid) Fresh PBMCs were transfected with pmaxGFP® Plasmid in a 100 μL Nucleocuvette® Vessel or a 20 μL Nucleocuvette® Vessel using the Next Generation 4D-Nucleofector® X Unit, the 96-well Unit or the Nucleofector® Shuttle® Add-on for reference. Transfection efficiency in CD3-positive T cells was analyzed 24 hours post Nucleofection® Procedure. Plasmid data represent the mean of various independent experiments. Live cell discrimination was done with Propidium Iodide.

Mesenchymal stem cells modifications for enhanced bone targeting and bone regeneration

Yuliya Safarova[1,2], Bauyrzhan Umbayev[1], Gonzalo Hortelano[3] & Sholpan Askarova*,[1] (iD)
[1]Center for Life Sciences, National Laboratory Astana, Nazarbayev University, Nur-Sultan, Kazakhstan
[2]School of Engineering & Digital Sciences, Nazarbayev University, Nur-Sultan, Kazakhstan
[3]School of Sciences & Humanities, Nazarbayev University, Nur-Sultan, Kazakhstan
*Author for correspondence: Tel.: +7 717 270 6514; +7 777 772 7828; shaskarova@nu.edu.kz

In pathological bone conditions (e.g., osteoporotic fractures or critical size bone defects), increasing the pool of osteoblast progenitor cells is a promising therapeutic approach to facilitate bone healing. Since mesenchymal stem cells (MSCs) give rise to the osteogenic lineage, a number of clinical trials investigated the potential of MSCs transplantation for bone regeneration. However, the engraftment of transplanted cells is often hindered by insufficient oxygen and nutrients supply and the tendency of MSCs to home to different sites of the body. In this review, we discuss various approaches of MSCs transplantation for bone regeneration including scaffold and hydrogel constructs, genetic modifications and surface engineering of the cell membrane aimed to improve homing and increase cell viability, proliferation and differentiation.

A bone fracture is a common medical condition, which can be due to traumatic injury or as a result of pathological weakening of the bones. The severity of the injury depends on the fracture (type, magnitude and location) and increases with age [1]. Some fractures require only temporary fixation and protection, while other serious fractures (in elderly, critical size bone defects, bone tumor surgery, pathologic fractures etc.) undergo a more difficult process of natural regeneration and often fail to heal. These conditions are called a 'nonunion' and a 'delayed union' of fractures.

Osteoporosis is the most common systemic bone disorder that predisposes the affected individuals to pathological bone fractures. Furthermore, fractures in elderly osteoporotic patients are challenging to treat due to prolonged healing time and the complexity of surgical fracture fixation in a weakened bone [2]. Second, the most common pathological bone condition is Paget's disease of bone [3]. The etiology of the Paget's disease of bone is still unknown and may include genetic factors as well as environmental. In this condition, the normal bone equilibrium is shifted toward the bone resorption processes which inevitably alters the fracture healing process [4]. Both disorders are primarily diagnosed in older people and in rare cases in people less than 55 years old [3,5]. Besides the aging-associated pathological conditions, there is also a group of genetically induced bone disorders. The genetic condition known as osteogenesis imperfecta is characterized by a defect in the collagen production genes (*COL1A1* or *COL1A2* gene), which results in bone malformation and impairment in the bone regeneration process [6]. Some other conditions are also able to worsen bone regeneration. For example, bacterial osteomyelitis impairs bone remodeling and leads to uncontrolled bone loss [7]. There are also a group of auto-inflammatory bone diseases that can affect proper bone healing including chronic nonbacterial osteomyelitis, Majeed syndrome, deficiency of IL-1 receptor antagonist and cherubism [8].

Many innovative therapeutic strategies have been identified in recent years to improve bone regeneration, and mesenchymal stem cell (MSCs) transplantation is one of the promising approaches. Overall the properties of MSCs make them very suitable biological material for transplantation in bone-associated conditions and fractures. MSCs are able to differentiate into the target tissue; they have advantageous immune modulating properties and

Future
Medicine

provide growth factors to facilitate the repair process. The stimulation of the natural repairing processes by providing osteoblasts precursors (MSCs) that will home and attach firmly to the site of injury increases the rate of regeneration of bone structures and improve healing. Transplantation of MSCs into the injured area can promote healing not only by directly increasing the number of precursor cells but also through a paracrine effect by releasing growth factors and immunomodulatory cytokines and chemokines to induce regeneration [9].

MSCs have been isolated so far from various types of tissues, including bone marrow, adipose tissue, synovial membrane and fluid, human placenta, umbilical cord, amniotic fluid or various fetal tissues. Although MSCs from these different sources have been applied in preclinical models, bone marrow-derived MSCs (BM-MSCs) and adipose-derived MSCs (AD-MSCs) are the most commonly used cell types for bone regeneration [10,11]. BM-MSCs are isolated at a relatively low density and must be expanded *in vitro*, in contrast with AD-MSCs that can be harvested in higher quantities [12]. However, BM-MSCs show more expression of osteogenic differentiation genes [11], while AD-MSCs show stronger angiogenic potential [13], and is a promising tool in the treatment of vascular ischemic conditions [14].

There are two main routes of transplantation of MSCs: systemic and local. Systemic administration involves intravenous (IV) and intra-arterial (IA) injection of the cells, while local administration involves direct injection of the cells into the regeneration site. Systemic route is often less invasive and keeps the cells close to the source of oxygen and nutrients with the ability to extravasate into the target tissue [15]. However, previous research in this area showed that, upon systemic administration, most of the transplanted MSCs are concentrated in the lungs [16–19], though after 10 days, the percentage drops dramatically – to 2% compared with the initial 35% [20]. Migration of transplanted MSCs from the lungs is believed to be driven by inflamed organs [21]. Due to their nature, MSCs can sense chemokine CCL21 in vessels near the sites of inflammation and some MSCs escape the lungs and home to inflamed tissue [22]. Thus, the efficacy of systemic MSCs administration in cases of bone pathology could be affected by other underlying chronic conditions. Another disadvantage of the systemic MSCs administration is the aggregation of the transplanted cells in the areas of abnormal cancerous cell proliferations such as breast or ovary cancer [23].

There are several ways to target MSCs to the tissue of interest. The targeting moiety can be induced by an independently administered component, for example, an injection of parathyroid hormone (PTH). It has been shown that therapy with PTH together with MSCs transplantation increases cell migration to the site of the bone defects and improves further differentiation of the cells [24]. In general, recruitment of the MSCs to the site of fracture is activated through the stromal cell-derived factor 1/C-X-C CXCR4 axes. However, PTH administration shifts the mechanism of MSCs recruitment to the amphiregulin pathway in which EGF-like ligand is secreted in the damaged area [24,25].

Another approach is a local transplantation of MSCs to the site of bone fracture. A major advantage of local cell delivery is the close proximity of the transplanted cells to the areas of bone defect. However, the survival of those cells is questionable since oxygen and nutrients are not always available at the sites of injection. Therefore, in order to increase the degree of cell engraftment, the delivery system must place cells at, or allow MSCs to migrate to the site of bone defect. Thus, the main focus of this review is modifications of MSCs that are aimed at improving the bone targeting potential of the MSCs and enhancing survival of cells upon therapeutic transplantations.

In this review, we refer to MSCs as a multipotent stem cells that according to International Society for Cell and Gene Treatment fulfills three main criteria: first, MSCs are adherent to plastic in culture; second, they express CD73, CD90, CD105 on their cell surface membrane and lack CD14, CD34, CD45 and human leukocyte antigen – DR isotype HLA-DR) expression; finally, MSCs can differentiate down the osteogenic, chondrogenic and adipogenic lineage [10].

Scaffolds & hydrogels

The use of biomaterial scaffolds is one of the most widely used strategies to enhance repair processes in bone tissue. The organic and inorganic materials implemented in scaffold manufacturing, including polymeric constructs, ceramics, metals and natural matrices are summarized in the scheme below (Figure 1). A precise review of all currently available scaffold materials for bone tissue engineering was given by Ghassemi *et al.* [26]. The authors concluded that different approaches should be combined in order to provide the scaffold with better mechanical strength (that lack both synthetic and natural polymeric scaffolds), less fragility (than ceramics scaffolds) and the incorporation of biologically active agents in order to promote osteoinductivity.
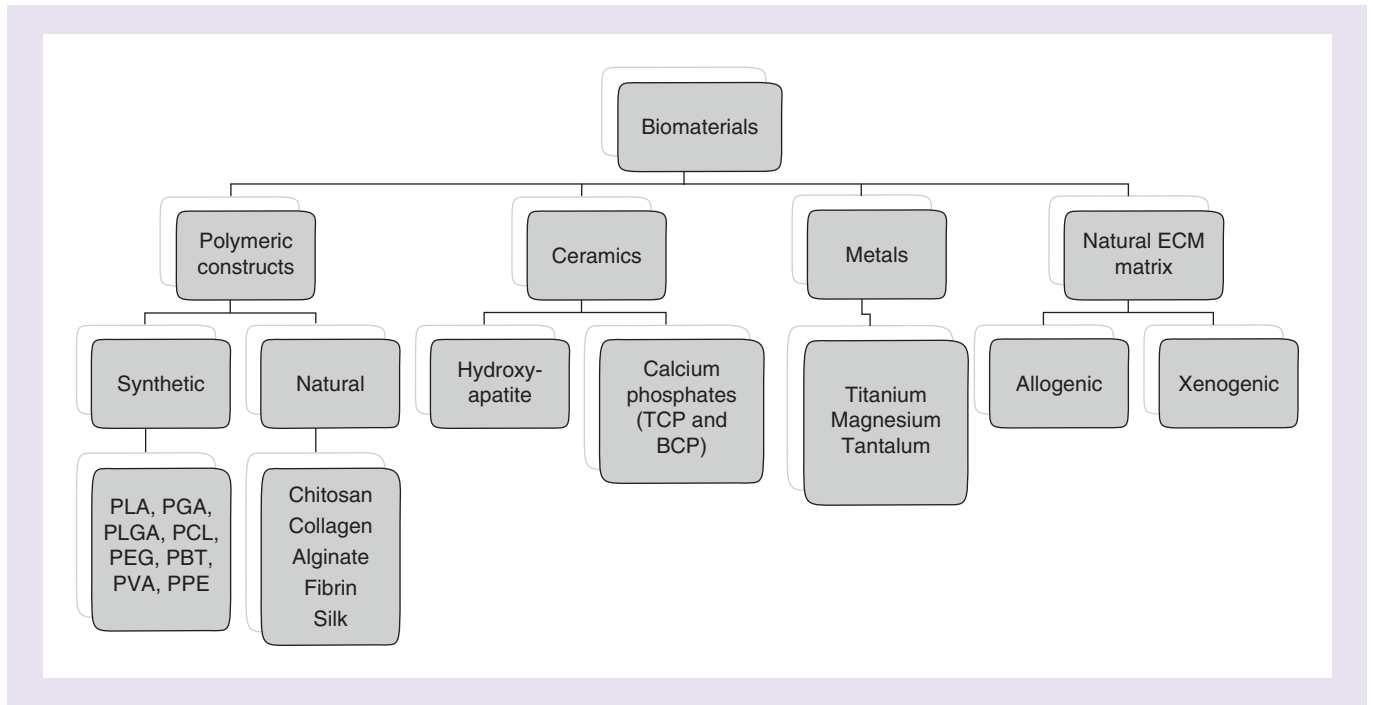
Figure 1.   Materials implemented in scaffold manufacturing.
ECM: Extracellular matrix; PBT: Polybutylene terephthalate; PCL: Polycaprolactone; PEG: Polyethylene glycol; PGA: Polyglycolic acid; PLA: Polylactic acid; PLGA: Poly(lactic-co-glycolic acid); PPE: Polyphenyl ether; PVA: Polyvinyl alcohol; TCP: Tricalcium phosphate.

Seeding scaffolds with osteoblast precursor cells is a promising approach to increase the efficacy of scaffold transplants. Ceramic scaffolds are very suitable for filling critical size bone defects because the scaffold matrix provides mechanical support for the cells to proliferate, differentiate into osteoblasts and eventually calcify. In a study by Agacayak and colleagues, the combination of MSCs, platelet rich plasma and biphasic calcium phosphate construct has been demonstrated to be a more effective approach for inducing osteogenesis in rat calvarial bone defect than the use of ceramic bone scaffold alone [27]. Similarly, hydroxyapatite ceramic scaffolds seeded with culture-expanded BM-MSCs were able to regenerate critical size bone defects of tibia diaphysis in sheep to a greater extent than synthetic bone substitute alone [28]. Several clinical cases were reported on the use of β-tricalcium phosphate scaffolds to meet craniomaxillofacial applications [29–33]. A β-TCP scaffold loaded with AD-MSCs and BMP-2 was used to reconstruct a maxillary defect left after the removal of keratocyst. The construct was first implanted into a muscle for ectopic bone formation and then transplanted into the maxillary area and led to successful healing 4 month after surgery [31].

Yet, the interactions between scaffolds and MSCs involve many factors affecting stem cell survival, proliferation and differentiation. One of the very important issues in cell-scaffold constructs is the lack of oxygen supply and nutrients, since vessel formation is a slow process. In this regard, a number of recent studies have been directed toward creating bioactive scaffolds and hydrogels that promote angiogenesis while supporting cell proliferation and differentiation (Table 1) [34,35].

For example, Yu *et al.* seeded the polycaprolactone–hydroxyapatite scaffolds with a combination of osteoblast precursor cells and endothelial cells to enhance angiogenesis, which significantly improved the bone regeneration process [38]. Porous silk scaffolds seeded with BM-MSCs in a study carried out by Zhang *et al.* was successful and provided evidence for increased rate of regeneration of cranial critical size bone defects in rats [39]. The authors showed that cells were able to survive up to 8 weeks due to the presence of VEGF and BMP-2 factors that promoted angiogenesis and the subsequent differentiation of cells along the osteogenic lineage. Similarly, transplantation of MSCs entrapped into the collagen sponge/hyaluronic acid-based hydrogel complex scaffolds containing VEGF and BMP-2 resulted in a significant increase of bone mineral density at canine maxillary alveolar bone defects [40]. Zhao *et al.* encapsulated BMSCs and BMP-2 into photocross-linkable hydrogel microspheres composed of gelatin-methacryloyl chloride and demonstrated improved bone formation of the rabbit femoral ankle [41].

Table 1. Bioactive hydrogels and scaffolds for bone regeneration.

Scaffold/hydrogel carrier	Biologically active agent	Outcome	Ref.
Poly(lactic-co-glycolic acid)	VEGF	Bone formation in an irradiated rat calvarial defect	[36]
A 3D honeycomb-like PCL scaffold	rhBMP2-PCL	Promotes bone healing in a large bone defect of rabbit ulna.	[37]
Cylindrical porous PCL-HA scaffolds	Osteoblasts and ECs	A widely distributed capillary network, osteoid generated by osteoblasts and absent ischemic necroses in a 0.4-cm-long segmental femur defect of BALB/c mice	[38]
Silk scaffolds	BMSCs, VEGF and BMP-2	Regeneration of critical size cranial bone defects in rats	[39]
Collagen sponge/hyaluronic acid-based hydrogel complex scaffolds	VEGF and BMP-2	Increase of bone mineral density at canine maxillary alveolar bone defects	[40]
Photocrosslinkable hydrogel microspheres composed of gelatin-methacryloyl chloride	BMSCs and BMP-2	Improved bone formation in rabbit femoral ankle	[41]
Nano calcium sulfate/alginate scaffold	BMP-2 transfected MSCs	Bone bridging of critical-sizes calvarial bone defects in rats.	[42]
Alginate microcapsules	Fibrinogen, fibronectin or RGD	Increased viability, proliferation and osteogenic differentiation of enclosed MSCs	[43–45]
High guluronic acid-content alginates at hydrogel with elasticity of 60 kPa	hMSCs	Bone formation in nude rats with cranial defects	[46]
Hydrogel scaffolds derived from bone extracellular matrix	Dental pulp stem cells	Cell survival, upregulated expression of RUNX-2, osteocalcin and bone sialoprotein	[47]
β-tricalcium phosphate and BMP-2	Adipose derived stem cells	Maxillary defect healing	[30,31]

bECM: Bone extracellular matrix; BM-MSC: Bone marrow derived mesenchymal stem cell; EC: Endothelial cell; hMSC: Human mesenchymal stem cell; MSC: Mesenchymal stem cell; HA: Hydroxyapatite; PCL: Polycaprolactone; RGD: The tripeptide Arg–Gly–Asp.

He *et al.* demonstrated that encapsulation of BMP-2-transfected MSCs into nano calcium sulfate/alginate scaffold resulted in bone bridging of critical-sizes calvarial bone defects in rats [42]. Sayyar *et al.* enclosed human MSCs in biomimetic microcapsules made with alginate, a natural carbohydrate from seaweed. The decoration of alginate with fibrinogen, fibronectin or RGD (the tripeptide Arg–Gly–Asp) led to a higher viability of encapsulated human MSCs [43]. Furthermore, alginate decorated with either fibrinogen or fibronectin, but not RGD increased cell proliferation and osteogenic differentiation of enclosed MSCs [44,45].

To enrich the hydrogel scaffold with oxygen available to MSCs, Kimelman-Bleich used perfluorotributylamine (PFTBA) [48]. PFTBA is a type of perfluorocarbons that traps oxygen due to high oxygen solubility, in other words, 35 mm compared with the 2.2 mm of oxygen in water. Hydrogel with PFTBA was mixed with the cells and injected in the area of ectopic bone formation. Results showed a 2.5-fold increase in bone formation compared with the hydrogel without PFTBA as well as increase in cell survival and in osteocalcin expression [48]. Study of synthetic oxygen carriers by Benjamin *et al.* has also led to the conclusion that PFTBA promotes cell survival especially if MSCs are encapsulated. Availability of oxygen to MSCs significantly downregulated hypoxia-related genes as well as promoted osteogenic over chondrogenic differentiation [49].

Hydrogel scaffolds could also be derived from decellularization of the extracellular matrix (ECM). ECM scaffolds hold a great potential as they contain proinflammatory cytokines, BMPs and various growth factors including VEGF [50]. Besides the biological properties, ECM also has structural properties that allow mechanical support of the cells. In a study of Paduano *et al.* decellularized bone ECM with dental pulp stem cells was examined *in vivo*. The construct of bone ECM showed an upregulated expression of RUNX-2, bone sialoprotein and osteocalcin compared with the cells cultured on the collagen Type I hydrogel scaffold [47].

Huebsch *et al.* were able to improve survival rate of human mesenchymal stem cell (hMSC) by modulating elastic modulus of the hydrogels composed of high guluronic acid-content alginates (medium viscosity high-guluronic acid alginate [MVG]; FMC BioPolymer). The authors used as model nude rats with cranial defects and demonstrated that the most prominent regenerative effect occurred using a hydrogel elasticity of 60 kPa [46]. This finding suggests that the biophysical properties of scaffold/hydrogel carriers may also play an important role in promoting the effectiveness of stem-cell based therapies.

Table 2. Preclinical *in vivo* studies of genetic modified mesenchymal stem cells for bone disease treatment

Genetic modifications	Cell type	Cellular mechanisms	Gene transfer type	Ref.
BMP-2	Rat bone marrow cells	Osteoblast differentiation	Adenovirus	[59]
	Human bone marrow MSCs		Adenovirus	[56]
	Murine bone marrow MSCs		Adenovirus-associated virus	[60]
	C3H10T1/2 MSCs		Liposome	[61]
	Murine bone marrow MSCs		Adenovirus-associated virus	[62]
	Human adipose tissue-derived MSCs		Adenovirus	[57]
	C3H10T1/2 MSCs		Liposome	[63]
BMP-2 and BMP-7	Sheep adipose-derived MSCs	Osteoblast differentiation	Adenovirus	[64]
	Rat adipose-derived stem cell	Osteoblast differentiation	Lentivirus	[65]
BMP-2 and VEGF	Human periosteum-derived cells	Osteoblast differentiation	Plasmid	[66]
	Rabbit bone marrow stromal cell	Osteoblast differentiation	Adenovirus	[67]
BMP-2 and miR-148b	Human adipose-derived MSCs	Osteoblast differentiation	Baculovirus	[68]
BMP-4	Rat adipose-derived stromal cells	Osteoblast differentiation and ectopic bone	Adenovirus	[69]
	Rat unfractioned bone marrow stromal cell	Osteoblast differentiation	Retroviral vector	[70]
BMP-4 and VEGF	Murine muscle-derived stem cells	Osteoblast differentiation, ectopic bone, and vasculogenesis	Retroviral vector	[71]
BMP-6	Porcine adipose-derived stem cells	Osteoblast differentiation	Lentivirus	[72]
BMP-6 or BMP-2	Porcine adipose and bone marrow MSCs	Osteoblast differentiation	Nucleofection	[73]
BMP-6	Porcine bone marrow MSCs	Osteoblast differentiation	Nucleofection	[74]
BMP-6 and VEGF	Rat bone marrow MSCs	Osteoblast differentiation and vasculogenesis	Adenovirus-associated virus	[75]
BMP-7	New Zealand white rabbit's bone marrow MSCs	Osteoblast differentiation	Adenovirus	[76]
BMP-9	Human MSCs	Osteoblast differentiation, ectopic bone	Adenovirus	[77]
	Human MSCs	Osteoblast differentiation	Adenovirus	[78]
	Rat bone marrow stromal cells	Osteoblast differentiation	Adenovirus	[79]
BMP-9 or BMP-2	Human bone marrow cells	Osteoblast differentiation	Nucleofection	[80]
Interleukin-4	Murine bone marrow MSCs	Accelerates bone mineralization	Lentivirus	[81]
bFGF	Murine adipose-derived MSCs	Stimulates endogenous angiogenesis and osteogenesis	Lentivirus	[82]
CXCR4, Cbfa1	Murine C3H10T1/2 cells	MSCs homing	Adenovirus	[83]
CXCR4	Murine bone marrow MSCs	MSCs homing	Retroviral vector	[84]
RANK-Fc	Murine bone marrow MSCs	Inhibits osteoclast differentiation and activation	Retroviral vector	[84,85]
Alpha-1 Antitrypsin	Murine adipose tissue-derived MSCs	Inhibition of osteoclast-associated bone resorption	Lentivirus	[86]
Sox-11	Rat bone marrow MSCs	MSCs differentiation and homing	Lentivirus	[87]
Runx2	Rat bone marrow MSC spheroids	Osteoblast differentiation	Plasmid	[88]
Jarid1a knockdown	Rat bone marrow MSCs	Activation of Runx2 and subsequent osteoblast differentiation	Transfection of small-interfering RNAs	[89]
miR-135	Rat adipose-derived MSCs	Osteoblast differentiation	Lentivirus	[90]
miR-31	Rat adipose-derived MSCs	Osteoblast differentiation	Lentivirus	[91]

Jarid1a: Histone demethylase Jumonji AT-rich interactive domain 1A; miR: MicroRNA; MSC: Mesenchymal stem cell; RANK-Fc: A recombinant protein of receptor activator of NF-κB; Runx2: Runt-related transcription factor 2; Sox-11: Sry-related high-mobility group box 11.

Genetic modifications of MSCs

MSCs can be genetically modified to enhance their survival rate, homing efficiency and differentiation potential [51–54]. Since the late 90s, many researches have been actively conducted to develop strategies of *ex vivo* gene therapy for bone engineering [10,51,52,54–58]. The strategies of *ex vivo* gene therapy are based on three pillars: the cell type, molecular target and gene transfer type (viral or nonviral; Table 2 & Figure 2). As mentioned before, MSCs from different tissue sources have been applied in preclinical models, yet BM-MSCs and AD-MSCs are the most commonly used cell types for bone regeneration (Table 2).
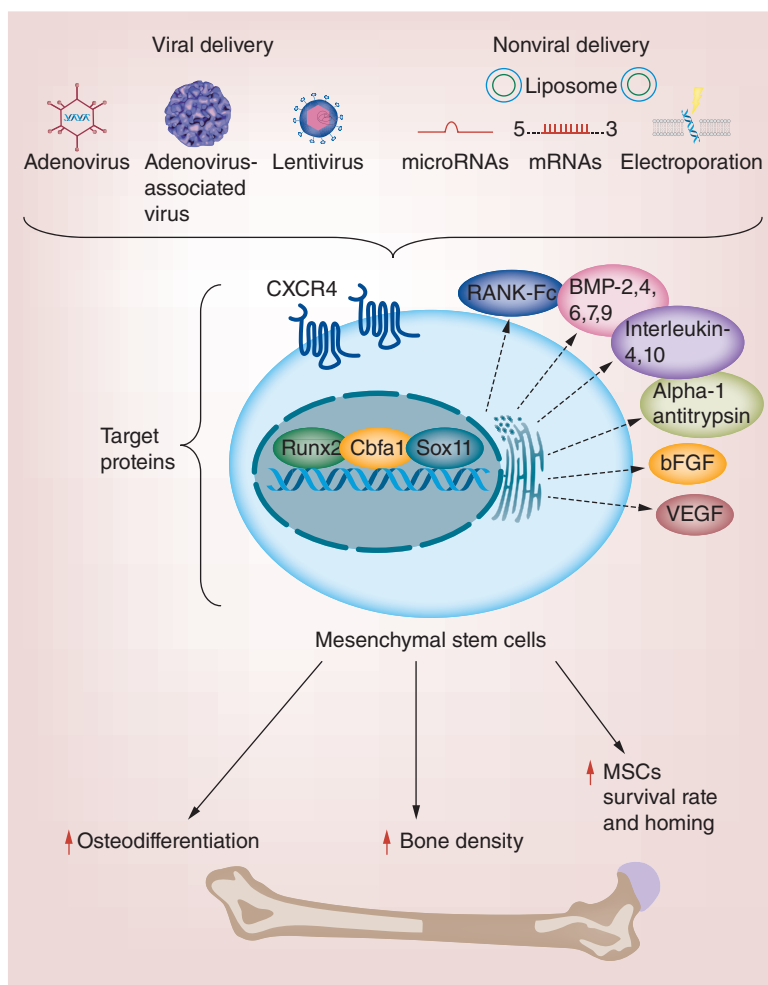
Figure 2. Viral and nonviral genetic modifications of mesenchymal stem cells for bone regeneration and treatment of bone diseases. A targeting strategy for genetic modifications of MSCs is mainly focused on three aspects: **(A)** activation of cytokines' secretion (BMPs, IL-4, IL-10, bFGF, VEGF) to promote MSC survival and osteogenic differentiation; **(B)** increasing expression of the cell surface receptors responsible for cell homing (CXCR4) or inhibition of osteoclast differentiation and activation (RANK-Fc); **(C)** activation of transcription factors and other proteins responsible for differentiation and migration of MSCs (Runx2, Cbfa1, Sox11). MSC: Mesenchymal stem cell; RANK-Fc: Recombinant RANK-L antagonist synthesized based on fusing the extracellular domain of RANK to the Fc portion of human immunoglobulin G(1); Runx: Runt-related transcription factor 2; Sox11: Sry-related high-mobility group box 11.

Molecular targeting strategies for genetic modifications of MSCs are mainly focused on three aspects: activation of cytokines' secretion (e.g., BMP-2, BMP-6, BMP-7, IL-4 and IL-10) in order to to promote MSC differentiation; increasing expression of the cell surface receptors responsible for cell rolling and eventual migration to the targeted tissue (e.g., CXCR4); and activation of transcription factors and other proteins responsible for differentiation and homing of MSCs (e.g., Sry-related high-mobility group box 11 [Sox11] and runt-related transcription factor 2 [Runx2]; Table 2 & Figure 2).

Bone morphogenetic proteins are the most important molecular targets for bone-targeted genetic engineering of MSCs [92]. BMPs are the multifunctional cytokines belonging to a TGFβ superfamily [93]. Kang *et al.* demonstrated that BMP-2, BMP-4, BMP-6, BMP-7 and BMP-9 possess the highest orthotopic bone-forming activity among 14 types of human BMPs [94], and recombinant human BMP-2 and BMP-7 were approved by US FDA for treating open tibia shaft fractures and long bone nonunions, respectively [95].

Numerous investigations, pioneered by the studies of Lieberman's [59], Huard's [96] and Gazit's [56], applied BMP-2 for *ex vivo* gene therapy. In various experimental models, the treatment of bone defects with BM-MSCs, AD-MSCs and C3H10T1/2 cells overexpressing BMP-2 led to increased bone regeneration [56–63]. A recent study has also demonstrated that BMP-2 transduced adipose-derived stem cells had higher osteogenic potential compared with BM-MSCs *in vitro* [97].

BMP- 4 is a key player in development of axial and craniofacial structures of the skeleton and in the early phase of fracture healing [98]. Lin *et al.* reported new bone formation in athymic mice transplanted with BMP-4-modified adipose-derived stromal cells from Sprague–Dawley rats [69]. In another study, the transplantation of unfractioned BM-MSCs transfected with BMP-4 improved healing of a critical-sized femur defect in adult rats [70]. Rose *et*

al. have reported that BMP-4-engineered muscle-derived cells demonstrated superior results when compared with BM-MSCs in terms of improving healing of the segmental defects [99].

BMP-6 and BMP-7 are the cytokines that also possess high osteoinductive properties. For example, injection of adipose-derived stem cells overexpressing *BMP-6* gene was capable of repairing the vertebral bone void in nude rats [72]. In another study, implantation of BMP-6-modified stem cells accelerated bone regeneration of the lumbar vertebral body in the mini pig animal model [74]. Furthermore, there is data demonstrating that AD-MSCs and BM-MSCs transfected with rhBMP-6 had higher osteogenic differentiation potential compared with transfection with rhBMP-2 *in vitro* and *in vivo* [73]. In turn, BMP-7 demonstrated great therapeutic potential in the treatment of fractures resistant to healing [100]. It was reported that New Zealand white rabbit's BM-MSCs with high expression of BMP-7 combined with an nano-hydroxyapatite/collagen (NHAC) scaffold effectively repaired a rabbit radius defect [76].

A BMP-9 probably is the most effective osteoinductive growth factor among BMPs family [94]. A number of studies have demonstrated that *ex vivo* modification of hMSCs with BMP-9 activated endochondral bone formation [77] and promoted spinal fusion [78] in rodents. Wang *et al.* have revealed that BM-MSCs transfected with BMP-9 induces callus formation in rats with osteoporotic fracture [79]. Recently, it was reported that functional Notch signaling in MSCs plays a role in osteogenesis induced by BMP-9 [101].

In addition to BMPs, some other growth factors may be implicated in osteogenesis and bone regeneration. As an example, Zhang and coauthors demonstrated that MSCs, genetically modified to express bFGF, improved bone fracture healing and enhanced bone strength in mice by stimulating endogenous angiogenesis, osteogenesis and rapid cartilage turnover through endochondral ossification [82].

It is worth mentioning that bone formation is a complex process that requires fine-tuning of many signaling pathways and for optimal bone regeneration the effects of several proteins are desired [102]. In this regard, a number of studies have revealed that the use of the BMPs is the most efficient for bone formation when combined with VEGF. For example, formation of ectopic bone was more prominent after implantation of human periosteum-derived cells cotransfected with BMP-2 and VEGF [66]. Similarly, regeneration of critical-sized bone defects in rabbits was more successful when treated with a coral scafold loaded with BMP2- and VEGF-expressing BM-MSCs compared with any single factor [67]. BM-MSCs co-expressing VEGF and BMP-6 injected to avascular necrosis of the femoral head in nude mice led to the enhancement of blood vessels and bone formation [75]. In another study, Peng *et al.* found that combined transplantation of VEGF- and BMP-4-expressing muscle-derived stem cells lead to a more optimal bone formation compared with transplantation of BMP4-expressing cells alone [71]. Some studies have also revealed enhanced efficiency of new bone formation on a model of tibial fracture in sheep and rat models of femurs defects after the transplantation of AD-MSCs co-transfected with both BMP-2 and BMP-7 compared with those with cells expressing only BMP-2 or BMP-7 [64,65]. Furthermore, there is evidence that co-transfection of MSCs with microRNA (miR)-148b enhances BMP2-induced osteogenesis [68], and MSCs engineered with BMP-7- and IL-4 cDNA accelerates bone repair in mice [81].

CXC chemokine receptors (CXCRs) belong to a family of transmembrane proteins that specifically bind to CXC chemokines. At the moment, there are seven known CXCRs, and CXCR4 presented on the surface of MSCs is considered to be a key mediator of MSCs' rolling and engraftment [103–106]. It has been demonstrated that transduction of MSCs with adenovirus carrying CXCR4 and Cbfa1 increased homing of MSCs to the defect site [83]. Using this rationale, Cho *et al.* prevented bone loss in ovariectomized (OVX) mice by intravenous transplantation of CXCR4-transfected MSCs [84]. Monocyte chemotactic protein, MIP-1α and RANTEs are also involved in the process of MSCs homing, but to a lesser extent [107].

Cho *et al.* also demonstrated that bone loss in OVX mice could be reversed by MSCs overexpressing receptor activator of NF-κB (RANK-Fc) [84], and this finding was confirmed by Kim *et al.* [85]. RANK-Fc is a recombinant protein of RANK which acts as a soluble antagonist of RANKL to prevent osteoclastogenesis [108]. In a similar study, Akbar *et al.* demonstrated the indirect influence of AD-derived MSCs expressing Alpha-1 Antitrypsin on bone repair in OVX mice [86]. Alpha-1 Antitrypsin is a proteinase inhibitor which suppresses the release of proinflammatory cytokines, enhances the production of anti-inflammatory cytokine and reduces osteoclast-associated bone resorption [109].

Sox11 is a transcription factor which plays an important role in differentiation and migration of MSCs via activation of Runx2 and CXCR4 expression [87,110]. Recently, Xu *et al.* demonstrated that genetically modified MSCs displaying high expression of Sox11 enhanced the differentiation and migration of MSCs and improved bone fracture healing in an open fracture model on Sprague–Dawley rats [87].

Runx2 has been identified as one of the transcription factors involved in osteoblast differentiation of MSCs [94]. Recent results showed that treatment of rat femurs bone defects with MSC genetically modified with Runx2 in spheroid cell implants accelerated bone repair as compared with nontransfected MSC spheroids [88]. Similarly, Deng and coauthors showed that knockdown of histone demethylase Jumonji AT-rich interactive domain 1A (Jarid1a) in bone MSCs of rats led to activation of Runx2 and subsequent improvement of calvarial bone defect regeneration [89].

As mentioned above, there are viral and nonviral vectors for the generation of genetically modified MSCs. Nonviral gene transfer for MSCs may generally be categorized in two groups: physical methods and chemical methods. Physical methods include gene guns, electroporation and sonoporation [73,74,111]. Another sufficiently effective method of a physical gene transfer is a nucleofection which is a variant of electroporation. The effectiveness of this method has been demonstrated in the studies where nucleofection of *BMP-6* gene was capable of enhancing osteogenic differentiation of AD-MSCs and BM-MSCs *in vitro* and *in vivo* [73,74]. Aslan *et al.* have reported that transplantation of hMSCs transfected with human *BMP-2* or *BMP-9* genes via nucleofection induced ectopic bone formation in NOD/SCID mice [80]. Chemical gene transfer approach involves application of the different nonviral carriers such as cationic lipids (liposome-based transfection) polymer-based systems and others [63,112,113]. In a comparison study, Park *et al.* evaluated liposome-mediated and adenoviral BMP-2 gene transfer of BM-MSCs in order to regenerate critical-size bone defects in rats [112]. The authors have established that liposome-mediated gene delivery into BM-MSCs was able to enhance bone repair albeit it took longer period than the adenoviral transfection.

The use of viral vectors has shown to be very effective in inducing the desired biological modifications in MSCs. This is in great part due to the very high level of transgene expression achieved by viral vectors. Among them, lentiviral vectors have the unique feature of allowing sustained transgene expression even after MSCs differentiation [114], which is often sought. Although integrating viral vectors such as adenovirus-associated virus, retrovirus and lentiviral vectors lead to persistent transgene expression, they also pose the potential risk of insertional mutagenesis, particularly retrovirus [115]. While the risk appears to be relatively small based on the information available today, it should still be taken into account when designing novel therapeutic strategies.

Notwithstanding the proven advantageous properties of MSCs in homing to sites of injury, inflammation and regeneration, there is evidence suggesting that MSCs may also promote tumor angiogenesis and development. Galderisi *et al.* indicate that tumors may be seen by MSCs as injury or regeneration sites, and as such may help create a microenvironment that promotes angiogenesis and metastasis of tumor cells [116]. Therefore, a word of caution in carefully selecting the applications of MSCs is also recommended. Even though the effect of MSCs on tumor progression has not been satisfactorily elucidated and can be considered debatable, the evidence of MSCs recruitment to tumors is quite strong [23]. Furthermore, the effect of MSCs on cancer stem cells demands important consideration and not fully established. Nevertheless, it is reasonable to assume that the context (such as the type of cancer cell line used in the study or the cytokines' profile) plays a key role in determining the ultimate effect of MSCs in promoting or inhibiting tumors. In this regard, simple activation or genetic engineering of MSCs may alter the context of the relationship between MSCs and tumor microenvironment leading to unforeseen consequences.

A further consideration is that for certain applications the expression of the therapeutic gene is only required for a short period of time, after which it is no longer required, and at times even unwanted. For instance, the time required for cytokines to exert its biological activity is quite short. Therefore, long-term expression of cytokines is often neither required nor recommended. Similarly, the cocktail of genes required to differentiate MSCs into the osteoblastic lineage is only required during the short period of time that it takes for the expressed transgene to induce changes in the cellular gene expression pattern. Once the differentiation process is underway the expression of the transgenes is no longer needed. Therefore, for certain applications, it is preferable to modify genetically MSCs transiently rather than permanently. In this regard, the use of episomal nonviral vectors potentially increases the safety of the treatment, although it is at the expense of lower transgene expression [117,118].

Additionally, newer transient cell engineering strategies based not on DNA but on the delivery of mRNA are available and have proven effective [119]. Mice transplanted with MSCs transiently transfected with mRNA for IL-10 and for homing ligands induced the homing to the cells to site of inflammation and reduced the inflammation without the need for persistent IL-10 expression [119]. MiRs are another key molecules that regulate the processes of cell differentiation [120], and there are several *in vitro* and *in vivo* studies indicating that miRs are capable of inducing osteogenic differentiation of human and rat AD-MSCs [68,91,120].

Table 3. Target moiety and corresponding agents for surface modifications of cells.		
Target moiety	**Agent**	**Ref.**
Hydroxyapatites	Bisphosphonates	[122,123]
CXC4R	SDF-1	[124]
E-selectins	CD44 glycoform	[125]
P-selectins	SLeX	[126]
SDF-1: Stromal cell-derived factor-1; sLeX: Sialyl Lewis X.		

Surface modifications of MSCs

According to Wu *et al.* at least 19 receptors are expressed on the surface of MSCs and all of them can potentially be used for cell targeting and homing [121]. These naturally occurring receptors may be effective in direct transplantation of MSCs without prior expansion *in vitro.* However, during *in vitro* proliferation of MSCs most of the receptors are found to be absent on the surface of culture-expanded cells [103]. This creates a whole niche for receptor or ligand engineering for targeted delivery of MSCs (Table 3).

For example, a receptor of particular interest, CX4CR, promotes MSCc rolling and binding to SDF-1 that is present in bone marrow and ischemic tissue [104,105]. In this regards, Jones *et al.* primed MSCs with SDF-1 for 1 h before transplantation to increase the transcription expression level of CXCR4 receptor, and obtained an increased cell engraftment rate both in wild-type and in osteogenesis imperfecta mice, as well as improved bone quality and plasticity in response to fracture, especially in osteogenesis imperfecta mice animals [124].

As previously mentioned, MSCs have high affinity to inflamed tissues and there are data indicating that MSCs are actively recruited to the sites of inflammation via endothelial expressed P- and E- selectins [127]. The selectins belong to a family of Type 1 transmembrane cell adhesion molecules that mediate the initial step of leukocyte recruitment in the inflammatory process. The physiological ligands for selectins are numerous glycoproteins, including P-selectin glycoprotein ligand 1, E-selectin ligand 1, CD34 and CD44, and CD44 is present on the MSCs [127]. Sackstein *et al.* used a glycan engineering approach to enhance MSCs trafficking (targeting?) to bone. MSCs were modified *ex vivo* to change native CD44 glycoform on the surface of MSCs into hematopoietic cell E-selectin/L-selectin ligand. The results showed that MSCs accumulated in bone marrow within hours after systemic infusion [125]. Similarly, Sarkar *et al.* proposed the use of a nanometer-scale polymer construct containing sialyl Lewis X, also known as cluster of differentiation 15s (CD15s) or stage-specific embryonic antigen 1 to target MSCs to bone marrow. This molecule is a tetrasaccharide carbohydrate which is usually presented on the surface of leukocytes as an active binding site of selectins' ligands [128,129] and promotes rolling and engraftment into the inflamed tissue with high expression of P-selectins [126].

In another study, researchers developed a two-end construct that binds to cell surface via a synthetic peptidomimetic ligand coupled to bisphosphonate (alendronate, Ale) [122]. The complex induced MSCs migration and differentiation along the osteogenic lineage *in vitro.* Intravenous injection of modified cells showed increased bone formation (especially trabecular) in estrogen deficient mice (role model of osteoporosis) by improving homing and retention of MSCs in bone tissue. The same polymer construct was also used in the study of D'Souza *et al.* [123]. Hydroxyl succinyl group was used for cell surface binding and alendronate was applied as a bone seeking agent. The polymer was synthesized using novel atom transfer radical polymerization (ATRP) technique to allow controlled polymerization of functional chains. *In vitro* data showed enhanced bone affinity compared with the polymer without bisphosphonate group. The polymer was not found to be toxic and therefore, opens the opportunity for its further testing *in vivo.*

Conclusion

MSCs cell therapy is undoubtedly becoming a reality for the treatment of bone-related conditions and fracture healing. Different approaches for cell transplantation and successful engraftment are being exploited to improve the healing outcomes. In this regard, cell engineering for bone regeneration attracts a lot of scientific attention making it of great clinical interest. There are three main strategies to increase the efficacy of MSCs transplantation: effective scaffold and hydrogel carriers, genetic modifications of MSCs and cell surface membrane engineering. Biomaterial scaffolds place the cells directly into the injury site; the genetic modifications of MSCs are aimed at improving the degree of engraftment via overexpression of genes controlling MSCs homing, proliferation and differentiation, whereas, the chemical engineering of the cell surface membrane provide bone targeting moieties to

MSCs. Transplanting scaffolds populated with MSCs is a very suitable strategy for filling critical size bone defects, while transplantation of genetically or chemically modified MSCs would manage the inflammatory conditions that do not require scaffolds stability and can result in significantly enhanced bone regeneration in pathological fractures. All of the approaches discussed here hold a great potential for present and future clinical practices related to bone regeneration.

Future perspective

MSCs applications for bone regeneration have been extensively used in numerous preclinical and clinical studies. Despite the increasing interest of MSC-based regenerative therapies for bones and its promising clinical potentials, the limited therapeutic effects of MSC treatment remain a major challenge suggesting that the modifications of MSC are required. A comprehensive review of the available literature indicates that most efforts are focused on scaffolds development and genetic modifications of MSCs, while the number of studies aimed at nongenetic chemical cell surface modifications are limited. Although, the use of genetic modifications has shown to be very effective in conferring the desired biological properties to MSCs, they also pose potential mutagenesis and carcinogenesis risks and more studies are required to address biosafety issues. In contrast to genetic modifications that are mostly used to manipulate nucleic acids, cell surface engineering may be used to manipulate lipids, proteins or glycans on plasma membrane, potentially increasing the safety of the treatment. In our view, cell surface engineering that involves multidisciplinary approach and convergence of chemists and cell biologists is a very promising research direction that may lead to the development of safe and clinically relevant technologies of MSCs' based cell therapy. In any event, there is a need to further understand the biology of MSCs in the context of chemical/genetic modifications and its behavior upon transplantation.

Executive summary

- In pathological bone fracture conditions natural processes of bone regeneration are hindered, and, in this case, transplantation of mesenchymal stem cells (MSCs) is a promising therapeutic method to facilitate the healing processes.
- Managing homing affinity and improvement of cell viability, proliferation and differentiation are the primary tasks in MSC transplantation for bone regeneration.

Scaffolds & hydrogels
- Seeding scaffolds with MSCs is a promising approach to increase the efficacy of scaffold transplants.
- One of the very important issues in cell-scaffold constructs is the lack of oxygen supply and nutrients.
- A number of recent studies have been directed toward creating bioactive scaffolds and hydrogels that increase the amount of oxygen available to MSCs, promote angiogenesis and support cell proliferation and differentiation.

Genetic modifications of MSCs
- Molecular targeting strategies for genetic modifications of MSCs are mainly focused on the activation of cytokines' secretion to promote MSC differentiation, increasing expression of the cell surface receptors responsible for cell rolling and migration and activation of transcription factors and other proteins responsible for the differentiation of MSCs.
- The use of viral vectors can give more stable results in terms of cell viability, proliferation and homing, though encounters major safety issues.
- The use of nonviral transfection potentially increases the safety of the treatment, although it is at the expense of lower transgene expression.

Surface modifications of MSCs
- During *in vitro* proliferation of MSCs, most of the receptors are found to be absent on the surface of culture-expanded cells and this creates a whole niche for receptor or ligand engineering for targeted delivery of MSCs.
- Surface binding of the different ligands to the cell membrane significantly reduces the potential risk of mutagenesis while allowing navigation of the cells precisely to the site of interest.

Conclusion & future perspective
- All of the approaches discussed here hold a great potential for present and future clinical practices related to bone regeneration, yet there is a need to further understand the biology of MSCs in the context of chemical/genetic modifications and its behavior upon transplantation.

References

Papers of special note have been highlighted as: ● of interest;

1. Ensrud KE. Epidemiology of fracture risk with advancing age. *J. Gerontol. A Biol. Sci. Med. Sci.* 68(10), 1236–1242 (2013).

2. Pesce V, Speciale D, Sammarco G, Patella S, Spinarelli A, Patella V. Surgical approach to bone healing in osteoporosis. *Clin. Cases Miner. Bone Metab.* 6(2), 131–135 (2009).

3. Alonso N, Calero-Paniagua I, Del Pino-Montes J. Clinical and genetic advances in Paget's disease of bone: a review. *Clin. Rev. Bone Miner. Metab.* 15(1), 37–48 (2017).

4. Shaker JL. Paget's disease of bone: a review of epidemiology, pathophysiology and management. *Ther. Adv. Musculoskelet. Dis.* 1(2), 107–125 (2009).

5. Marcucci G, Brandi ML. Rare causes of osteoporosis. *Clin. Cases Miner. Bone Metab.* 12(2), 151–156 (2015).

6. Chan JK, Gotherstrom C. Prenatal transplantation of mesenchymal stem cells to treat osteogenesis imperfecta. *Front. Pharmacol.* 5, 223 (2014).

7. Croes M, Van Der Wal BCH, Vogely HC. Impact of bacterial infections on osteogenesis: evidence from *in vivo* studies. *J. Orthop. Res.* 37(10), 2067–2076 (2019).

8. Stern SM, Ferguson PJ. Autoinflammatory bone diseases. *Rheum. Dis. Clin. North Am.* 39(4), 735–749 (2013).

9. Egusa H, Sonoyama W, Nishimura M, Atsuta I, Akiyama K. Stem cells in dentistry–Part II: clinical applications. *J. Prosthodont. Res.* 56(4), 229–248 (2012).

10. Klingemann H, Matzilevich D, Marchand J. Mesenchymal stem cells – sources and clinical applications. *Transfus. Med. Hemother.* 35(4), 272–277 (2008).

11. Panepucci RA, Siufi JL, Silva WA Jr. *et al.* Comparison of gene expression of umbilical cord vein and bone marrow-derived mesenchymal stem cells. *Stem Cells* 22(7), 1263–1278 (2004).

12. Strioga M, Viswanathan S, Darinskas A, Slaby O, Michalek J. Same or not the same? Comparison of adipose tissue-derived versus bone marrow-derived mesenchymal stem and stromal cells. *Stem Cells Dev.* 21(14), 2724–2752 (2012).

13. Ullah I, Subbarao RB, Rho GJ. Human mesenchymal stem cells – current trends and future prospective. *Biosci. Rep.* 35(2), e00191 (2015).

14. Kim Y, Kim H, Cho H, Bae Y, Suh K, Jung J. Direct comparison of human mesenchymal stem cells derived from adipose tissues and bone marrow in mediating neovascularization in response to vascular ischemia. *Cell. Physiol. Biochem.* 20(6), 867–876 (2007).

15. De Becker A, Riet IV. Homing and migration of mesenchymal stromal cells: how to improve the efficacy of cell therapy? *World J. Stem Cells* 8(3), 73–87 (2016).

16. Schrepfer S, Deuse T, Reichenspurner H, Fischbein MP, Robbins RC, Pelletier MP. Stem cell transplantation: the lung barrier. *Transplant. Proc.* 39(2), 573–576 (2007).

17. Fischer UM, Harting MT, Jimenez F *et al.* Pulmonary passage is a major obstacle for intravenous stem cell delivery: the pulmonary first-pass effect. *Stem Cells Dev.* 18(5), 683–692 (2009).

18. Nystedt J, Anderson H, Tikkanen J *et al.* Cell surface structures influence lung clearance rate of systemically infused mesenchymal stromal cells. *Stem Cells* 31(2), 317–326 (2013).

19. Eggenhofer E, Benseler V, Kroemer A *et al.* Mesenchymal stem cells are short-lived and do not migrate beyond the lungs after intravenous infusion. *Front. Immunol.* 3, 297 (2012).

20. Gholamrezanezhad A, Mirpour S, Bagheri M *et al. In vivo* tracking of 111In-oxine labeled mesenchymal stem cells following infusion in patients with advanced cirrhosis. *Nucl. Med. Biol.* 38(7), 961–967 (2011).

21. Ma S, Xie N, Li W, Yuan B, Shi Y, Wang Y. Immunobiology of mesenchymal stem cells. *Cell Death Differ.* 21(2), 216–225 (2014).

22. Sasaki M, Abe R, Fujita Y, Ando S, Inokuma D, Shimizu H. Mesenchymal stem cells are recruited into wounded skin and contribute to wound repair by transdifferentiation into multiple skin cell type. *J. Immunol.* 180(4), 2581–2587 (2008).

23. Kidd S, Spaeth E, Dembinski JL *et al.* Direct evidence of mesenchymal stem cell tropism for tumor and wounding microenvironments using *in vivo* bioluminescent imaging. *Stem Cells* 27(10), 2614–2623 (2009).

24. Cohn Yakubovich D, Sheyn D, Bez M *et al.* Systemic administration of mesenchymal stem cells combined with parathyroid hormone therapy synergistically regenerates multiple rib fractures. *Stem Cell Res. Ther.* 8(1), 51 (2017).

25. Sheyn D, Shapiro G, Tawackoli W *et al.* PTH induces systemically administered mesenchymal stem cells to migrate to and regenerate spine injuries. *Mol. Ther.* 24(2), 318–330 (2016).

26. Ghassemi T, Shahroodi A, Ebrahimzadeh MH, Mousavian A, Movaffagh J, Moradi A. Current concepts in scaffolding for bone tissue engineering. *Arch. Bone Jt. Surg.* 6(2), 90–99 (2018).

• **Ghassemi *et al.* provided a comprehensive overview of all current concept of scaffold production.**

27. Agacayak S, Gulsun B, Ucan MC, Karaoz E, Nergiz Y. Effects of mesenchymal stem cells in critical size bone defect. *Eur. Rev. Med. Pharmacol. Sci.* 16(5), 679–686 (2012).

28. Cancedda R, Mastrogiacomo M, Bianchi G, Derubeis A, Muraglia A, Quarto R. Bone marrow stromal cells and their use in regenerating bone. *Novartis Found. Symp.* 249 133–143 discussion 143-137, 170-134, 239–141 (2003).

29. Paduano F, Marrelli M, Amantea M *et al.* Adipose tissue as a strategic source of mesenchymal stem cells in bone regeneration: a topical review on the most promising craniomaxillofacial applications. *Int. J. Mol. Sci.* 18(10), E2140 (2017).

30. Sandor GK, Numminen J, Wolff J *et al.* Adipose stem cells used to reconstruct 13 cases with cranio-maxillofacial hard-tissue defects. *Stem Cells Transl. Med.* 3(4), 530–540 (2014).

31. Mesimaki K, Lindroos B, Tornwall J *et al.* Novel maxillary reconstruction with ectopic bone formation by GMP adipose stem cells. *Int. J. Oral Maxillofac. Surg.* 38(3), 201–209 (2009).

32. Wolff J, Sandor GK, Miettinen A *et al.* GMP-level adipose stem cells combined with computer-aided manufacturing to reconstruct mandibular ameloblastoma resection defects: experience with three cases. *Ann. Maxillofac. Surg.* 3(2), 114–125 (2013).

33. Sandor GK, Tuovinen VJ, Wolff J *et al.* Adipose stem cell tissue-engineered construct used to treat large anterior mandibular defect: a case report and review of the clinical application of good manufacturing practice-level adipose stem cells for bone regeneration. *J. Oral Maxillofac. Surg.* 71(5), 938–950 (2013).

34. Liu Y, Chan JK, Teoh SH. Review of vascularised bone tissue-engineering strategies with a focus on co-culture systems. *J. Tissue Eng. Regen. Med.* 9(2), 85–105 (2015).

35. Bai X, Gao M, Syed S, Zhuang J, Xu X, Zhang X-Q. Bioactive hydrogels for bone regeneration. *Bioact. Mater.* 3(4), 401–417 (2018).

36. Kaigler D, Wang Z, Horger K, Mooney DJ, Krebsbach PH. VEGF scaffolds enhance angiogenesis and bone regeneration in irradiated osseous defects. *J. Bone Miner. Res.* 21(5), 735–744 (2006).

37. Bae JH, Song HR, Kim HJ *et al.* Discontinuous release of bone morphogenetic protein-2 loaded within interconnected pores of honeycomb-like polycaprolactone scaffold promotes bone healing in a large bone defect of rabbit ulna. *Tissue Eng. Part A* 17(19-20), 2389–2397 (2011).

38. Yu H, Vandevord PJ, Gong W *et al.* Promotion of osteogenesis in tissue-engineered bone by pre-seeding endothelial progenitor cells-derived endothelial cells. *J. Orthop. Res.* 26(8), 1147–1152 (2008).

39. Zhang W, Zhu C, Ye D *et al.* Porous silk scaffolds for delivery of growth factors and stem cells to enhance bone regeneration. *PLoS ONE* 9(7), e102371 (2014).

40. Kim SK, Cho TH, Han JJ, Kim IS, Park Y, Hwang SJ. Comparative study of BMP-2 alone and combined with VEGF carried by hydrogel for maxillary alveolar bone regeneration. *Tissue Eng. Regen. Med.* 13(2), 171–181 (2016).

41. Zhao X, Liu S, Yildirimer L *et al.* Injectable stem cell-laden photocrosslinkable microspheres fabricated using microfluidics for rapid generation of osteogenic tissue constructs. *Adv. Funct. Mater.* 26(17), 2809–2819 (2016).

42. He X, Dziak R, Mao K *et al.* Integration of a novel injectable nano calcium sulfate/alginate scaffold and *BMP2* gene-modified mesenchymal stem cells for bone regeneration. *Tissue Eng. Part A* 19(3-4), 508–518 (2013).

43. Sayyar B, Dodd M, Marquez-Curtis L, Janowska-Wieczorek A, Hortelano G. Cell-matrix Interactions of Factor IX (FIX)-engineered human mesenchymal stromal cells encapsulated in RGD-alginate vs. Fibrinogen-alginate microcapsules. *Artif. Cells Nanomed. Biotechnol.* 42(2), 102–109 (2014).

44. Sayyar B, Dodd M, Wen J *et al.* Encapsulation of factor IX-engineered mesenchymal stem cells in fibrinogen–alginate microcapsules enhances their viability and transgene secretion. *J. Tissue Eng.* 3(1), 2041731412462018 (2012).

45. Sayyar B, Dodd M, Marquez-Curtis L, Janowska-Wieczorek A, Hortelano G. Fibronectin-Alginate microcapsules improve cell viability and protein secretion of encapsulated Factor IX-engineered human mesenchymal stromal cells. *Artif. Cells Nanomed. Biotechnol.* 43(5), 318–327 (2015).

46. Huebsch N, Lippens E, Lee K *et al.* Matrix elasticity of void-forming hydrogels controls transplanted-stem-cell-mediated bone formation. *Nat. Mater.* 14(12), 1269–1277 (2015).

47. Paduano F, Marrelli M, White LJ, Shakesheff KM, Tatullo M. Odontogenic differentiation of human dental pulp stem cells on hydrogel scaffolds derived from decellularized bone extracellular matrix and collagen Type I. *PLoS ONE* 11(2), e0148225 (2016).

48. Kimelman-Bleich N, Pelled G, Sheyn D *et al.* The use of a synthetic oxygen carrier-enriched hydrogel to enhance mesenchymal stem cell-based bone formation *in vivo*. *Biomaterials* 30(27), 4639–4648 (2009).

• **Interesting approach to use synthetic oxygen carrier to improve cell survival in hydrogel scaffold.**

49. Benjamin S, Sheyn D, Ben-David S *et al.* Oxygenated environment enhances both stem cell survival and osteogenic differentiation. *Tissue Eng. Part A* 19(5-6), 748–758 (2013).

50. Papadimitropoulos A, Scotti C, Bourgine P, Scherberich A, Martin I. Engineered decellularized matrices to instruct bone regeneration processes. *Bone* 70, 66–72 (2015).

51. Wei W, Huang Y, Li D, Gou H-F, Wang W. Improved therapeutic potential of MSCs by genetic modification. *Gene therapy* 25, 538–547 (2018).

52. Jin YZ, Lee JH. Mesenchymal stem cell therapy for bone regeneration. *Clin. Orthop. Surg.* 10(3), 271–278 (2018).

53. Lu CH, Chang YH, Lin SY, Li KC, Hu YC. Recent progresses in gene delivery-based bone tissue engineering. *Biotechnol. Adv.* 31(8), 1695–1706 (2013).

54. Nowakowski A, Walczak P, Lukomska B, Janowski M. Genetic engineering of mesenchymal stem cells to induce their migration and survival. *Stem Cells Int.* 2016, 4956063–4956063 (2016).

55. Freitas J, Santos SG, Gonçalves RM, Teixeira JH, Barbosa MA, Almeida MI. Genetically engineered-MSC therapies for non-unions, delayed unions and critical-size bone defects. *Int. J. Mol. Sci.* 20(14), 3430 (2019).

56. Turgeman G, Pittman D, Müller R *et al.* Engineered human mesenchymal stem cells: a novel platform for skeletal cell mediated gene therapy. *J. Gene Med.* 3, 240–251 (2001).

57. Peterson B, Zhang J, Iglesias R *et al.* Healing of critically sized femoral defects, using genetically modified mesenchymal stem cells from human adipose tissue. *Tissue Eng.* 11(1-2), 120–129 (2005).

58. Miyazaki M, Zuk PA, Zou J, Yoon SH, Wei F, Morishita Y, Sintuu C, Wang JC *et al.* Comparison of human mesenchymal stem cells derived from adipose tissue and bone marrow for *ex vivo* gene therapy in rat spinal fusion model. *Spine* 33(8), 863–869 (2008)

59. Lieberman J, Daluiski A, Stevenson S *et al.* The effect of regional gene therapy with bone morphogenetic protein-2 producing bone marrow cells on the repair of segmental defects in rats. *J. Bone Joint Surg. Am.* 81, 905–917 (1999).

60. Kumar S, Nagy TR, Ponnazhagan S. Therapeutic potential of genetically modified adult stem cells for osteopenia. *Gene Ther.* 17(1), 105–116 (2010).

61. Pelled G, Tai K, Sheyn D *et al.* Structural and nanoindentation studies of stem cell-based tissue-engineered bone. *J. Biomech.* 40(2), 399–411 (2007).

62. Fernandes G, Wang C, Yuan X, Liu Z, Dziak R, Yang S. Combination of controlled release platelet-rich plasma alginate beads and bone morphogenetic protein-2 genetically modified mesenchymal stem cells for bone regeneration. *J. Periodontol.* 87(4), 470–480 (2016).

63. Tai K, Pelled G, Sheyn D *et al.* Nanobiomechanics of repair bone regenerated by genetically modified mesenchymal stem cells. *Tissue Eng. Part A* 14(10), 1709–1720 (2008).

64. Hernandez-Hurtado AA, Borrego-Soto G, Marino-Martinez IA *et al.* Implant composed of demineralized bone and mesenchymal stem cells genetically modified with AdBMP2/AdBMP7 for the regeneration of bone fractures in ovis aries. *Stem Cells Int.* 2016, 12 (2016).

65. Qing W, Guang-Xing C, Lin G, Liu Y. The osteogenic study of tissue engineering bone with *BMP2* and *BMP7* gene-modified rat adipose-derived stem cell. *J. Biomed. Biotechnol.* 2012, 7 (2012).

66. Samee M, Kasugai S, Kondo H, Ohya K, Shimokawa H, Kuroda S. Bone morphogenetic protein2 (BMP2) and vascular endothelial growth factor (VEGF) transfection to human periosteal cells enhances osteoblast differentiation and bone formation. *J. Pharmacol. Sci.* 108, 18–31 (2008).

67. Xiao C, Zhou H, Liu G *et al.* Bone marrow stromal cells with a combined expression of BMP-2 and VEGF-165 enhanced bone regeneration. *Biomed. Mater.* 6(1), 015013 (2011).

68. Liao Y-H, Chang Y-H, Sung L-Y *et al.* Osteogenic differentiation of adipose-derived stem cells and calvarial defect repair using baculovirus-mediated co-expression of BMP-2 and miR-148b. *Biomaterials* 35(18), 4901–4910 (2014).

69. Lin L, Fu X, Zhang X *et al.* Rat adipose-derived stromal cells expressing BMP4 induce ectopic bone formation *in vitro* and in vivo1. *Acta Pharmacol. Sin.* 27, 1608–1615 (2007).

70. Rose T, Peng H, Shen H-C *et al.* The role of cell type in bone healing mediated by *ex vivo* gene therapy. *Langenbecks Arch. Surg.* 388, 347–355 (2003).

71. Peng H, Wright V, Usas A *et al.* Synergistic enhancement of bone formation and healing by stem cell-expressed VEGF and bone morphogenetic protein-4. *J. Clin. Invest.* 110(6), 751–759 (2002).

72. Sheyn D, Kallai I, Tawackoli W *et al.* Gene-modified adult stem cells regenerate vertebral bone defect in a rat model. *Mol. Pharm.* 8(5), 1592–1601 (2011).

73. Mizrahi O, Sheyn D, Tawackoli W *et al.* BMP-6 is more efficient in bone formation than BMP-2 when overexpressed in mesenchymal stem cells. *Gene Ther.* 20(4), 370–377 (2013).

74. Pelled G, Sheyn D, Tawackoli W *et al.* BMP6-engineered MSCs induce vertebral bone repair in a pig model: a pilot study. *Stem Cells Int.* 2016, 6530624–6530624 (2016).

• **Shows that delivery of bone morphogenetic protein 6-modified mesenchymal stem cells (MSCs) can enhance bone formation in a in a clinically relevant, large animal pig model.**

75. Liao H, Zhong Z, Liu Z, Li L, Ling Z, Zou X. Bone mesenchymal stem cells co-expressing VEGF and BMP-6 genes to combat avascular necrosis of the femoral head. *Exp. Ther. Med.* 15(1), 954–962 (2018).

76. Yan X, Zhou Z, Guo L *et al.* BMP7-overexpressing bone marrow-derived mesenchymal stem cells (BMSCs) are more effective than wild-type BMSCs in healing fractures. *Exp. Ther. Med.* 16(2), 1381–1388 (2018).

77. Dayoub H, Dumont RJ, Li JZ *et al.* Human mesenchymal stem cells transduced with recombinant bone morphogenetic protein-9 adenovirus promote osteogenesis in rodents. *Tissue Eng.* 9(2), 347–356 (2003).

78. Dumont R, Dayoub H, Li J *et al. Ex Vivo* bone morphogenetic protein-9 gene therapy using human mesenchymal stem cells induces spinal fusion in rodents. *Neurosurgery* 51 1239–1244 discussion 1244 (2002).

79. Wang X, Huang J, Huang F *et al.* Bone morphogenetic protein 9 stimulates callus formation in osteoporotic rats during fracture healing. *Mol. Med. Rep.* 15(5), 2537–2545 (2017).

80. Aslan H, Zilberman Y, Arbeli V *et al.* Nucleofection-based *ex vivo* nonviral gene delivery to human stem cells as a platform for tissue regeneration. *Tissue Eng.* 12(4), 877–889 (2006).

81. Lin T, Pajarinen J, Kohno Y *et al.* Transplanted interleukin-4–secreting mesenchymal stromal cells show extended survival and increased bone mineral density in the murine femur. *Cytotherapy* 20(8), 1028–1036 (2018).

82. Zhang H, Kot A, E Lay YA *et al.* Acceleration of fracture healing by overexpression of basic fibroblast growth factor in the mesenchymal stromal cells. *Stem Cells Translational Medicine* 6(10), 1880–1893 (2017).

83. Lien C-Y, Chih-Yuan Ho K, Lee OK, Blunn GW, Su Y. Restoration of bone mass and strength in glucocorticoid-treated mice by systemic transplantation of CXCR4 and Cbfa-1 co-expressing mesenchymal stem cells. *J. Bone Miner. Res.* 24(5), 837–848 (2009).

84. Cho SW, Sun HJ, Yang J-Y *et al.* Transplantation of mesenchymal stem cells overexpressing RANK-Fc or CXCR4 prevents bone loss in ovariectomized mice. *Mol. Ther.* 17(11), 1979–1987 (2009).

85. Kim D, Cho SW, Her SJ *et al.* Retrovirus-mediated gene transfer of receptor activator of nuclear factor-κB-Fc prevents bone loss in ovariectomized mice. *Stem Cells* 24(7), 1798–1805 (2006).

86. Akbar MA, Lu Y, Elshikha AS *et al.* Transplantation of adipose tissue-derived mesenchymal stem cell (ATMSC) expressing alpha-1 antitrypsin reduces bone loss in ovariectomized osteoporosis mice. *Hum. Gene Ther.* 28(2), 179–189 (2016).

87. Xu L, Huang S, Hou Y *et al.* Sox11-modified mesenchymal stem cells (MSCs) accelerate bone fracture healing: sox11 regulates differentiation and migration of MSCs. *FASEB J.* 29(4), 1143–1152 (2014).

88. Yanagihara K, Uchida S, Ohba S, Kataoka K, Itaka K. Treatment of bone defects by transplantation of genetically modified mesenchymal stem cell spheroids. *Mol. Ther. Meth. Clin. Dev.* 9, 358–366 (2018).

• **Demonstrates of osteogenic potential of transplanting genetically modified MSC spheroids with the *Runx2* gene.**

89. Deng Y, Guo T, Li J, Guo L, Gu P, Fan X. Repair of calvarial bone defect using Jarid1a-knockdown bone mesenchymal stem cells in rats. *Tissue Eng Part A* 24(9-10), 711–718 (2018).

90. Xie Q, Wang Z, Zhou H *et al.* The role of miR-135-modified adipose-derived mesenchymal stem cells in bone regeneration. *Biomaterials* 75, 279–294 (2016).

91. Deng Y, Zhou H, Zou D *et al.* The role of miR-31-modified adipose tissue-derived stem cells in repairing rat critical-sized calvarial defects. *Biomaterials* 34(28), 6717–6728 (2013).

92. Salazar VS, Gamer LW, Rosen V. BMP signalling in skeletal development, disease and repair. *Nat. Rev. Endocrinol.* 12(4), 203–221 (2016).

93. Wang RN, Green J, Wang Z *et al.* Bone morphogenetic protein (BMP) signaling in development and human diseases. *Genes Dis.* 1(1), 87–105 (2014).

94. Kang Q, Song W-X, Luo Q *et al.* A comprehensive analysis of the dual roles of BMPs in regulating adipogenic and osteogenic differentiation of mesenchymal progenitor cells. *Stem Cells Dev.* 18(4), 545–559 (2009).

95. El Bialy I, Jiskoot W, Reza Nejadnik M. Formulation, delivery and stability of bone morphogenetic proteins for effective bone regeneration. *Pharm. Res.* 34(6), 1152–1170 (2017).

96.   Musgrave DS, Bosch P, Ghivizzani S, Robbins PD, Evans CH, Huard J. Adenovirus-mediated direct gene therapy with bone morphogenetic protein-2 produces bone. *Bone* 24(6), 541–547 (1999).

97.   Bougioukli S, Sugiyama O, Pannell W *et al.* Gene therapy for bone repair using human cells: superior osteogenic potential of bone morphogenetic protein 2-transduced mesenchymal stem cells derived from adipose tissue compared to bone marrow. *Hum. Gene Ther.* 29(4), 507–519 (2018).

•   **Indicates that adipose tissue might be a preferable source of MSCs to develop a regional gene therapy approach to treat difficult bone-repair scenarios.**

98.   Tsuji K, Cox K, Bandyopadhyay A, Harfe BD, Tabin CJ, Rosen V. BMP4 is dispensable for skeletogenesis and fracture-healing in the limb. *J. Bone Joint Surg. Am.* 90(Suppl. 1), 14–18 (2008).

99.   Rose T, Peng H, Shen H-C *et al.* The role of cell type in bone healing mediated by *ex vivo* gene therapy. *Langenbecks Arch. Surg.* 388(5), 347–355 (2003).

100. Cecchi S, Bennet SJ, Arora M. Bone morphogenetic protein-7: review of signalling and efficacy in fracture healing. *J. Orthop. Transl.* 4, 28–34 (2016).

101. Cui J, Zhang W, Huang E *et al.* BMP9-induced osteoblastic differentiation requires functional Notch signaling in mesenchymal stem cells. *Lab. Invest.* 99(1), 58–71 (2019).

102. Li B, Wang H, Qiu G, Su X, Wu Z. Synergistic effects of vascular endothelial growth factor on bone morphogenetic proteins induced bone formation *in vivo*: influencing factors and future research directions. *Biomed. Res. Int.* 2016, 2869572–2869572 (2016).

103. Karp JM, Leng Teo GS. Mesenchymal stem cell homing: the devil is in the details. *Cell Stem Cell* 4(3), 206–216 (2009).

104. Shi M, Li J, Liao L *et al.* Regulation of CXCR4 expression in human mesenchymal stem cells by cytokine treatment: role in homing efficiency in NOD/SCID mice. *Haematologica* 92(7), 897–904 (2007).

105. Potapova IA, Brink PR, Cohen IS, Doronin SV. Culturing of human mesenchymal stem cells as three-dimensional aggregates induces functional expression of CXCR4 that regulates adhesion to endothelial cells. *J. Biol. Chem.* 283(19), 13100–13107 (2008).

106. Su P, Tian Y, Yang C *et al.* Mesenchymal stem cell migration during bone formation and bone diseases therapy. *Int. J. Mol. Sci.* 19(8), (2018).

107. Ito H. Chemokines in mesenchymal stem cell therapy for bone repair: a novel concept of recruiting mesenchymal stem cells and the possible cell sources. *Mod. Rheumatol.* 21(2), 113–121 (2011).

108. Hsu H, Lacey DL, Dunstan CR *et al.* Tumor necrosis factor receptor family member RANK mediates osteoclast differentiation and activation induced by osteoprotegerin ligand. *Proc. Natl Acad. Sci. USA* 96(7), 3540–3545 (1999).

109. Janciauskiene S, Larsson S, Larsson P, Virtala R, Jansson L, Stevens T. Inhibition of lipopolysaccharide-mediated human monocyte activation, in vitro, by α1-antitrypsin. *Biochem Biophys Res Commun* 321(3), 592–600 (2004).

110. Larson BL, Ylostalo J, Lee RH, Gregory C, Prockop DJ. Sox11 is expressed in early progenitor human multipotent stromal cells and decreases with extensive expansion of the cells. *Tissue Eng. Part A* 16(11), 3385–3394 (2010).

111. Li W, Wei H, Xia C *et al.* Gene gun transferring-bone morphogenetic protein 2 (BMP-2) gene enhanced bone fracture healing in rabbits. *Int. J. Clin. Exp. Med.* 8, 19982–19993 (2016).

112. Park J, Ries J, Gelse K *et al.* Bone regeneration in critical size defects by cell-mediated BMP-2 gene transfer: a comparison of adenoviral vectors and liposomes. *Gene Ther.* 10(13), 1089–1098 (2003).

113. Raftery RM, Mencía-Castaño I, Sperger S *et al.* Delivery of the improved BMP-2-Advanced plasmid DNA within a gene-activated scaffold accelerates mesenchymal stem cell osteogenesis and critical size defect repair. *J. Control. Release* 283, 20–31 (2018).

114. Zhang XY, La Russa VF, Bao L, Kolls J, Schwarzenberger P, Reiser J. Lentiviral vectors for sustained transgene expression in human bone marrow-derived stromal cells. *Mol. Ther.* 5(5 Pt 1), 555–565 (2002).

115. Hacein-Bey-Abina S, Von Kalle C, Schmidt M *et al.* LMO2-associated clonal T cell proliferation in two patients after gene therapy for SCID-X1. *Science* 302(5644), 415–419 (2003).

116. Galderisi U, Giordano A, Paggi MG. The bad and the good of mesenchymal stem cells in cancer: boosters of tumor growth and vehicles for targeted delivery of anticancer agents. *World J. Stem Cells* 2(1), 5–12 (2010).

117. Yin H, Kanasty RL, Eltoukhy AA, Vegas AJ, Dorkin JR, Anderson DG. Non-viral vectors for gene-based therapy. *Nat. Rev. Genet.* 15(8), 541–555 (2014).

118. Hamann A, Nguyen A, Pannier AK. Nucleic acid delivery to mesenchymal stem cells: a review of nonviral methods and applications. *J. Biol. Eng.* 13, 7–7 (2019).

119. Levy O, Zhao W, Mortensen LJ *et al.* mRNA-engineered mesenchymal stem cells for targeted delivery of interleukin-10 to sites of inflammation. *Blood* 122(14), e23–32 (2013).

120. Bartel DP. MicroRNAs: target recognition and regulatory functions. *Cell* 136(2), 215–233 (2009).

121. Wu Y, Zhao RC. The role of chemokines in mesenchymal stem cell homing to myocardium. *Stem Cell Rev.* 8(1), 243–250 (2012).

122. Guan M, Yao W, Liu R *et al.* Directing mesenchymal stem cells to bone to augment bone formation and increase bone mass. *Nat. Med.* 18(3), 456–462 (2012).

• **Shows the use of bisphopsphonate affinity for bone targeting polymer construct to navigate the MSCs.**

123. D'souza S, Murata H, Jose MV *et al.* Engineering of cell membranes with a bisphosphonate-containing polymer using ATRP synthesis for bone targeting. *Biomaterials* 35(35), 9447–9458 (2014).

• **Proposes the novel method of bisphosphonate polymer synthesis using ATRP for navigation of MSCs to the bone surface.**

124. Jones GN, Moschidou D, Lay K *et al.* Upregulating CXCR4 in human fetal mesenchymal stem cells enhances engraftment and bone mechanics in a mouse model of osteogenesis imperfecta. *Stem Cells Transl. Med.* 1(1), 70–78 (2012).

125. Sackstein R. Directing stem cell trafficking via GPS. *Methods Enzymol.* 479, 93–105 (2010).

126. Sarkar D, Spencer JA, Phillips JA *et al.* Engineered cell homing. *Blood* 118(25), e184–e191 (2011).

• **One of the pioneering ideas of cell surface modification for enhance targeting to the inflamed tissue.**

127. Yilmaz G, Vital S, Yilmaz CE, Stokes KY, Alexander JS, Granger DN. Selectin-mediated recruitment of bone marrow stromal cells in the postischemic cerebral microvasculature. *Stroke* 42(3), 806–811 (2011).

128. Vestweber D, Blanks JE. Mechanisms that regulate the function of the selectins and their ligands. *Physiol. Rev.* 79(1), 181–213 (1999).

129. Zhang X, Bogorin DF, Moy VT. Molecular basis of the dynamic strength of the sialyl Lewis X–selectin interaction. *Chemphyschem* 5(2), 175–182 (2004).

Inducible Cas9 T Cells: An Innovative Platform for Allogeneic CAR-T Cell Generation

Lonza

Marian Nicola[1], Ariel Gilert[1], Christian Fischer[2], Alessandro Di Cara[2], Frida Grynspan[1]
[1]Lonza Biologics R&D, CIC Haifa, IL; [2]Lonza Biologics R&D, Basel, CH

Background

- CAR-T cells show great promise in treating many types of cancers
- Genetically engineered allogeneic T cells have the potential to provide universal CAR-T cells to treat large number of patients
- CRISPR/Cas9 is used for generating allogeneic T cells
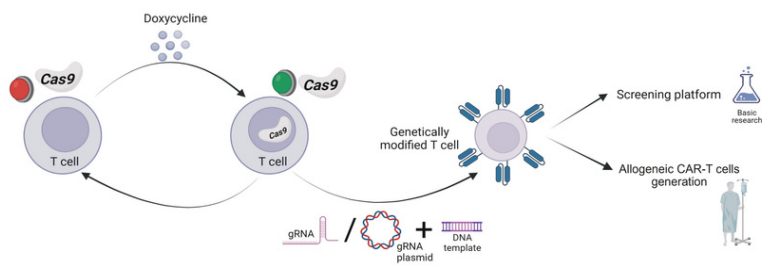
Why is it Necessary?

The use of autologous CAR-T cells requires individual manufacturing for each patient which is challenging in terms of quality, mass production and logistics. Allogeneic CAR-T cells have the potential to address these challenges

Method
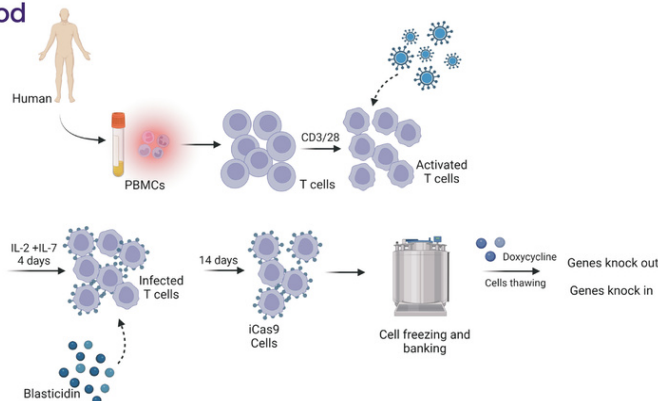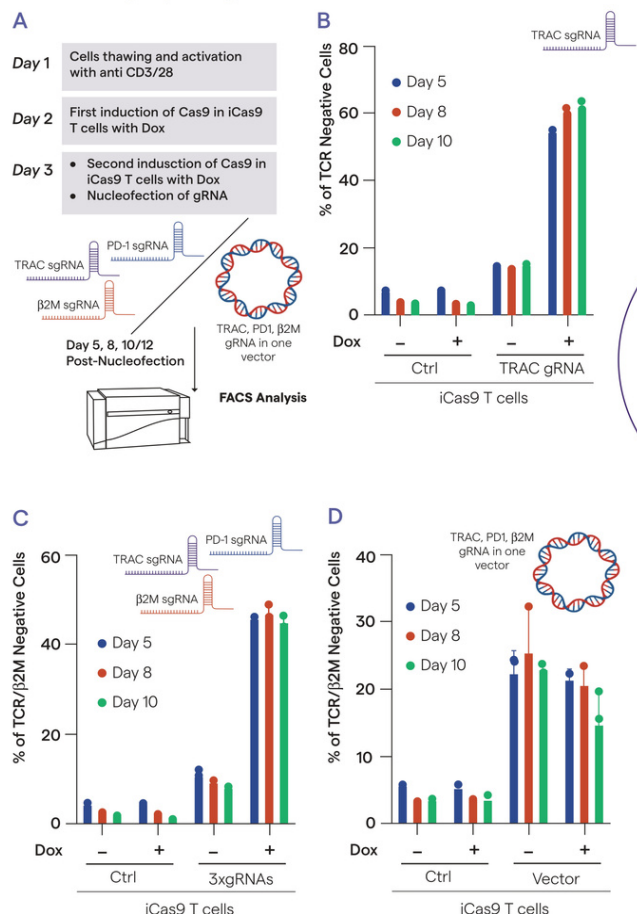

Knock-out (KO) Using iCas9 T Cells

Figure 1. Establishing single or multiple genes' KO in iCas9 T cells
(A) Schematic representation showing the workflow of genes KO in iCas9 T cells. iCas9 T cells transfected with: (B) single gRNA targeted to TRAC gene (C) β2M-/TCR- knock out (from PD1 negative cells) of iCas9 T cells transfected with multiple gRNAs targeted to TRAC, β2M and PD1 genes. (D) β2M-/TCR- knock out (from PD1 negative cells) of iCas9 T cells transfected with single vector expressing multiple gRNAs targeted to TRAC, β2M and PD1. In (B-D), iCas9 T cells were induced (Dox) and compared to uninduced control. All experiments were performed using FACS. Two factor repeated measures ANOVA was performed for all comparisons.
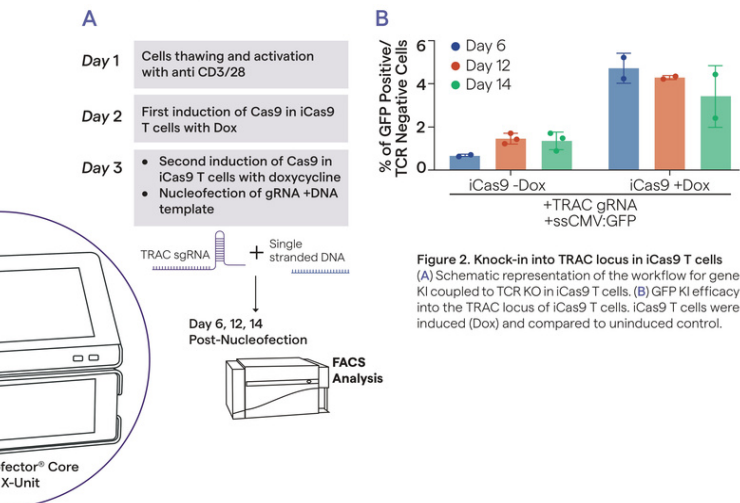
Knock-in (KI) Using iCas9 T Cells

Figure 2. Knock-in into TRAC locus in iCas9 T cells
(A) Schematic representation of the workflow for gene KI coupled to TCR KO in iCas9 T cells. (B) GFP KI efficacy into the TRAC locus of iCas9 T cells. iCas9 T cells were induced (Dox) and compared to uninduced control.

Generation of CAR-T Cells Using iCas9 T Cells vs Cas9 RNP
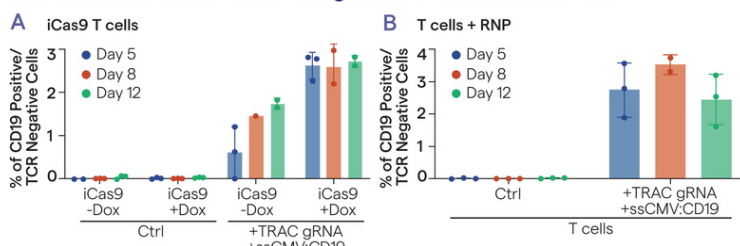

Figure 3. CAR T cells generation in iCas9 T cells and T cells
(A) FACS analysis showing CD19 KI efficacy into the TRAC locus of <u>iCas9 T cells</u> (B) FACS analysis showing CD19 KI efficacy into the TRAC locus of <u>T cells</u>. Two factor repeated measures ANOVA was performed for all comparisons.

Conclusions

- Successful generation of inducible Cas9 expressing T cells
- Generation of inducible Cas9 expressing T cells master cell bank
- The platform allows for single/multiple knock-outs and knock-ins using iCas9 T cells transfected with single/multiple gRNAs and/or plasmid encoding multiple gRNAs
- Transfection of single stranded DNA template with promoter yield the highest knock-in efficiency in iCas9 T cells
- iCas9 T cells and Cas9-RNP reach comparable KO and KI efficiencies

Take Home Message

The iCas9 T cells platform is an innovative approach for the generation of allogeneic CAR-T cells that allows the KO of genes involved in a range of immunogenic responses at high efficiency and more importantly for KI of relevant CARs.

Marian Nicola is a speaker in Lonza's virtual live event "CRISPR in Drug Discovery". Please register here to join the event on September 26 2023 or watch it on-demand after that.

References:
1. Waldman, A.D. *et al.* A guide to cancer immunotherapy: from T cell basic science to clinical practice. Nat Rev Immunol. 2020; 20; 651–668.
2. Gaj T, *et al.* ZFN, TALEN, and CRISPR/Cas-based methods for genome engineering. Trends Biotechnol. 2013; 31(7):397-405

Efficient transient genetic labeling of human CD34+ progenitor cells for *in vivo* application

Juliane MI Wiehe¹*,
Carola Niesler²*,
Jan Torzewski¹†,
Oliver Zimmermann¹,
Markus Wiesneth³,
Michael Schmitt⁴,
Klaus Schwarz³,
Hartmut Döhner⁴,
Vinzenz Hombach¹
& Jochen Greiner⁴

†*Author for correspondence*
¹*University of Ulm,*
Department of Internal
Medicine II,
Robert-Koch Str. 8,
89081 Ulm,
Germany
Tel.: + 49 731 500 24370;
Fax: + 49 731 500 24442;
E-mail: jan.torzewski@
uniklinik-ulm.de
²*University of Stellenbosch,*
Department of Physiological
Sciences, Private Bag X1,
Stellenbosch, 7602,
South Africa
³*University of Ulm, Institute*
for Clinical Transfusion
Medicine and
Immunogenetics, Ulm,
Germany
⁴*University of Ulm,*
Department of Internal
Medicine III, Ulm,
Germany
*Both authors contributed
equally.

Genetic labeling of human hematopoietic progenitor cells (HPC) and their consecutive fate-mapping *in vivo* is an approach to answer intriguing questions in stem cell biology. We recently reported efficient transient genetic labeling of human CD34+ HPC with the truncated low-affinity nerve growth factor receptor (ΔLNGFR) for *in vivo* application. Here we investigate whether HPC labeling with ΔLNGFR affects lineage-specific cell differentiation, whether ΔLNGFR expression is maintained during lineage-specific cell differentiation and which leukemia cell line might be an appropriate cell culture model for human CD34+ HPC. Human CD34+ peripheral blood stem cells and various leukemia cell lines were characterized by immunophenotyping. Cells were transfected using nucleofection. Hematopoietic differentiation was studied by colony-forming assays. ΔLNGFR expression was assessed using reverse transcription-PCR, immunofluorescence and flow cytometry. Nucleofection was efficient and did not significantly reduce hematopoietic cell differentiation. Mature myeloid cells (CD66b+) derived from human CD34+ HPC and Mutz2 cells maintained ΔLNGFR expression at a high percentage (70 ± 2% and 58 ± 2%, respectively). Mutz2 cells may serve as an *in vitro* model for human myeloid HPC. The method described herein has been adopted to Good Manufacturing Practices (GMP) guidelines and is ready for *in vivo* application.

Adult stem cells, especially hematopoietic progenitor cells (HPC), are well characterized and have been routinely used for autologous and allogeneic transplantation to treat various diseases [1–4]. HPC are isolated from bone marrow or peripheral blood mobilized by granulocyte colony-stimulating factor (G-CSF). Recent studies suggest that HPC and bone marrow cells are also able to participate in the regeneration of nonhematopoietic tissues and organs [5–8]. Following transplantation of HPC, donor-derived cells have been detected in various organs [9,10]. These results suggest that HPC might have the ability to home to different tissues and contribute to the regeneration of damaged tissues by 'transdifferentiation' into organ cells [11,12]. However, this proposed plasticity of HPC remains a controversial issue. The interpretation of experimental data ranges from the suggestion of a high efficiency of transdifferentiation of adult bone marrow stem cells [5–8], to the notion that there is no evidence of transdifferentiation at all [13,14] and that endogenous stem cells may be recruited to differentiate into, or fuse with, organ cells [15]. Although repair of damaged tissue with autologous HPC has been proposed as a novel therapeutic option for myocardial infarction [16–18], the molecular mechanisms of homing or transdifferentiation of autologous HPC in humans have not yet been studied *in vivo* [19]. To

this end, labeling of HPC and their consecutive fate-mapping *in vivo* is desirable. Labeling of HPC prior to application in humans, however, must be efficient and safe. Genetic cell markers are appropriate to track transplanted HPC *in vivo*. However, the method of gene transfer into stem cells is critical, as viral vector transduction involves the risk of tumor induction by nonspecific genomic integration [20–22], whereas nonviral transfection often fails due to low transfection efficiency [23]. Electroporation of CD34+ HPC, for example, is reported to achieve transfection efficiencies within the range of 20–25% [24–26], whereas lipofection is repeatedly reported to be inefficient [27,28].

Our group and others have recently described the method of nucleofection to facilitate a rapid, specific and highly efficient transient transfection of hematopoietic or embryonic stem cells [29,30]. Nucleofection is a novel technology based on electroporation, which involves introducing extrinsic nucleic acids gently and directly into the cell nucleus. Using this method, a high transfection efficiency was achieved without a marked decrease in cell viability. Importantly, no clonal integration of the transgene was observed [29], and thus, the risk of side effects, such as tumor induction by nonspecific viral promoter integration into the genome, was markedly reduced. Most *in vivo* studies in humans have been performed using the

future medicine

truncated low-affinity nerve growth factor receptor (ΔLNGFR) or neomycin phosphotransferase (NPT) as marker genes. Unfortunately, no antibody is available to detect NPT in cells by immunostaining and therefore ΔLNGFR was deemed the more appropriate marker for our studies. Although earlier studies have demonstrated that ΔLNGFR enhances signaling through neurotrophin receptors of the tropomyosin receptor kinase (TRK) family and thereby may increase the risk of cellular transformation and possibly metastasis, recent data have confirmed its safety for *in vivo* application in humans [31].

This study has been designed to investigate whether nucleofection of CD34+ HPC with ΔLNGFR affects hematopoietic cell differentiation and whether ΔLNGFR expression is maintained during hematopoietic cell differentiation after transient transfection. Furthermore, we have characterized the immunophenotype, transfection efficiency and hematopoietic cell differentiation of transfected leukemia cell lines to decide which cell line may be an appropriate model for human CD34+ HPC.

Materials & methods
Cell culture
Human CD34+ HPC: CD34+ cells stimulated with G-CSF were prepared by leukapheresis. Informed consent was taken from all patients treated in a framework of studies approved by the local ethics committee. Immunomagnetic selection of CD34+ cells was performed using the CliniMACS® system (Miltenyi Biotech GmbH, Germany). Flow cytometry (FACS) analysis using anti-CD34 antibody conjugated with phycoerythrin (PE) (Becton Dickinson GmbH, Germany) showed a purity of more than 98% for CD34+ HPC. Cells were cryopreserved as described [32]. Cryopreserved CD34+ HPC were thawed and washed with phosphate buffered saline (PBS). Cells were cultured in Roswell Park Memorial Institute (RPMI) medium (Biochrom, Germany), supplemented with 10% fetal calf serum (FCS), 1% penicillin, streptomycin and glutamine (PSG) at 37°C, 5% CO_2. Medium was changed every other day. After nucleofection, cells were stimulated for lineage-specific differentiation.

Cell lines
The human chronic myeloid leukemia (CML) cell line K562 and the human acute myeloid leukemia (AML) cell lines HL60 (FAB M2), Kasumi1 (FAB M2) and KG1 (FAB M7) were obtained from American-type culture collection (ATCC) (Manassas, VA, USA). Cell lines were cultured in RPMI 1640 medium, FCS, 10% (v/v), L-glutamine (2 mM), penicillin (100 units/ml) and streptomycin (100 units/ml). Mutz2 (the German Resource Centre for Biological Material-DSMZ, Braunschweig, Germany) is a human cell line established from cells of a patient with ALL. Mutz2 cells were cultured in αMEM-medium (PAA Laboratories GmbH, Linz, Austria) supplemented with 10% FCS, 2% PSG and 10% conditioned medium from the cell line 5637 (DSMZ, Germany), a carcinoma cell line from the urinary bladder. Cells were cultured at 37°C, 5% CO_2. Medium was changed every other day. After nucleofection, cells were stimulated for hematopoietic cell differentiation.

Immunophenotyping of human CD34+ HPC & Mutz2 cells
Human CD34+ HPC and Mutz2 cells were tested for expression of cell-surface antigens with the following antibodies: CD1A-PE (DakoCytomation-Glostrup, Denmark), CD2-FITC, CD3-PC5 (Beckman Coulter GmbH, Germany), CD7-FITC, CD10-FITC, CD13-PE (DakoCytomation), CD14-PE, CD19-PC5, CD33-PC5 (Beckman Coulter), CD34-FITC (Becton Dickinson), CD45-PC5 (Beckman Coulter), CD56-PE (Bekton Dickinson), CD61-FITC (DakoCytomation), CD65-FITC (Caltec), CD117-PC5 (Beckman Coulter), HLA-DR-PE (Bekton Dickinson), κ-FITC, Lambda-PE (DakoCytomation), and 7.1-PE (Beckman Coulter).

The antigens recognized are found in the following cell types:
- T cells: CD1A, CD2, CD3, CD7
- B cells: CD10, CD19, CD79
- Myeloid lineage: CD13, CD14 and CD33
- Hematopoietic stem cells and endothelial cells: CD34
- Leukocytes: CD45, CD61
- Hematopoietic stem cells: CD117 (ckit; stem cell factor)
- Natural killer cells: CD56

Myeloperoxidase (MPO)-fluorescein isothiocyanate (FITC) (DakoCytomation) was used as a cytoplasmatic marker. Expression was analyzed using the FACS Calibur flow cytometer (Becton Dickinson).

ΔLNGFR labeling
Vector construction
The ΔLNGFR vector was generated by cloning the human truncated *LNGFR* gene into the eukaryotic pVAX1 expression vector (Invitrogen

Table 1. Comparison of human CD34 HPC with the leukemia cell line Mutz2.		
	CD34-selected HPC	**Unselected Mutz2 cells**
CD34	>98%	83%
Granularity	Low	Low
Transfection efficiency	41 ± 2%	55 ± 5%
Differentiation potential	Granulocytes, erythrocytes, macrophages, megakaryocytes	Granulocytes, macrophages, megakaryocytes
Derivation	Normal HPC	Cell line, leukemic blasts
Availability	Limited	Unlimited

HPC: Hematopoietic progenitor cells.

GmbH, Germany). The ΔLNGFR 834 bp fragment was amplified by polymerase chain reaction (PCR) as described [29].

Nucleofection
CD34⁺ HPC and Mutz2 cells were pelleted and resuspended in human CD34 Cell Nucleofector™ Solution or Cell Line Nucleofector Solution V (Amaxa GmbH, Köln, Germany), respectively, at $2–3 \times 10^6$/100 µl. Cells were nucleofected with 2 µg plasmid DNA (pVAX1/ΔLNGFR or pVAX1 (Invitrogen Life Technologies)) using program U-08 (for HPC) or G-09 (for Mutz2) of the nucleofector device.

After nucleofection, cells were immediately mixed with 500 µl prewarmed culture medium and transferred into 6-well plates containing prewarmed medium. Cells were incubated at 37°C over a time period of 10 days.

LNGFR expression
Reverse transcription (RT)-PCR
To analyze ΔLNGFR mRNA in transfected and nontransfected CD34⁺ cells, RT-PCR was performed. Total RNA was extracted using the RNeasy Minikit™ (Qiagen, Germany) and transcribed using Omniscript RT kit (Qiagen). cDNA was subjected to RT-PCR for a 250 bp fragment of the *LNGFR* gene (forward primer 5´-caggacaagcagaacaacgtg-3´, reverse primer 5´-cgtgctggctatgaggtcttg-3´) and a 220 bp fragment of the housekeeping gene Glyceraldehyde-3-phosphate dehydrogenase (*GAPDH*) (forward primer 5´-aagagaggcatcctcaccct-3´, reverse primer 5´-tacatggtcggggtgttgaa-3´) using the Hot Star Taq Master Mix kit (Qiagen). The ΔLNGFR–vector construct was used as a positive control.

FACS analysis
Expression of ΔLNGFR was evaluated in nontransfected, mock-transfected and ΔLNGFR-transfected HPC and leukemia cell lines, using FACS analysis. Cells were incubated with nonconjugated purified mouse monoclonal anti-human nerve growth factor (NGF) antibody (CL10012) (Cedarlane Laboratories Limited, Canada). Data were analyzed using the Cellquest Version 3.1 software (Becton Dickinson). To examine ΔLNGFR surface expression of CD34⁺ HPC and Mutz2 cell lines during differentiation into CD66b⁺ cells, FACS analysis was performed at 1, 4, 7 and 10 days after transfection using the anti-human NGF antibody and the monoclonal FITC-labeled CD66b antibody (Beckman Coulter GmbH).

Figure 1. Representative immunophenotyping of human CD34⁺ HPC and unselected Mutz2 cells.
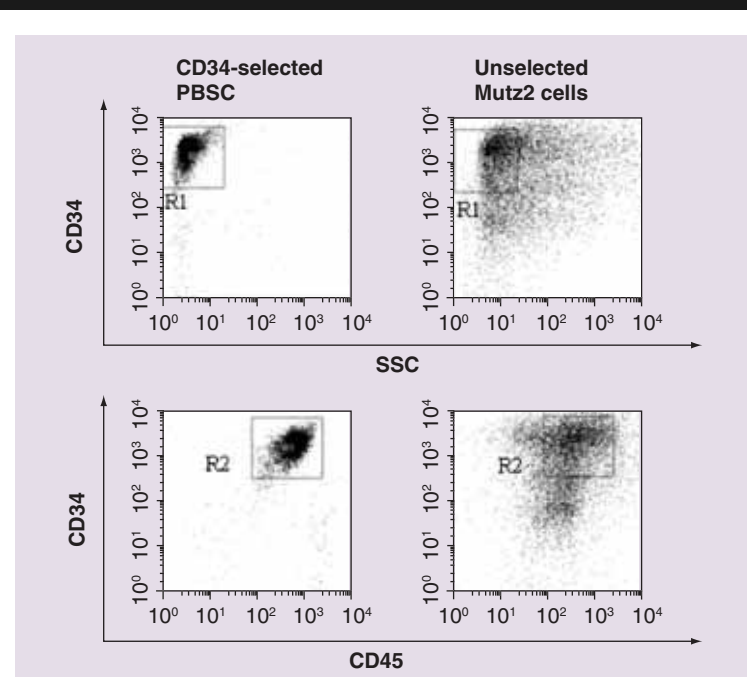
The main population of both CD34⁺ HPC and unselected Mutz2 cells expressed the cell-surface antigens CD34 and CD45, and is characterized by low granularity. PBSC: Peripheral blood stem cells; SSC: Side scatter.

Figure 2. Representative immunophenotyping of human CD34⁺ HPC.
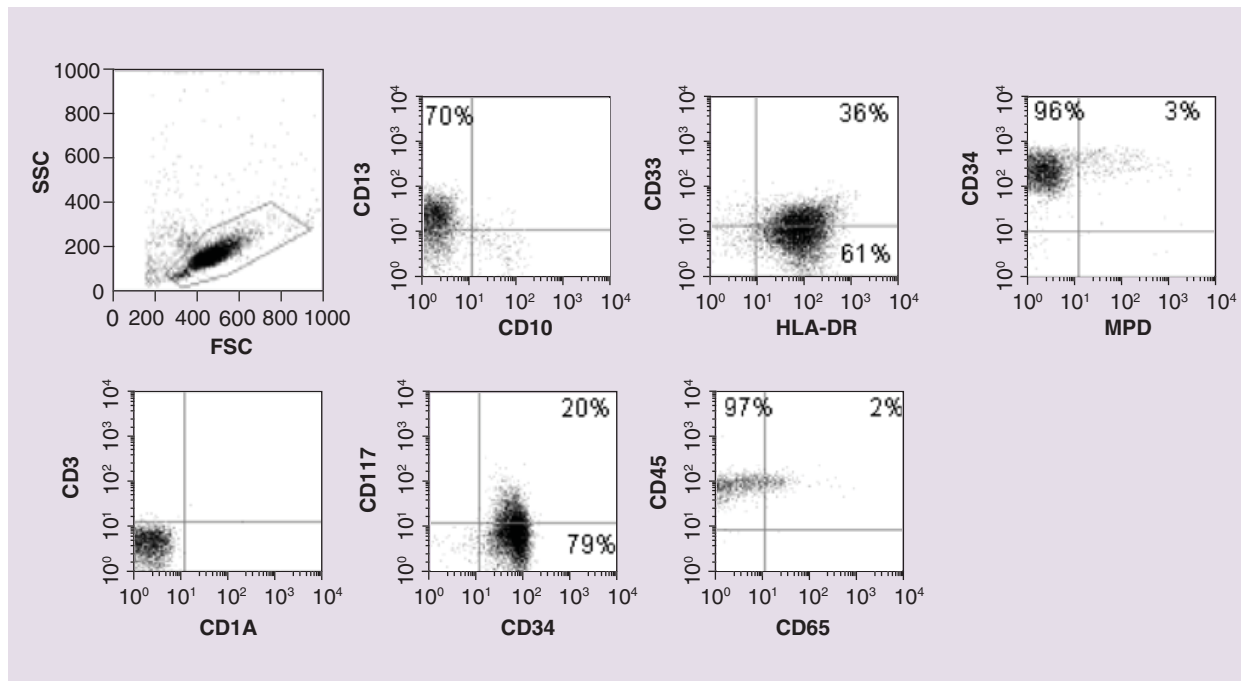
The main population of CD34⁺ HPC expressed the cell-surface antigens CD34 and CD45. Human CD34⁺ HPC expressed CD34, CD45, HLA-DR , CD13 and, to a lesser extent, CD33 and CD117. FSC: Forward scatter; HPC: Hematopoietic progenitor cells; SSC: Side scatter.

The CD66b⁺ population as well as the CD66b/ΔLNGFR double-positive population was quantified.

Immunofluorescence microscopy
For immunofluorescence microscopy, 10 μl of the cell suspension used for FACS analysis was mounted on a microscopic slide and fixed using the Dako fluorescent mounting medium (Dako-Cytomation). Cells were visualized by immunofluorescence microscopy using a blue and green fluorescent filter (Zeiss, Germany).

Differentiation capacity
Differentiation of CD34⁺ HPC & Mutz2 cells into CD66b⁺ cells
ΔLNGFR positivity of CD34⁺ HPC and Mutz2 cells was assessed during differentiation into cells expressing CD66b⁺, a cell-surface marker for granulocytes [33]. Cells were plated at a density of $5–10 \times 10^5$ cells/ml in Cellgro medium (Cell Genix, Germany) supplemented with 10% FCS, 2% PSG, 0.5×10^{-4} α-thioglycerol, and recombinant human (rh) cytokines Epo (1 U/ml), rh-interleukin (IL)-3 (20 ng/ml) and rh-stem cell factor (SCF) (100 ng/ml) (R&D Systems, Germany). Medium was changed every other day.

Cells were harvested by centrifugation. The CD66b⁺ population and the CD66b/ΔLNGFR double-positive populations were measured.

Methylcellulose assays
To evaluate differentiation capacity, HPC were examined in burst-forming unit (BFU) and colony-forming unit (CFU) assays using non-, mock- and ΔLNGFR-transfected CD34⁺ HPC and Mutz2 cells. For evaluation of BFU and CFU granulocyte, erythrocyte, macrophage and megakaryocyte (GEMM) assays, $0.05–0.2 \times 10^5$/ml viable cells were plated in methylcellulose medium and 1000 mU/ml rh-Epo, 20 ng/ml rh-IL-3 and 100 ng/ml rh-SCF were added, while CFU-C were evaluated using 2 ng/ml GM-CSF, 20 ng/ml rh IL-3 and 100 ng/ml rh-SCF. Colonies were assessed 14 days after plating.

Endomyocardial biopsies/
immunohistochemical staining for LNGFR
Right ventricular (septal) endomyocardial biopsies were obtained from patients with dilated cardiomyopathy presenting with the clinical symptoms of cardiac failure and echocardiographic ventricular dysfunction [40,41]. Coronary artery disease was excluded by coronary angiog-

Figure 3. CD66b FACS staining of CD34+ HPC.

The main population of both CD34+ HPC and unselected Mutz2 cells expressed the cell-surface antigens CD34 and CD45. CD34+ HPC did not express CD66b. FACS: Fluorescence activated cell sorting; FSC: Forward scatter; HPC: Hematopoietic progenitor cells; SSC: Side scatter.

Chirurgische Produkte GmbH, Karlstein, Germany). All procedures were performed in accordance with ethical standards and with the informed consent of the patients.

Five sequential sections (6 µm) from endomyocardial biopsies were immunohisto-chemically analyzed by Avidin-Biotin-Staining for LNGFR expression using the mouse mono-clonal anti-human NGF-receptor antibody (Cedarlane, Canada) at a dilution of 1:25, followed by a second antibody staining with a biotinylated horse anti-mouse antibody at a dilution of 1:100. Cardiomyocytes were stained with Troponin I (Hytest, Finland) at a dilution of 1:2500 followed by a second antibody staining with an anti-mouse biotinylated antibody at a dilution of 1:100.

Statistical analysis
All experiments were carried out three times with three independent samples. The mean value and the standard deviation were calculated using Microsoft Excel and statistical analysis was performed using SigmaStat version 2.0 software. Tests included One-Way Analysis of Variance (ANOVA), Tukey-Test, and student's t-test. $p < 0.05$ was considered statistically significant.

raphy. Furthermore, valvular and congenital heart disease was excluded. Biopsies were performed by standard technique using the percutaneous transvenous femoral approach with a Pilling Weck bioptome (Bioptom 1.8 × 1000 mm, REF, MDZ-4, Lot D0601,

Figure 4. Representative immunophenotyping of unselected Mutz2 cells.

The main population of unselected Mutz2 cells expressed the cell-surface antigens CD34 and CD45. Mutz2 cells expressed CD34 and the antigens CD45, HLA-DR, CD13, CD33, and CD65. FSC: Forward scatter; SSC: Side scatter.
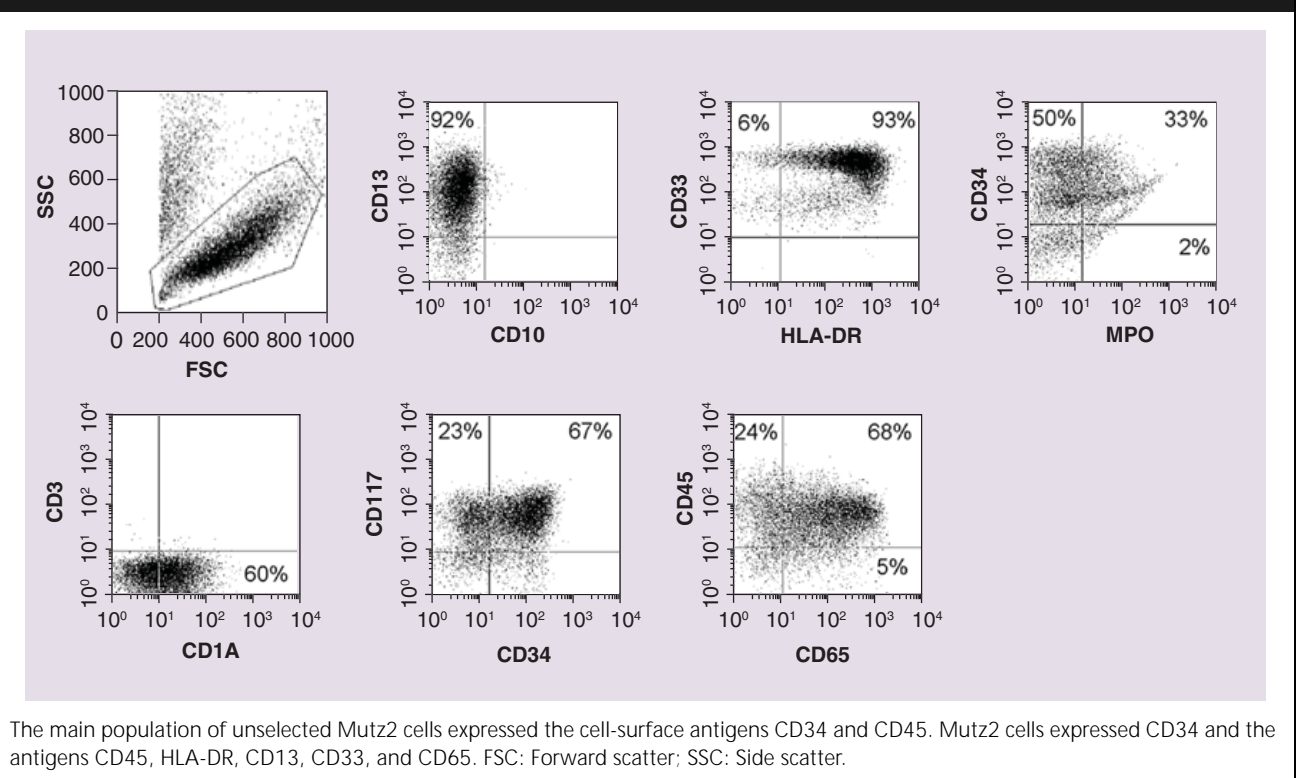
Figure 5. Lack of constitutive mRNA expression of ΔLNGFR in human CD34⁺ HPC and Mutz2 cells.

Untreated CD34⁺ HPC **(1)** and Mutz2 cells **(2)** do not express ΔLNGFR.
(3) Negative control. The plasmid containing ΔLNGFR served as a positive control. **(4)** GAPDH was used as housekeeping gene. GADPH: Glyceraldehyde-3-phosphate dehydrogenase; HPC: Hematopoietic progenitor cells; ΔLNGFR: Truncated low-affinity nerve growth factor receptor.

Results

Immunophenotyping of CD34⁺ HPC & Mutz2 cells

Human HPC were positively selected for the cell-surface antigen CD34. A purity of more than 98% was achieved **(Figure 1, Table 1)**. CD34⁺ HPC were characterized by FACS analysis according to standards applied for leukemia typing [34]: they expressed CD34 (99%), CD45 (99%), HLA-DR (97%), CD13 (70%) and, to a lesser extent, CD33 (36%) and CD117 (20%) (representative experiment shown in **Figure 2**). Cells did not express CD66b **(Figure 3)**. Due to the difficulties (both availability and ethically) in obtaining human CD34⁺ primary cells, we went on to characterize leukemia cell lines as potential *in vitro* models of CD34⁺ HPC. The Mutz2 cell line showed high expression of CD34 and the highest transfection efficiency of all leukemia cell lines studied **(Table 2)**. Similarly to CD34⁺ HPC, Mutz2 cells expressed CD34 (83%) as well as CD45 (92%), HLA-DR (93%), CD13 (92%),

CD33 (99%) and CD117 (90%). They also showed significant expression of the antigens CD65 (75%), CD1A (60%) and MPO (35%) **(Figure 4)**. The expression pattern characterizes these cells as leukemic blasts of an acute myeloid leukemia, FAB type M2. No expression of the antigens CD2, CD3, CD7, CD10, CD14, CD19, CD56, CD61, CD79a, 7.1, κ and λ light chain was found in the human HPC and Mutz2 cells. Typical characteristics of CD34⁺ HPC and Mutz2 cells are listed in **Table 1**.

Neither CD34⁺ HPC nor Mutz2 cells express LNGFR

RT-PCR amplification of a 250 bp ΔLNGFR fragment of cDNA was used to investigate whether LNGFR is expressed in untreated HPC and Mutz2. No LNGFR expression was detectable in CD34⁺ HPC nor in Mutz2 cells. The vector plasmid containing ΔLNGFR cDNA was used as a positive control and *GAPDH* as a housekeeping gene **(Figure 5)**. In order to further confirm the transient character of ΔLNGFR nucleofection, we performed PCR, 21 and 28 days after nucleofection, which showed complete loss of the marker gene after 28 days.

High transfection efficiency of CD34⁺ HPC & Mutz2 cells

Human CD34⁺ HPC and Mutz2 cells were transfected with ΔLNGFR by nucleofection. Transfection of both human CD34⁺ HPC and Mutz2 cells is highly efficient **(Figure 6)**. **Figure 6A** shows a representative example of FACS analysis on day 1 after transfection. **Figure 6B** depicts the mean transfection efficiency of Mutz2 cells compared with human CD34⁺ HPC: 41% (± 2%) of human CD34⁺ HPC and 55% (± 5%) of Mutz2 cells were positive for the marker gene ΔLNGFR after transient transfection. No statistically significant differences were observed (n = 3). As an additional control we

Table 2. CD34 expression and transfection efficiency of different leukemia cell lines 1 day post transfection.

AML cell line	CD34 positivity	Transfection efficiency
CD34⁺ HPC	98%	41%
Mutz2	83%	55%
K562	13%	53%
Kasumi-1	96%	25%
HL60	12%	24%
KG1	66%	6%

AML: Acute myeloid leukemia; HPC: Hematopoietic progenitor cells.

Figure 6. Transfection efficiency of human CD34+ HPC and Mutz2 cells using nucleofection.

A representative FACS-dotblot shows that transfection with ΔLNGFR is highly efficient on day 1 after transfection **(A)**. 41 ± 2% of human CD34+ HPC and 55 ± 5% of Mutz2 cells were positive for ΔLNGFR 1 day post transfection (n = 3) **(B)**. ns: Not significant.
FSC: Forward scatter; HPC: Hematopoietic progenitor cells; LNGFR: Low-affinity nerve growth factor receptor; PBSC: Peripheral blood stem cells.

also found high transfection efficiencies using the marker gene enhanced green fluorescent protein (EGFP) [data not shown].

### Hematopoietic cell differentiation of transfected cells

To investigate whether HPC and Mutz2 cells are still able to differentiate after nucleofection with ΔLNGFR, we performed colony-forming assays. Non-, mock- and ΔLNGFR-transfected CD34+ HPC differentiated into blood cells of different hematopoietic cell lines (erythrocytes, granulocytes, macrophages, megakaryocytes). Non-, mock- and ΔLNGFR-transfected Mutz2 cells showed differentiation into granulocytes, macrophages and megakaryocytes, but not into erythrocytes. Colonies derived from human CD34+ HPC and Mutz2 are shown in **Figure 7A & B**, respectively. A significant decrease of colonies was observed between untreated and ΔLNGFR-transfected CD34+ HPC in burst forming units with erythrocytes (BFU-E) (3210 ± 1473 vs 606 ± 526; p < 0.05) and CFU-GEMM (2678 ± 498 vs 681 ± 243; p < 0.01), as well as in CFU-GEMM of untreated compared with

mock-transfected CD34+ HPC (2678 ± 498 vs 1300 ± 1032; p < 0.05). Similarly, a significant decrease in colony number was seen in untreated versus ΔLNGFR-transfected Mutz2 cells in CFU-GEMM (716 ± 136 vs 194 ± 19; p < 0.01) and CFU-GM (444 ± 140 vs 94 ± 35; p < 0.05) assays. However, no statistically significant differences were found between mock- and ΔLNGFR-transfected cells in both HPC and Mutz2 cells (n = 3) **(Figure 7C & D)**.

Maintenance of marker expression during hematopoietic cell differentiation

CD66b, a cell-surface antigen characteristically expressed in mature myeloid cells such as granulocytes, was used as a surrogate marker for lineage-specific cell differentiation to investigate whether differentiated cells maintain ΔLNGFR expression. **Figure 8A** shows immunofluorescent images of CD34+ HPC and Mutz2 cells cultured for 4 days after nucleofection in a differentiation medium. Whereas both cells shown in the panels express CD66b (green), only one of these also expresses the marker gene ΔLNGFR (red) **(Figure 8A)**. **Figure 8B** shows a

Figure 7. Hematopoietic cell differentiation of transfected human CD34+ HPC.
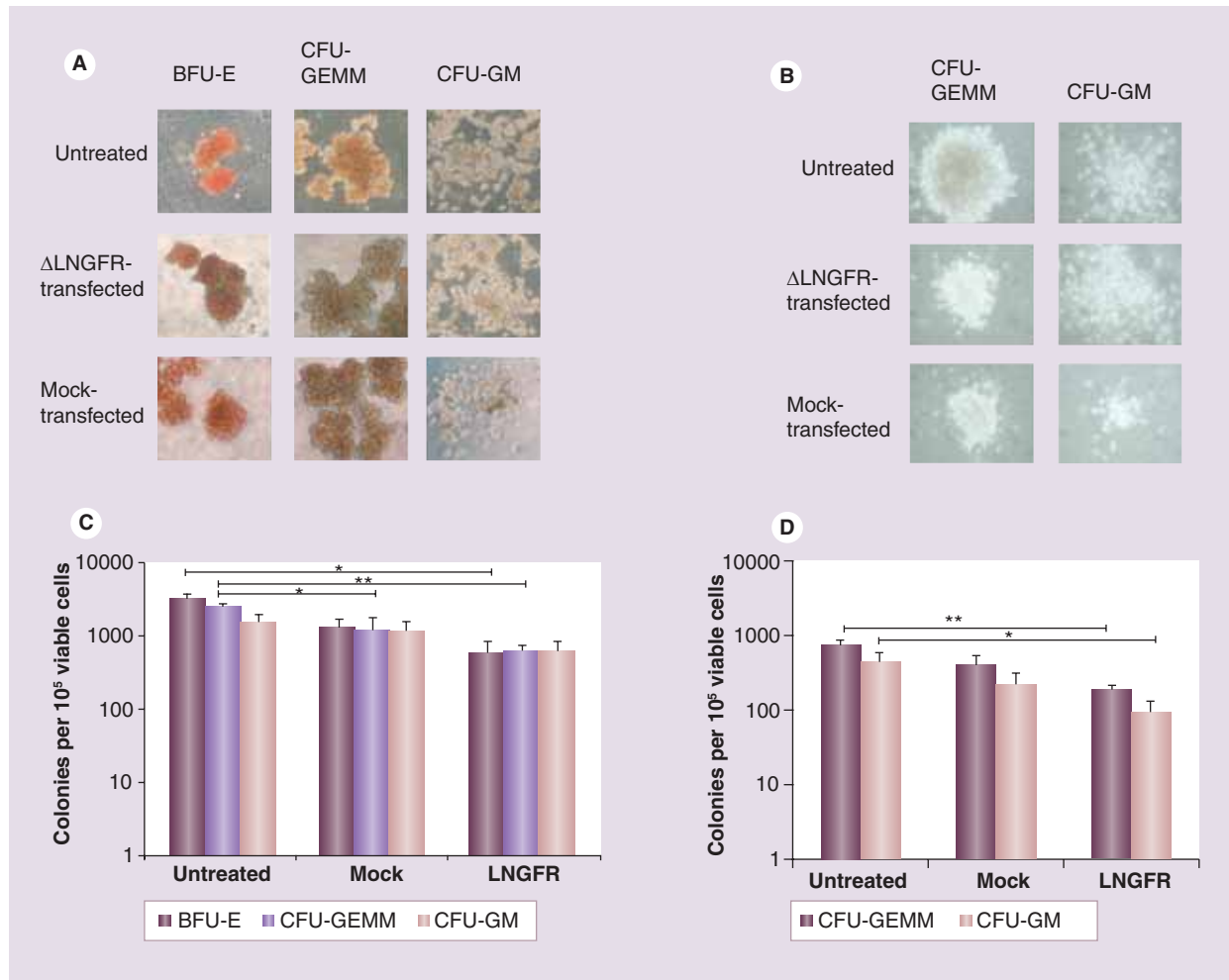
Methylcellulose assays of untreated, mock-, and ΔLNGFR-transfected human CD34+ HPC formed all colonies (BFU-E, CFU-GEMM, CFU-GM) **(A)**. For Mutz2 cells **(B)** CFU-GEMM and CFU-GM colonies were formed, but not BFU-E. Quantitative analysis of lineage-specific cell differentiation of transfected CD34+ HPC **(C)** and Mutz2 **(D)** into hematopoietic cell lines.
BFU-E: Burst-forming units with erythroctyes; CFU-GEMM: Colony-forming units with granulocytes, erythrocytes, megakaryocytes and macrophages; CFU-GM: Colony-forming units with granulocytes and macrophages; HPC: Hematopoietic progenitor cells; LNGFR: Low-affinity nerve growth factor receptor. (n = 3; *p < 0.05; **p < 0.01)
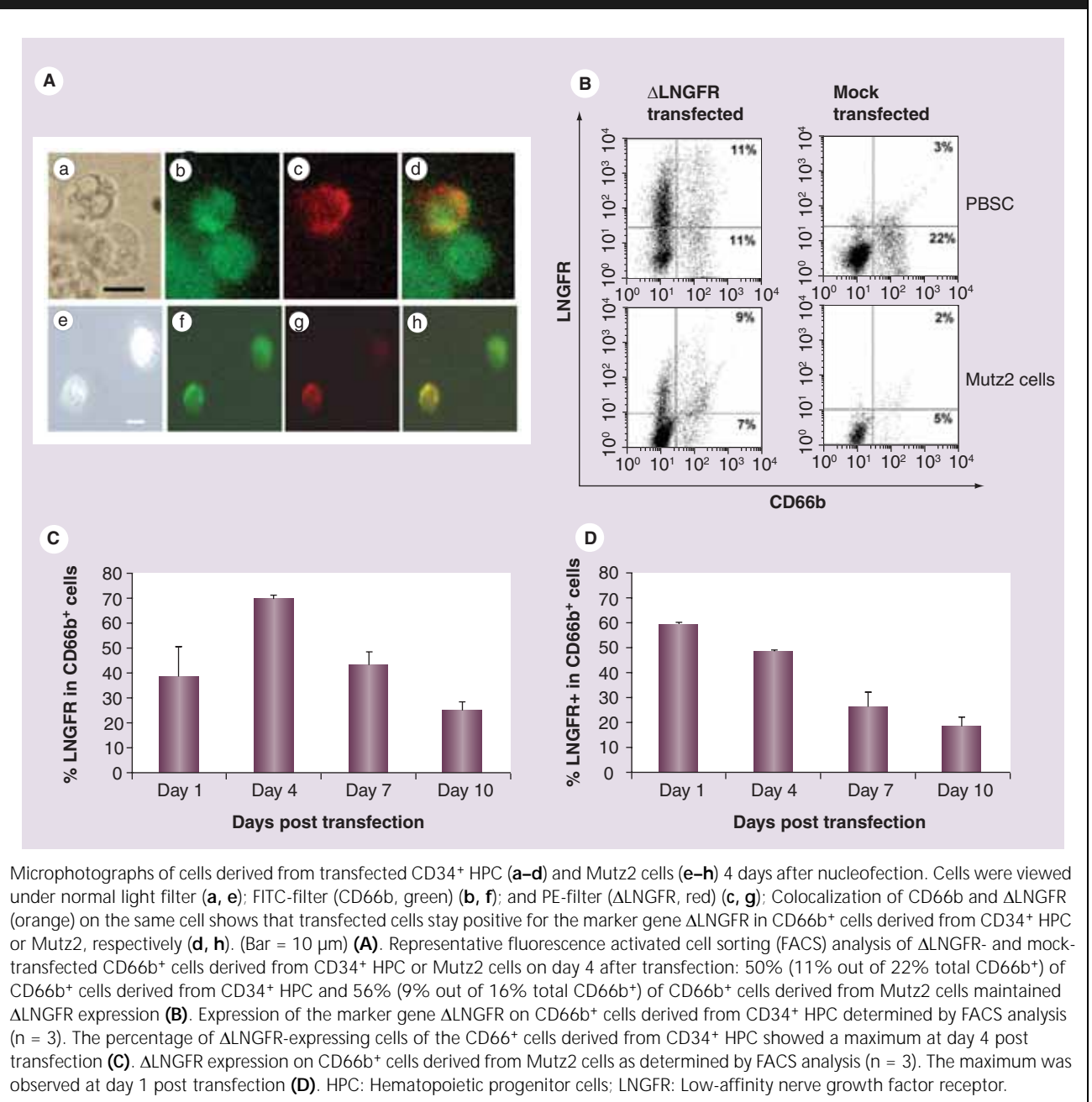
representative FACS analysis of the percentage of transfected HPC and Mutz2 cells that maintain ΔLNGFR expression after differentiation into CD66b+ cells on day 4. The kinetics of ΔLNGFR expression during differentiation of transfected CD34+ HPC and Mutz2 cells into CD66b+ cells was also assessed over 10 days by FACS analysis. The percentage of ΔLNGFR expression in CD66b+ cells derived from CD34+ HPC showed a maximum at day 4 post transfection (70 ± 2%), and decreased to 43 ± 6% on day 7 and 24 ± 4% on day 10 (n = 3, **Figure 8C**). Similarly, the number of ΔLNGFR expressing CD66b+ cells derived from Mutz2 cells decreased over time. Maximal

expression was measured at day 1 post transfection with 58 ± 1%, which decreased to 48 ± 1% at day 4, 26 ± 6% at day 7 and 19 ± 3% at day 10 (n = 3, **Figure 8D**).

LNGFR-expression in endomyocardial biopsies

In order to define ΔLNGFR as a suitable marker gene in human myocardium we stained endomyocardial biopsies immunohistochemically with anti-human NGF receptor antibody. Physiologically, human cardiomyocytes (positive for troponin I) were negative for LNGFR. Only intramyocardial nerve strands showed positive staining for LNGFR **(Figure 9)**.

Figure 8. Maintenance of ΔLNGFR expression in CD66b+ cells derived from CD34+ HPC and Mutz2 cells.

Microphotographs of cells derived from transfected CD34+ HPC (**a–d**) and Mutz2 cells (**e–h**) 4 days after nucleofection. Cells were viewed under normal light filter (**a, e**); FITC-filter (CD66b, green) (**b, f**); and PE-filter (ΔLNGFR, red) (**c, g**); Colocalization of CD66b and ΔLNGFR (orange) on the same cell shows that transfected cells stay positive for the marker gene ΔLNGFR in CD66b+ cells derived from CD34+ HPC or Mutz2, respectively (**d, h**). (Bar = 10 μm) **(A)**. Representative fluorescence activated cell sorting (FACS) analysis of ΔLNGFR- and mock-transfected CD66b+ cells derived from CD34+ HPC or Mutz2 cells on day 4 after transfection: 50% (11% out of 22% total CD66b+) of CD66b+ cells derived from CD34+ HPC and 56% (9% out of 16% total CD66b+) of CD66b+ cells derived from Mutz2 cells maintained ΔLNGFR expression **(B)**. Expression of the marker gene ΔLNGFR on CD66b+ cells derived from CD34+ HPC determined by FACS analysis (n = 3). The percentage of ΔLNGFR-expressing cells of the CD66+ cells derived from CD34+ HPC showed a maximum at day 4 post transfection **(C)**. ΔLNGFR expression on CD66b+ cells derived from Mutz2 cells as determined by FACS analysis (n = 3). The maximum was observed at day 1 post transfection **(D)**. HPC: Hematopoietic progenitor cells; LNGFR: Low-affinity nerve growth factor receptor.

Discussion

CD34+ HPC are commonly used in clinical settings for allogeneic and autologous transplantation and are targets for gene therapy studies [35,36]. HPC may also contribute to the regeneration of damaged tissue in other organs [5–8], especially in the heart [16–18]. However, homing of HPC to nonhematopoietic tissues and the potential of HPC to transdifferentiate into various organ cells is still a very controversial issue [6,13,14]. Genetic labeling of human HPC and their consecutive fate-mapping is an approach to *in vivo*-monitoring of stem cells. Attempts at such labeling have been reported as early as 1964. However, two major obstacles must still be overcome. First, toxicity of genetic labeling [20,21,22] and second, dilution and loss of the genetic marker.

It is important to note that genetic labeling of stem cells for *in vivo* use is accompanied by the risk of certain side effects, the most important being the induction of transformation and undesirable immune reactions [20–22]. In contrast to

viral vectors, transient transfection by nucleofection, as reported in this study, reduces the risk of side effects caused by stable genomic integration. In addition, nucleofection is a highly efficient method for transient transfection of HPC with, for example, ΔLNGFR [29] or of embryonic stem cells with EGFP [30]. ΔLNGFR, the truncated, nonfunctional form of the LNGFR, is currently the only marker gene which is easily detectable by immunohistochemistry and FACS analysis and can be applied in humans without toxic side effects [31].
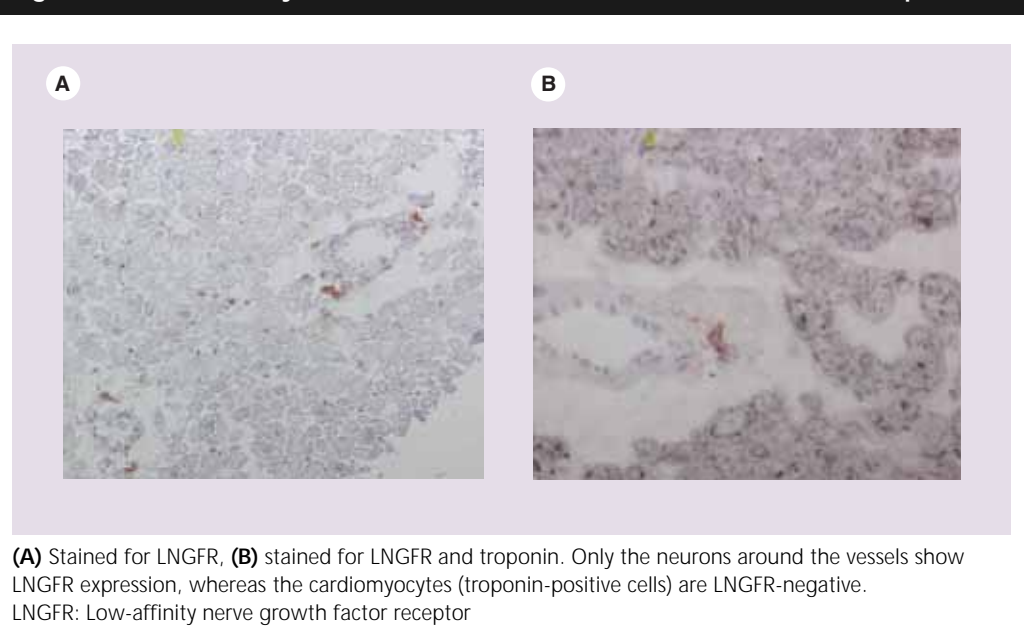
In the current study, we have investigated the toxicity and efficiency of ΔLNGFR nucleofection of CD34+ HPC during hematopoietic cell differentiation. Colony-forming assays were performed in order to analyze whether ΔLNGFR nucleofection influences lineage-specific cell differentiation. Despite the fact that the total number of colonies was decreased when comparing nontransfected with transfected cells, there was no statistically significant difference between ΔLNGFR- and mock-transfected cells. This indicates that although nucleofection itself influences the potential for proliferation and differentiation, the marker gene ΔLNGFR does not. The observation that ΔLNGFR labeling does not qualitatively interfere with hematopoietic cell differentiation would infer that transdifferentiation of CD34+ HPC into organ cells, if present, would not be substantially influenced by ΔLNGFR transfection.

A second major observation in our study is the fact that mature blood cells derived from ΔLNGFR-transfected CD34+ HPC obviously maintain ΔLNGFR expression at a higher percentage than proliferating cell cultures. Blood cells derived from transfected CD34+ HPC-expressing CD66b+, a cell-surface marker for granulocytes, displayed a high coexpression of ΔLNGFR with a maximum of 70 ± 2% at day 4 after transfection. This demonstrates a remarkable maintenance rate of ΔLNGFR-expression in differentiated cells. Even 10 days after transient transfection, a high percentage of CD66b+ cells maintained expression of the marker gene ΔLNGFR. Therefore, cell maturation obviously reduces the extinction of this transient marker gene in contrast to proliferating cells. Taken together, the observations that: although nucleofection reduces the number of colonies, transient ΔLNGFR labeling allows substantial lineage-specific cell differentiation and; that mature blood cells derived from ΔLNGFR transfected CD34+ HPC obviously maintain ΔLNGFR expression, both suggest that ΔLNGFR nucleofection may be an adequate method to study homing, differentiation and potentially also transdifferentiation of human HPC *in vivo*.

Due to the difficulties in obtaining sufficient quantities of human CD34+ HPC for *in vitro* experiments, appropriate cell lines are desirable tools to establish and optimize transfection conditions and differentiation protocols. In earlier studies, the differentiation of myeloid leukemia cell lines has been induced by cytokines or various therapeutic agents [37–39].

Figure 9. Sections of myocardial tissue, stained for LNGFR or LNGFR and troponin.

(A) Stained for LNGFR, **(B)** stained for LNGFR and troponin. Only the neurons around the vessels show LNGFR expression, whereas the cardiomyocytes (troponin-positive cells) are LNGFR-negative.
LNGFR: Low-affinity nerve growth factor receptor

We aimed to characterize a cell line that might be useful as an *in vitro* model for CD34⁺ HPC. Mutz2 cells showed the highest transfection efficiency (55% ± 4.9) of the leukemia cell lines tested in this study. Similar to the observations made with CD34⁺ HPC [29], the percentage of ΔLNGFR-positive Mutz2 cells decreased with time, confirming the transient character of nucleofection. Furthermore, Mutz2 cells were also found to have the potential to differentiate into all hematopoietic lineages, except erythrocytes. Importantly, no significant differences were found in colony-forming cells for ΔLNGFR-transfected compared with mock-transfected Mutz2 cells. In analogy to HPC, Mutz2 leukemia cells maintained expression of the marker gene ΔLNGFR with a maximum of 58 ± 2% after differentiation into CD66b⁺ cells.

Conclusion

In conclusion, the leukemia cell line Mutz2 may be an appropriate model of CD34⁺ HPC for transfection and myeloid cell differentiation experiments. Furthermore, nucleofection of human CD34⁺ HPC with ΔLNGFR does not affect their ability to differentiate into all hematopoietic cell lines, and differentiated CD66b⁺ myeloid cells maintain expression of the transient marker gene up to 10 days post transfection. Although the time-frame is relatively short, ΔLNGFR nucleofection could be an appropriate method for labeling HPC for *in vivo* studies investigating homing and (possibly) transdifferentiation of CD34⁺ HPC in the human heart, for example in dilated cardiomyopathy, where myocardial biopsies are routinely performed [40,41].

Future perspective

The methodology described herein may be applied in animal studies; for example, in non-obese diabetic severe combined immunodeficient (SCID) mice, in order to study the fate of human HPC and to study potential side effects. However, it is also ready for *in vivo* application in humans; that is, it has been accepted by the ethical committees of Germany. To our knowledge, this is the first description of a genetic labeling technique for human adult stem cells that is ready for autologous *in vivo* application. It may thus be widely useful for homing and, possibly, transdifferentiation studies in humans.

Executive summary

- Nucleofection was efficient and did not significantly reduce hematopoietic cell differentiation.

- Mature myeloid cells (CD66b⁺) derived from human CD34⁺ hematopoietic progenitor cell (HPC) and Mutz2 cells maintained expression of the truncated low-affinity nerve growth factor receptor (ΔLNGFR) at a high percentage.

- Mutz2 cells may serve as an *in vitro* model for human myeloid HPC.

- The method described herein has been adopted to Good Manufacturing Practices (GMP) guidelines and is ready for *in vivo* application.

Bibliography

1. de Lima M, Anagnostopoulos A, Munsell M *et al.*: Nonablative versus reduced-intensity conditioning regimens in the treatment of acute myeloid leukemia and high-risk myelodysplastic syndrome: dose is relevant for long-term disease control after allogeneic hematopoietic stem cell transplantation. *Blood* 104, 865–872 (2004).

2. Kolb HJ, Simoes B, Schmid C: Cellular immunotherapy after allogeneic stem cell transplantation in hematologic malignancies. *Curr. Opin. Oncol.* 16, 167–173 (2004).

3. Maloney DG, Molina AJ, Sahebi F *et al.*: Allografting with nonmyeloablative conditioning following cytoreductive autografts for the treatment of patients with multiple myeloma. *Blood* 102, 3447–3454 (2003).

4. Appelbaum FR, Rowe JM, Radich J, Dick JE: Acute myeloid leukemia. *Hematology*. (Am. Soc. Hematol. Educ. Program) 1, 62–86 (2001).

5. Lagasse E, Connors H, Al-Dhalimy M *et al.*: Purified hematopoietic stem cells can differentiate into hepatocytes *in vivo*. *Nat. Med.* 6, 1229–1234 (2000).

6. Orlic D, Kajstura J, Chimenti S *et al.*: Bone marrow cells regenerate infarcted myocardium. *Nature* 410, 701–705 (2001).

7. Toma C, Pittenger MF, Cahill KS, Byrne BJ, Kessler PD: Human mesenchymal stem cells differentiate to a cardiomyocyte phenotype in the adult murine heart. *Circulation* 105, 93–98 (2002).

8. Jiang Y, Vaessen B, Lenvik T, Blackstad M, Reyes M, Verfaillie CM: Multipotent progenitor cells can be isolated from postnatal murine bone marrow, muscle, and brain. *Exp. Hematol.* 30, 896–904 (2002).

9. Korbling M, Katz RL, Khanna A *et al.*: Hepatocytes and epithelial cells of donor origin in recipients of peripheral-blood stem cells. *N. Engl. J. Med.* 346, 738–746 (2002).

10. Muller P, Pfeiffer P, Koglin J *et al.*: Cardiomyocytes of non-cardiac origin in myocardial biopsies of human transplanted hearts. *Circulation* 106, 31–35 (2002).

11. Graf T: Differentiation plasticity of hematopoietic stem cells. *Blood* 99, 3089–3101 (2002).

12. Goodell MA, Jackson KA, Majka SM *et al.*: Stem cell plasticity in muscle and bone marrow. *Ann. NY Acad. Sci.* 938, 208–218; discussion 218–220 (2001).

13. Murry CE, Soonpaa MH, Reinecke H *et al.*: Haematopoietic stem cells do not transdifferentiate into cardiac myocytes in myocardial infarcts. *Nature* 428, 664–668 (2004).

14. Balsam LB, Wagers AJ, Christensen JL, Kofidis T, Weissman IL, Robbins RC: Haematopoietic stem cells adopt mature haematopoietic fates in ischaemic myocardium. *Nature* 428, 668–673 (2004).

15. Terada N, Hamazaki T, Oka M *et al.*: Bone marrow cells adopt the phenotype of other cells by spontaneous cell fusion. *Nature* 416, 542–545 (2002).

16. Strauer BE, Brehm M, Zeus T *et al.*: Repair of infarcted myocardium by autologous intracoronary mononuclear bone marrow cell transplantation in humans. *Circulation* 106, 1913–1918 (2002).

17. Assmus B, Schachinger V, Teupe C *et al.*: Transplantation of progenitor cells and regeneration enhancement in acute myocardial infarction (TOPCARE-AMI). *Circulation* 106, 53–61 (2002).

18. Wollert KC, Meyer GP, Lotz J *et al.*: Intracoronary autologous bone-marrow cell transfer after myocardial infarction: the BOOST randomised controlled clinical trial. *Lancet* 364, 141–148 (2004).

19. Wiehe JM, Zimmermann O, Greiner J *et al.*: Labeling of adult stem cells for *in vivo* application in the human heart. *Histol. Histopathol.* 20, 901–906 (2005).

20. Li Z, Dullmann J, Schiedlmeier B *et al.*: Murine leukemia induced by retroviral gene marking. *Science* 296, 497 (2002).

21. Hacein-Bey-Abina S, von Kalle C, Schmidt M *et al.*: A serious adverse event after successful gene therapy for X-linked severe combined immunodeficiency. *N. Engl. J. Med.* 348, 255–256 (2003).

22. Baum C, Dullmann J, Li Z *et al.*: Side effects of retroviral gene transfer into hematopoietic stem cells. *Blood* 101, 2099–2114 (2003).

23. Li LH, McCarthy P, Hui SW: High-efficiency electrotransfection of human primary hematopoietic stem cells. *FASEB* 15, 586–588 (2001).

24. Weissinger F, Reimer P, Waessa T *et al.*: Gene transfer in purified human hematopoietic peripheral-blood stem cells by means of electroporation without prestimulation. *J. Lab. Clin. Med.* 141, 138–149 (2003).

25. Wu MH, Smith SL, Danet GH *et al.*: Optimization of culture conditions to enhance transfection of human CD34+ cells by electroporation. *Bone Marrow Transplant* 27, 1201–1209 (2001).

26. Wu MH, Liebowitz DN, Smith SL, Williams SF, Dolan ME: Efficient expression of foreign genes in human CD34(+) hematopoietic precursor cells using electroporation. *Gene Ther.* 8, 384–390 (2001).

27. Van Tendeloo VF, Snoeck HW, Lardon F *et al.*: Nonviral transfection of distinct types of human dendritic cells: high-efficiency gene transfer by electroporation into hematopoietic progenitor- but not monocyte-derived dendritic cells. *Gene Ther.* 5, 700–707 (1998).

28. Lundqvist A, Noffz G, Pavlenko M *et al.*: Nonviral and viral gene transfer into different subsets of human dendritic cells yield comparable efficiency of transfection. *J. Immunother.* 25, 445–454 (2002).

29. Greiner J, Wiehe J, Wiesneth M *et al.*: Efficient transient genetic labeling of human CD34+ hematopoietic stem cells. *Transfus. Med. Hemother.* 31, 136–141 (2004).

30. Lakshmipathy U, Pelacho B, Sudo K *et al.*: Efficient transfection of embryonic and adult stem cells. *Stem Cells* 22, 531–543 (2004).

31. Bonini C, Grez M, Traversari C *et al.*: Safety of retroviral gene marking with a truncated NGF receptor. *Nat. Med.* 9, 367–369 (2003).

32. Wiesneth M, Schreiner T, Friedrich W *et al.*: Mobilization and collection of allogeneic peripheral blood progenitor cells for transplantation. *Bone Marrow Transplant* 21, 21–24 (1998).

33. Eades-Perner AM, Thompson J, van der Putten H, Zimmermann W: Mice transgenic for the human CGM6 gene express its product, the granulocyte marker CD66b, exclusively in granulocytes. *Blood* 91, 663–672 (1998).

34. Jennings CD, Foon KA: Flow cytometry: recent advances in diagnosis and monitoring of leukemia. *Cancer Invest.* 15, 384–399 (1997).

35. Mayhall EA, Paffett-Lugassy N, Zon LI: The clinical potential of stem cells. *Curr. Opin. Cell Biol.* 16, 713–720 (2004).

36. Larochelle A, Dunbar CE: Genetic manipulation of hematopoietic stem cells. *Semin. Hematol.* 41, 257–271 (2004).

37. Glasow A, Prodromou N, Xu K, von Lindern M, Zelent A: Retinoids and myelomonocytic growth factors cooperatively activate RARA and induce human myeloid leukemia cell differentiation via MAP kinase pathways. *Blood* 105, 341–349 (2005).

38. Johnson BS, Mueller L, Si J, Collins SJ: The cytokines IL-3 and GM-CSF regulate the transcriptional activity of retinoic acid receptors in different *in vitro* models of myeloid differentiation. *Blood* 99, 746–753 (2002).

39. Moldenhauer A, Nociari M, Lam G, Salama A, Rafii S, Moore MA: Tumor necrosis factor alpha-stimulated endothelium: an inducer of dendritic cell development from hematopoietic progenitors and myeloid leukemic cells. *Stem Cells* 22, 144–157 (2004).

40. Zimmermann O, Grebe O, Merkle N *et al.*: Myocardial biopsy findings and gadolinium-enhanced cardiovascular magnetic resonance in dilated cardiomyopathy. *Eur. J. Heart Fail.* 8(2), 162–166 (2005) (Epub ahead of print).

41. Zimmermann O, Kochs M, Zwaka TP *et al.*: Myocardial biopsy based classification and treatment in patients with dilated cardiomyopathy. *Int. J. Cardiol.* 104, 92–100 (2005).

Efficient transfection and sustained long term functionality of primary human hepatocytes

Lonza

Nicole Kukli[1], Stephan Schuell[1], Nazim El-Andaloussi[1], Maureen Bunger[2], Andrea Toell[1], Jenny Schroeder[1], Magdalene Stosik[1]
[1]Lonza Cologne GmbH, Cologne, Germany; [2]Lonza Walkersville, Inc., Walkersville, MD, USA

Purpose

Primary Human Hepatocytes (PHH) are the state-of-the art in vitro human liver model system in the field of toxicology. PHH are known to be difficult to transfect with classical transfection methods. Furthermore, PHH tend to lose their typical liver functions rapidly in culture. In this study, we optimized the thawing, transfection and culture procedure for cryopreserved PHH. Transfection efficiency and hepatocyte functionality were analyzed over 7 days.

Methods

Lonza's cryopreserved plateable human hepatocytes were transfected using the 4D Nucleofector® System. Prior transfection, cryopreserved PHH were gently thawed and resuspended in P3 Nucleofector® Solution. Following transfection using program EX-147 or DS-150, PHH were plated on collagen-coated cell culture vessels in Matrigel™ (Corning) sandwich culture. We characterized specific hepatocyte functions of the resulting transfected sandwich cultures for up to 7 days. Transfection efficiency of both pmaxGFP™ Plasmid DNA and Cleancap® mCherry RNA (TriLink) was assessed by fluorescence microscopy. PHH were analyzed for cell viability, bile canaliculi formation, albumin secretion and CYP3A4, CYP1A2 and CYP2B6 metabolite formation. Experimental details can be found in the figure legends below.

A) 4D-Nucleofector® Device

B) Transfection Process

Step 1 — Harvest cells of interest.
Step 2 — Mix and combine. Nucleofector® Solution with supplement. Cells. DNA or siRNA. Transfer to a Lonza certified cuvette.
Step 3 — Select Nucleofector® Program. Insert cuvette. Press » Start «.
Step 4 — Rinse cuvette with culture medium.
Step 5 — Transfer to culture dish. Expression can be detected as soon as 3 – 8 hours post Nucleofector® Experiment.
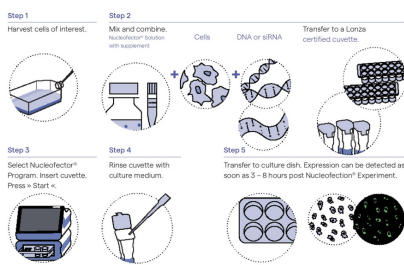
Figure 1: 4D Nucleofector® Device for efficient transfection of difficult to transfect primary cells and cell lines

Conclusion

We present reliable protocols for efficient DNA and mRNA expression in cryopreserved PHH. We demonstrate highly preserved functionality of transfected hepatocytes for 7 days when using program DS-150. Our protocols enable transfection of human hepatocytes for generation of more sophisticated long-term in vitro liver models.

Results
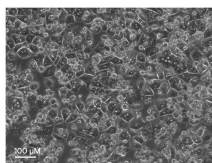
A) GFP-Fluorescence
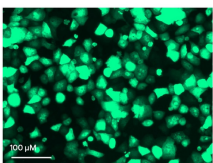
B) Bright-Field

Figure 2: High GFP expression 24 hours after transfection with the high efficiency program EX-147
24 hours after plating, GFP fluorescence and cell morphology was observed and documented by (A) fluorescence and (B) bright field microscopy. (Zeiss AxioObserver Z.1 microscope).
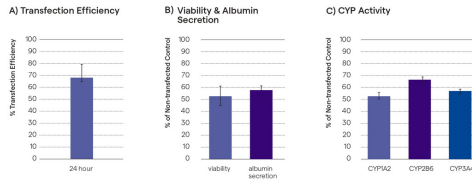

A) Transfection Efficiency **B) Viability & Albumin Secretion** **C) CYP Activity**

Figure 3: High GFP expression 24 hours after transfection with the high efficiency program EX-147
5x10^{6} cells were transfected with program EX-147 using 5 µg pmaxGFP™ Vector in 100 µL Nucleocuvette® Vessel. Cells were plated in collagen/Matrigel™ sandwich culture in 24-well plate. (A) For calculation of transfection efficiency, fluorescent cells were counted manually 24 hours post transfection. Data from 5 independent experiments with 4 different donors are shown, n=17. Error bars indicate standard deviation. (B) Viability was assessed with the CellTiter-Blue® Cell Viability Assay (Promega) 24 hours post transfection. Data of five independent experiments with five different donors is shown, n = 22. Albumin content in the supernatant was quantified with the Human Albumin ELISA Kit (Bethyl). Data from one representative donor HUM4235 are shown, n=3. The respective non-transfected sample was set to 100% for normalization. Error bars indicate standard deviation. (C) For measurement of CYP3A4 activity 24 hours post transfection cells were incubated with 200 µM testosterone for 15 minutes and the formation of 6ß-hydroxytestosterone was evaluated. For measurement of CYP2B6 activity PHH were incubated with 250 µM bupropion for 15 minutes and the formation of OH-bupropion was evaluated. For measurement of CYP1A2 activity PHH were incubated with 100 µM phenacetin for 15 minutes and the formation of acetaminophen was evaluated. All culture supernatants were analyzed by LC/MS/MS. The respective non-transfected sample was set to 100% for normalization. Results of one typical lot (HUM4253) are shown, n = 3. Error bars indicate standard deviation.

> With program EX-147, high DNA transfection efficiencies of 68% were observed. Albumin secretion and Cytochrome p450 activity were clearly detectable 24 hours post transfection, but partially not sustained for a longer period of time (data not shown). Therefore, we recommend program EX-147 for highly efficient short term DNA transfection.

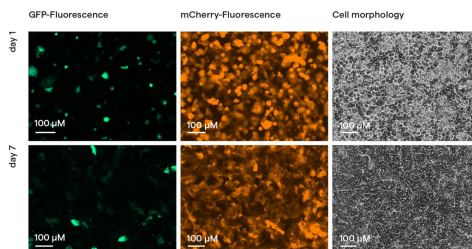**GFP-Fluorescence** **mCherry-Fluorescence** **Cell morphology**

day 1
day 7

Figure 4: Sustained plasmid DNA and efficient mRNA expression for 7 days in primary human hepatocytes maintaining typical healthy hepatocyte morphology after transfection with program DS-150
Primary human hepatocytes (lot HUM4235) were transfected with program DS-150 using 5 µg pmaxGFP™ Vector or 5 µg Cleancap® mCherry RNA (TriLink) in 100 µL Nucleocuvette® Vessel 4D-Nucleofector® Device. Cells were plated in collagen/Matrigel™ Sandwich culture in 24-well plate. On day 1 and 7 after transfection, transfection efficiency and cell morphology was observed and documented by fluorescence- and bright field microscopy.

A) pmaxGFP Transfection Efficiency **B) mCherry Transfection Efficiency**
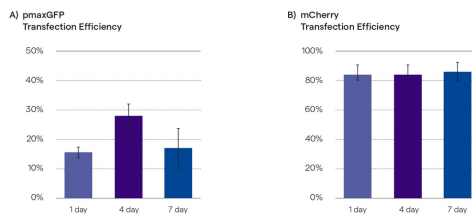

Figure 5: Sustained GFP and mCherry expression for at least 7 days after transfection with program DS-150
Primary human hepatocytes (lot HUM4235) were transfected with program DS-150 using (A) 5 µg pmaxGFP™ Vector or (B) 5 µg Cleancap® mCherry RNA (TriLink) in 100 µL Nucleocuvette® Vessel 4D-Nucleofector® Device. Cells were plated in collagen/Matrigel™ Sandwich culture in 24-well plates. For calculation of transfection efficiency, fluorescent cells were counted manually on day 1, 4 and 7 after plating.

A) Viability **B) Albumin Secretion**

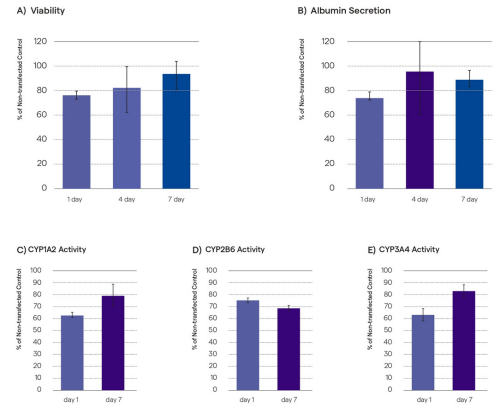**C) CYP1A2 Activity** **D) CYP2B6 Activity** **E) CYP3A4 Activity**

Figure 6: Preserved viability and typical hepatocyte functionality of the cells for at least 7 days after transfection with program DS-150
Primary human hepatocytes were transfected with program DS-150 using 5 µg pmaxGFP™ Vector in 100 µL Nucleocuvette® Vessel 4D-Nucleofector® Device. Cells were plated in collagen/Matrigel™ Sandwich culture in 24-well plates. (A) Viability was assessed with the CellTiter-Blue® Cell Viability Assay (Promega). (B) Albumin content in the supernatant was quantified with the Human Albumin ELISA Kit (Bethyl). (C) For measurement of CYP3A4 activity 24 h post transfection cells were incubated with 200 µM testosterone for 15 minutes and the formation of 6ß-hydroxytestosterone was evaluated. (D) For measurement of CYP2B6 activity PHH were incubated with 250 µM bupropion for 15 minutes and the formation of OH-bupropion was evaluated. (E) For measurement of CYP1A2 activity PHH were incubated with 100 µM phenacetin for 15 minutes and the formation of acetaminophen was evaluated. All culture supernatants were analyzed by LC/MS/MS. The respective non-transfected sample was set to 100% for normalization. For viability and albumin content, data of two donors (lot HUM4235 and HUM4108) are shown, n=6. For Cyp Acticity, data of one typical donor (lot HUM4235) is shown, n=3.
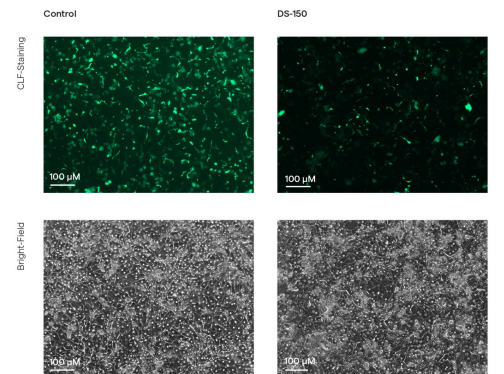
Control **DS-150**
CLF-Staining
Bright-Field

Figure 7: Branched bile canaliculi network in both transfected and non-transfected hepatocytes on day 4
Primary human hepatocytes (lot HUM4235) were transfected with program DS-150 using 5 µg Cleancap® mCherry RNA (TriLink) in 100 µL Nucleocuvette® Vessel 4D-Nucleofector® Device. Cells were plated in collagen/Matrigel™ Sandwich culture in 24-well plate. Culture medium was changed daily. On day 4, Cholyl-lysyl-fluorescein (CLF) staining (Corning) was used for visualization of bile canaliculi formation. Cells were incubated for 1 hour in medium containing 4 µM CLF followed by three washing steps with culture medium prior to examination by fluorescence microscopy. Typical results are shown.

> To address the needs of long-term culture of transfected hepatocytes, conditions preserving cell functionality over time were identified. Following transfection with program DS-150, efficiencies of up to 20% for DNA and up to 85% for mRNA were achieved and sustained for 7 days. Viability and albumin secretion at 24h after transfection were slightly reduced, but recovering over time. In comparison to control cultures, CYP1A2, CYP2B6 and CYP3A4 activity was between 60% and 80%. Transfected PHH formed complex, branched bile canaliculi network. We recommend program DS-150 for efficient transfection of siRNA and mRNA as well as intermediate levels of DNA transfection for long-term culture after transfection.

CRISPR-mediated modification of DNA methylation pattern in the new era of cancer therapy

Faezeh Maroufi[1] [ID], Amirhosein Maali[2,3] [ID], Meghdad Abdollahpour-Alitappeh[4] [ID], Mohammad Hossein Ahmadi[1] [ID] & Mehdi Azad*,[1] [ID]

[1]Department of Medical Laboratory Sciences, Faculty of Allied Medicine, Qazvin University of Medical Sciences, Qazvin, Iran
[2]Student Research Committee, Pasteur institute of Iran, Tehran, Iran
[3]Department of Medical Biotechnology, Faculty of Allied Medicine, Qazvin University of Medical Sciences, Qazvin, Iran
[4]Cellular & Molecular Biology Research Center, Larestan University of Medical Sciences, Larestan, Iran
*Author for correspondence: Tel.: +982 833 359 501; haematologicca@gmail.com

In the last 2 decades, a wide variety of studies have been conducted on epigenetics and its role in various cancers. A major mechanism of epigenetic regulation is DNA methylation, including aberrant DNA methylation variations such as hypermethylation and hypomethylation in the promoters of critical genes, which are commonly detected in tumors and mark the early stages of cancer development. Therefore, epigenetic therapy has been of special importance in the last decade for cancer treatment. In epigenetic therapy, all efforts are made to modulate gene expression to the normal status. Importantly, recent studies have shown that epigenetic therapy is focusing on the new gene editing technology, CRISPR-Cas9. This tool was found to be able to effectively modulate gene expression and alter almost any sequence in the genome of cells, resulting in events such as a change in acetylation, methylation, or histone modifications. Of note, the CRISPR-Cas9 system can be used for the treatment of cancers caused by epigenetic alterations. The CRISPR-Cas9 system has greater advantages than other available methods, including potent activity, easy design and high velocity as well as the ability to target any DNA or RNA site. In this review, we described epigenetic modulators, which can be used in the CRISPR-Cas9 system, as well as their functions in gene expression alterations that lead to cancer initiation and progression. In addition, we surveyed various species of CRISPR-dead Cas9 (dCas9) systems, a mutant version of Cas9 with no endonuclease activity. Such systems are applicable in epigenetic therapy for gene expression modulation through chemical group editing on nucleosomes and chromatin remodeling, which finally return the cell to the normal status and prevent cancer progression.

Cancer is one of the most common diseases around the world, causing a huge psychological and economic burden for society and many deaths worldwide [1]. Cancers are developed with both genetic and epigenetic abnormalities. More importantly, epigenetic abnormalities are even more frequent in most human cancers. Heritable modifications in gene expression caused by epigenetic factors can lead to suppression or activation of particular genes without directly altering DNA sequences [2]. Epigenetic profiles change in different steps of tumor development and progression. DNA methylation, as one of the major mechanisms of epigenetic regulation, not only can control gene expression but also plays a well-established role in the pathogenesis of many cancers [3]. DNA methylation occurs primarily on cytosine residues near the gene promoters with a higher concentration of CpG sites, known as CpG islands, via DNA methyltransferase (DNMT). Subsequently, chromatins are remodeled and gene transcription is inhibited through complexes such as histone deacetylase (HDAC), and some proteins such as heterochromatin protein 1. However, such alterations are reversible and return to the normal state through other enzymes such as ten-eleven translocation methylcytosine dioxygenase (TET).

Future Medicine

DNA methylation EpiEffectors

EpiEffectors are a huge collection of proteins that control epigenome structure and function. EpiEffectors consist of enzymes that are able to form covalent modifications (writers) including the addition of acetyl or methyl groups to particular amino acid residues or bases on the nucleosome; proteins that identify the added groups for the recognition and remodeling of specific genomic regions to modulate gene expression (readers); and enzymes that are capable of removing active and repressive marks (erasers), leading to the reversibility of such changes [4]. Table 1 indicates the main EpiEffectors and their functions used as targets in epigenetic therapy or in the CRISPR-Cas9 system.

The role of DNA methylation in cancer development

Aberrant DNA methylation is commonly found in tumors and marks the early stages of cancer development. Hypermethylation of CpG islands in gene promoters prevents transcriptional activation through blocking the access of transcriptional machineries to the gene promoter, finally leading to gene silencing. Promoter hypermethylation not only alters gene expression but also can change cell functions, cycle, signaling, adhering and proliferation, as well as DNA repair, apoptosis, angiogenesis, tumor invasion, protooncogene activation and downregulation of tumor suppressor genes. In the following, we mention some of the genes whose downregulation occurs commonly in cancers, including *p16INK4a*, *p15INK4b*, *Rb*, *p14ARF* (which are related to the cell cycle), *MGMT*, *BRCA1* [24], *hMLH1* (which play a role in DNA repair), *DAPK* (which contributes to apoptosis), *RARB2* (as a cell signaling gene), *ER* (which contribute to hormonal responses), *RASSF1A* (in Ras signaling), microRNAs, etc. [25]. Hypermethylation of CpG islands has the potential to turn off various tumor suppressor genes [26], allows cells to escape the normal checkpoints of cell division and promotes tumor growth, leading to tumorigenesis [27]. On the other hand, chromosomal instability, loss of genomic imprinting and reactivation of transposable elements are developed by gene promoter hypomethylation, which results in gene overexpression and cancer development (Figure 1). For example, hypomethylation was reported in the *BCL2* gene in lymphocytic lymphoma [28] and the *RRAS* gene in gastric carcinoma [29]. In addition, a wide variety of tumors frequently show mutations in genes encoding EpiEffectors. Abnormal DNA methylation (hypermethylation or hypomethylation) can stem from mutations in EpiEffectors or some other driving factors. Numerous studies demonstrated the critical role of mutations in the *DNMT* family, especially *DNMT3A*, in tumors, which leads to malignant transformation. Mutations in *DNMT3A* were reported in 23–36% of the acute myeloid leukemia (AML) patients with poor prognosis [30] and myelodysplastic syndromes [31]. Importantly, healthy individuals with *DNMT3A* mutations have a predisposition to development of malignant hematological disorders including AML [32]. Mutations in *DNMT1* were also observed in colorectal cancers and AML [33,34]. Most studies on *TET2*-mutant cancers revealed that TET loss-of-function is frequently observed in different types of cancers, including both solid tumors and blood malignancies such as T cell lymphomas [34]. Mutations occurring in epigenetic regulatory enzymes are either loss-of-function or gain-of-function. There is evidence demonstrating *EZH2* gain-of-function mutations in follicular lymphoma [35] and *IDH1/2* mutations in some patients with AML [36] and various solid tumors such as gliomas, prostate cancer and cholangiocarcinoma [37,38]. Mutations in HDAC-encoding genes were found to be related to cancer progression. There are studies indicating the role of frame-shift mutation-based dysfunction of HDAC2 expression in colorectal cancer and human epithelial cancers [39]. The prevalence of somatic mutations in HAT is more frequently observed in lymphomas, lung cancer and urothelial carcinoma [40]. A meta-analysis conducted in a variety of sequencing studies pointed that the SWI/SNF mutation occurs in about 20% of the human malignancies [41]. More recently, a variety of cancer types, such as ovarian, endometrial and colorectal cancers, have showed mutations in *ARID1A* [42]. Mutation or inhibition of *AID/APOBEC* was observed in many cancers [43]. All of these mutations promote metastasis and lead to poor prognosis in patients with such cancers. Therefore, epigenetic modulators play highly important roles in gene expression and cellular processes, whose dysfunctions lead to cancer development.

There are a wide variety of emerging strategies for the treatment and diagnosis of cancer [44], showing a great improvement to introduce novel therapeutic ways and tools [45,46]. In epigenetic therapy, all efforts are made to modulate gene expression to the normal status through several ways, for example, hypomethylating agents such as DNMT inhibitors or HDAC inhibitors. Of great note, CRISPR is a novel way to modulate gene expression. The CRISPR-Cas9 system is a site-specific genome editing tool that could be used to specifically target genes in eukaryotic cells [47]. In the following, we discuss CRISPR as a novel tool for cancer treatment, particularly its ability to edit gene expression.

Table 1. DNA methylation EpiEffectors and their functions.

EpiEffectors	Subtypes	Functions	Ref.
DNA methyl transferase (DNMT)	DNMT1 DNMT3A DNMT3B	DNMT1 is responsible for both *de novo* methylation and methylation maintenance DNMT3A and DNMT3B are *de novo* DNA methyl transferases that are involved mainly in methylation of new CpG sites in the DNA and have a critical role in genome regulation and development. The Arg836 residue from DNMT3A target recognition domain encounters with CpG, guaranteeing DNMT3A enzymatic function toward CpG sites in cells	[5]
SWItch/sucrose nonfermentable (SWI/SNF[BAF])	ARID1A ARID1B ARID2	The ATP-dependent nucleosome remodeling complex is bound extensively across the genome at promoters and enhancers; such complexes can serve as tumor suppressors, leading to both activation or repression of gene expression	[6]
Heterochromatin protein 1 (HP1)	HP1α HP1β HP1γ	HP1 is a transcriptional repressor that directly binds to the methylated histone H3 lysine 9 residue (H3K9me), a hallmark of histone modification for untranslatable heterochromatin. HP1 contains two conserved domains, including chromodomain at the N-terminus (directly bound to H3K9me) and chromo shadow domain at the C-terminus (cooperating in protein–protein interactions)	[7]
Methyl CpG-binding protein 2 (MeCP2)		MeCP2 is an important reader of DNA methylation. MeCP2 is an x-linked protein and has two functional domains, including a methyl-cytosine-binding domain that binds to the methylated CpG sites on the DNA strands and a transcriptional repression domain that interacts with SIN3A to apply HDAC	[8]
Insulator proteins	CTCF (CCCTC binding factor)	Insulator binding proteins (IBPs) regulate gene expression through binding to specific DNA sites and facilitate gene regulation specificity. A fundamental role of IBPs is to cover gene promoters from the activity of regulatory elements, leading to activation or silence of transcription. IBPs make target gene promoters inaccessible for the activating or silencing effects of adjacent regulatory elements CTCF produces chromatin loops between bound CTCF sites that separate the enhancer and promoter of a target gene, leading to the prevention of physical and regulatory contact between chromosomal regions present within the loop with those present outside. Mammalian CTCF supports long-distance regulation by approximating regulatory elements and promoters, and physically segregates loci to limit regulatory cross-talk.	[9,10]
Enhancer of zeste homolog 2 (EZH2)		EZH2 is a histone-lysine N-methyltransferase enzyme that plays a critical role in histone methylation and transcription repression. EZH2 facilitates the addition of methyl groups to histone H3 at lysine 27 by using a cofactor S-adenosyl-L methionine and functions as a gene suppressor. Methylation activity of EZH2 catalyzes heterochromatin formation, thereby silencing gene functions	[11]
Ten-eleven translocation methylcytosine dioxygenase (TET)	TET1 TET2 TET3	5mC is oxidized by the TET family of dioxygenases to generate 5-hydroxymethylcytosine (5hmC). TET enzymes produce 5-formylcytosine (5fC) and 5-carboxylcytosine (5caC) through hydroxylating 5hmC	[12]
Isocitrate dehydrogenase (IDH)	IDH1 IDH2	Isocitrate is metabolized to α-ketoglutarate (α-KG), either in the mitochondrion (by IDH2) or in the cytoplasm (by IDH1). The α-KG produced is used as a co-factor for α-KG-dependent dioxygenases, particularly for the TET family of DNA demethylases and the Jumonji (Jmj) family of histone demethylases. Gain of mutations in IDH1 or IDH2 results in decreased levels of α-KG, which leads to increased formation of D-2-hydroxyglutarate (2-HG). α-KG is an important co-factor needed for certain histones and DNA demethylases, while 2-HG functions as a competitive inhibitor of the DNA demethylases	[13]
Oxoguanine glycosylase 1 (OGG1)		Reactive oxygen species may attack guanine at the dinucleotide site, leading to the formation of 8-hydroxy-2′-deoxyguanosine (8-OHdG). This results in the formation of a 5mCp-8-OHdG dinucleotide site. The base excision repair enzyme OGG1 targets 8-OHdG. OGG1, present at the 5mCp-8-OHdG site, applies TET1, while TET1 oxidizes 5mC adjacent to 8-OHdG. This initiates demethylation of 5mC	[14]
Thymine DNA glycosylase (TDG)		TDG recognizes 5fC and 5caC. This leads to excision of the glycosidic bond, resulting in an apyrimidinic site in the oxidation pathway	[15]
Cytidine deaminase /Apolipoprotein B editing complex (AID/APOBEC)		5hmC can be deaminated by AID/APOBEC deaminases to form 5-hydroxymethyl uracil (5hmU) in an alternative oxidative deamination pathway. In addition, 5mC can be converted to thymine. TDG, methyl-CpG-binding protein 4 (MBD4), Nei-Like DNA Glycosylase 1 (NEIL1) and single-strand-selective monofunctional uracil-DNA glycosylase 1 (SMUG1) can potentially cleave 5hmU	[16,17]
Histone methylation erasers		Histone demethylases are able to remove methyl groups. Amino oxidase homolog lysine demethylase 1 (KDM1) and JmjC domain, which contain histone demethylases, are two categorized groups of histone methylation erasers	[18]
	KDM1A KDM1B	In the KDM1 family, also referred to as lysine-specific demethylase 1 (LSD1), KDM1A demethylates H3K9me1 and H3K9me2, leading to transcriptional activation. KDM1B specifically targets H3K4me1 and H3K4me2	[19]
	KDM2 KDM3 KDM4 KDM5 KDM6	JmjC KDMs contains a family of demethylases able to demethylate histones	[20]
Histone acetyltransferase (HAT/KAT)	Gcn5/PCAF (KAT2A/KAT2B) MYST (KAT5) p300/CBP (KAT3B/KAT3A) Rtt109 (KAT11)	The acetyl groups can be transferred from the acetyl-CoA cofactor to the Nζ nitrogen of a lysine side chain within histones by HAT/KAT. These enzymes participate in various transcription-mediated biological events, such as hormonal signaling, dosage compensation and cell-cycle progression.	[21]

| Table 1. DNA methylation EpiEffectors and their functions (cont.).			
EpiEffectors	**Subtypes**	**Functions**	**Ref.**
Bromodomain and extra-terminal (BET)	BRD2 BRD3 BRD4 BRDT	Proteins that are histone acetylation readers are enriched at promoter sites, particularly upstream of oncogenes, where they recruit other transcriptional factors capable of interacting with acetylated lysine residues on histone tails and an extra C-terminal domain, obtaining a functional link between acetylation-mediated protein–protein interactions and lysine acetylation in chromatin-mediated gene transcription	[22]
Histone deacetylase (HDAC)	HDAC1-11 sirtuins (SIRT1-7)	HDAC removes acetyl groups from lysine on the histone, allowing for histones to wrap DNA more tightly. Acetylation/deacetylation can regulate DNA expression	[23]
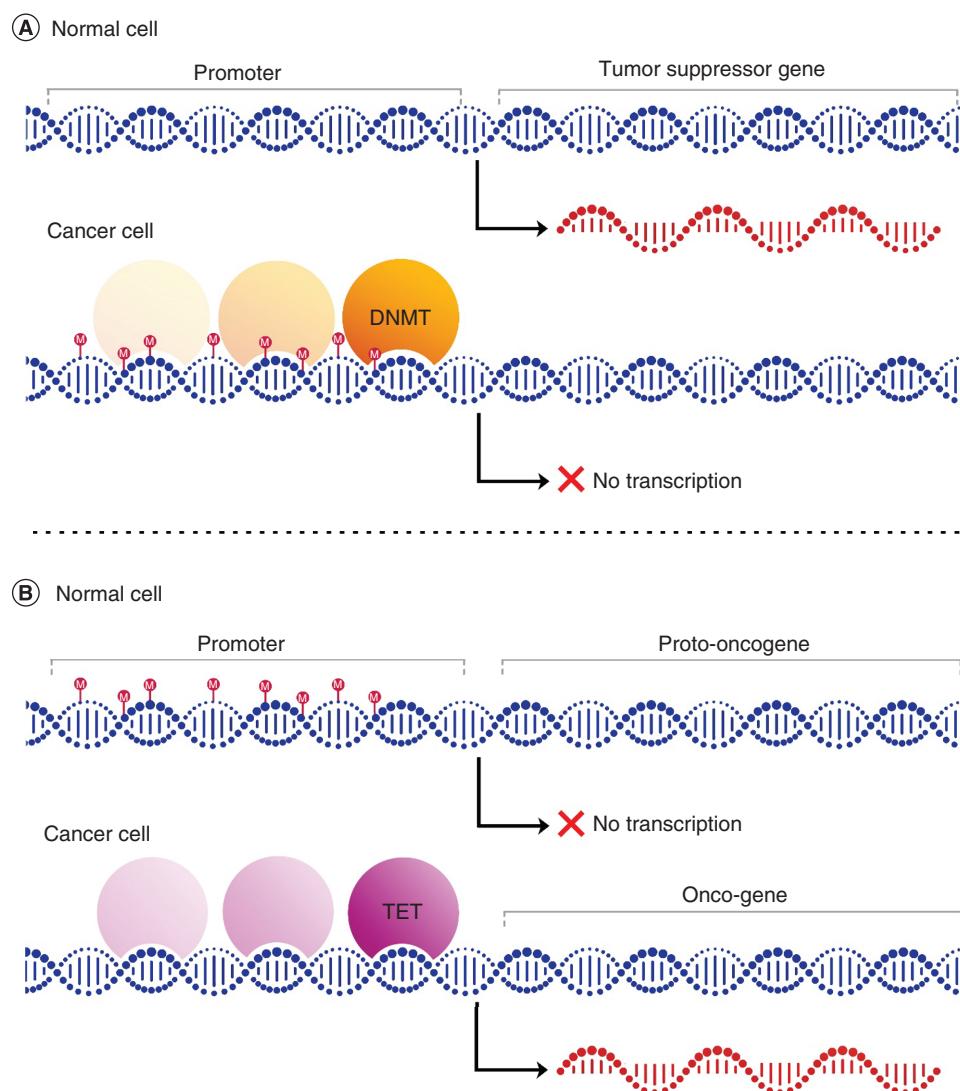
Figure 1.   The role of DNA methylation in cancer development. (A) Hypermethylation of the tumor suppressor gene promoter. Tumor suppressor genes are unmethylated in normal cells; when a promoter of a tumor suppressor gene is hypermethylated by DNMT, tumor suppressor gene transcription is inhibited and then turned off, allowing cells to escape the normal checkpoints of cell division, promoting tumor growth and finally leading to tumorgenesis. **(B)** Hypomethylation of proto-oncogene promoter. Oncogenes are methylated in normal cells as a suppressing regulatory mechanism. However, when proto-oncogene promoters are hypomethylated by the TET enzyme, the oncogenes are activated and overexpressed. This causes chromosomal instability, loss of genomic imprinting and tumorgenesis.

Workmanship & ingredients of the CRISPR-Cas9 system as a gene editing tool

Zinc finger nucleases, transcription activator-like effector nucleases, meganucleases and CRISPR-Cas9 systems are genome editing tools, functioning by targeting and altering almost any sequences in the genome of cultured cells or whole organisms. However, the CRISPR-Cas9 system overcomes the challenges associated with zinc finger nucleases and transcription activator-like effector nucleases due to its ease of design and use, more flexibility and higher efficiency [48]. CRISPR-based mechanisms are a natural adaptive immune system against bacteria-killing viruses found in bacteria to cleave viral genomes [49].

The CRISPR-Cas9 system consists of a Cas9 endonuclease that cleaves the target sequence in the genome, and a single guide RNA (sgRNA) that has two components including CRISPR RNA (crRNA) and a noncoding trans-activating crRNA as a homing device required for Cas9 cleavage [50]. crRNA, which contains approximately 20 base-pair sequences designed to complementarily bind to the target DNA site by Watson-Crick base-pairing, must be followed by a short DNA sequence (the protospacer-adjacent motif [PAM]) that is critical for compatibility with Cas9. sgRNA and Cas9 form a ribonucleoprotein complex guided to the target DNA site by sgRNA. Cas9 precisely cleaves DNA at approximately three nucleotides before PAM to produce double-strand breaks (DSBs). Cas9 has two catalytic sites, including RuvC and HNH capable of cleaving opposite DNA strands to generate DSBs [51]. Following the activation of Cas9 endonuclease, DSBs are repaired by cell machinery through one of two main mechanisms relying upon the existence of a repair template and the cell state, such as homology directed repair (HDR) and nonhomologous end joining (NHEJ) [52]. NHEJ, as an error-prone system, is commonly applied for the random insertions or deletions (indels) of nucleotides at the DSB site, and to induce particular gene knockout through the formation of frameshift mutations. NHEJ functions throughout the whole cell cycle, particularly in the absence of a donor DNA template (Figure 2). Therefore, exact genome editing will be achievable through providing a donor DNA template and sustaining the homology directed repair. Moreover, the CRISPR-Cas9 system employs simple alterations of the sgRNA sequence and introduces multiple DSBs for retargeting new DNA sequences [53]. In epigenetic editing, it is important to limit the nucleolytic activity of the CRISPR-Cas9 system. Recently, Cas9 has remodeled as inactive or dead Cas9 (dCas9) with two mutations in the catalytical site (D10A mutation in RuvC and H840A in the HNH nuclease domain) [54], which can be used for the alteration of gene expression and the rewriting of epigenetic marks without DSB production [55]. Newly-introduced CRISPR-dCas9 systems such as CRISPR activation (CRISPRa) and interference (CRISPRi) exert fused transcriptional regulators to repress or induce gene transcription in the direction of dCas9 to the transcription start site of the target gene [56].

Epigenome editing by CRISPR-dCas9

Three main strategies are suggested for modulating gene expression by the CRISPR-Cas9 system in the cells that lack normal activities of EpiEffectors. The first strategy includes CRISPR-Cas9-based approaches that knock-out the genes involved in cancer by introducing indels at the chosen genome loci of malignant cells. For example, *DNMT*, and its cognate protein, is one of the major genes correlated to cancer. In a study, He *et al.* designed a CRISPR-Cas9 system including Cas9 and sgRNA targeting *DNMT1* in ovarian cancer. They used a folate receptor-targeted liposome (F-LP) as a delivery tool for *in vivo* transfer. This system could effectively downregulate DNMT1 expression with fewer side effects in malignant cells [57]. This approach, although having a potential application for cancer therapy, is related to gene editing and not discussed here. The second strategy includes editing mutations occurring in EpiEffector genes. For example, point mutations in *TET1* genes can be repaired by the CRISPR-Cas9 system. However, this strategy faces delivery challenges and donor template application problems, showing that the technique needs more progression. The third strategy includes fusing EpiEffectors to catalytic-dCas9 by linkers in the CRISPR system. After recognizing and matching sgRNA and the complementary target sequence, the EpiEffector fulfills its duty at the target region and alters the gene expression profile. Of course, to obtain controlled results, it is recommended to simultaneously use the first and third strategies. A DNA-binding protein, an effector protein and a unique gRNA sequence are three basic requirements for CRISPR used as an epigenome editing tool. To date, three generations of dCas9 tools have been introduced (Figure 3). A transcriptional repressor or activator is the first generation of dCas9 tools that has the ability to be coupled with dCas9 (CRISPRa/i) for achieving gene activation or repression like many EpiEffectors such as TET and DNMT (Figure 3A); the second generation has been developed to improve the efficiency of dCas9, especially in the CRISPRa systems. These tools, which include SunTag, VP64, VPR, SAM, MS2, scRNA, or combinations of them with dCas9, are designed to fuse multiple copies of eppieffectors to dCas9 in order to amplify EppiEffectors (Figure 3B). The third generation of dCas9 tools includes three systems: (i) coupling or dimerization systems, in which chemical or light factors serve
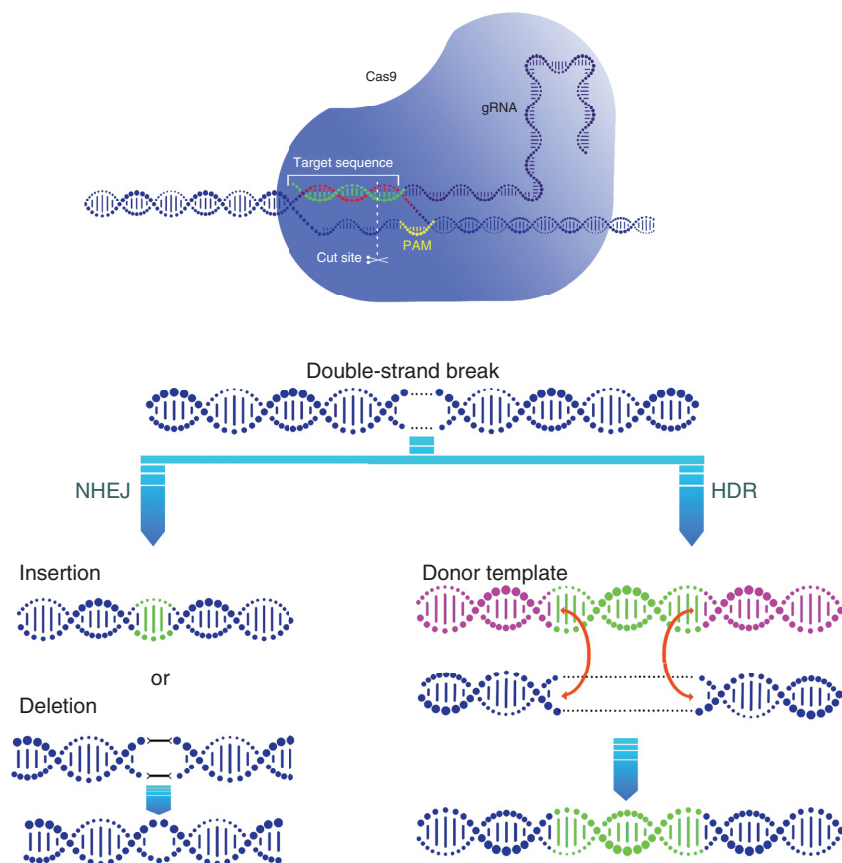
Figure 2. The CRISPR-Cas9 system as a gene editing tool. CRISPR consists of a Cas9 endonuclease (which cleaves the target sequence in the genome) and a single guide RNA (sgRNA; which contains two parts including (i) CRISPR RNA (crRNA) with an approximately 20-base-pair sequence binding to the target DNA site as a guide for Cas9 followed by a short DNA sequence known as PAM, which is essential for compatibility with the Cas9 nuclease, and (ii) Noncoding trans-activating crRNA (tracrRNA), as a homing device necessary for Cas9 cleavage. Cas9 cleaves DNA to produce DSBs. After Cas9 endonuclease activity, the cell machinery repairs DSBs by one of two main mechanisms, including HDR or NHEJ.
DSB: Double-strand break; HDR: Homology directed repair; NHEJ: Nonhomologous end joining; PAM: Protospacer-adjacent motif.

as receptors that separately fuse to EpiEffector and dCas9; these proteins, when coupling with their drives, activate EpiEffectors. This system includes PYL1, ABI (which are chemically activated by abscisic acid [ABA]), GID, GAI (which are chemically activated by gibberellin [GA]), PhyB and PIF (which are activated by light), which allow controlling CRISPR–dCas9 systems for inducible gene regulation. (ii) Split dCas9 systems that exert cleft dCas9, which is divided into two parts and, when these two parts connect with other in the target sequence, activates EpiEffectors. This system controls gene expression. (iii) Receptor-coupled systems, in which the EpiEffectors, when receptors couple with their ligands, are activated. In these systems, some molecular devices (G protein-coupled receptors, modular extracellular sensor architecture [MESA] and synthetic receptor tyrosine kinase systems) are involved for gene regulations (Figure 3C) [58]. Here, we reviewed various types of dCas-X proteins and their potential applications as well as crucial factors imperative for transcriptional modulation that can be used to simplify new generations of *in vivo* transcriptional therapeutics in Table 2.

CRISPRi blocks the transcriptional process and causes gene expression [83]. Kruppel-associated box (KRAB), known as a strong repressor complex, can fuse to dCas9 and result in a stronger and more specific gene repression [84]. dCas9-VP64 mediates gene activation in CRISPRa. VP64-P65-Rta (VPR), as a second generation of the CRISPR-based gene activation platform, can improve the dCas-VP64 strategy, leading to potent gene induction. dCas9-VPR contains dCas9 fused to a tripartite transactivation complex, including VP64, P65 (transcription activator) and Rta (transactivator) proteins [85]. Effectors directly fuse to the catalytic domain of dCas9 in most dCas9 systems, but can

Table 2. CRISPR-dCas9-X systems with their functions and examples for cancer treatment.

CRISPR-dCas9 System	Function	Example	Ref.
dCas9-DNMT3A	Increased DNA methylation and repressed gene transcription	McDonald et al. fused dCas9-DNMT3A to target the tumor suppressor gene cyclin dependent kinase inhibitor 2A (CDKN2A) [9p21.3]. They observed an increase in DNA methylation at the CDKN2A target locus	[59]
dCas9–DNMT3ACD	Increased DNA methylation and repressed gene transcription	Vojta et al. fused the catalytic domain of DNMT3A and dCas9 to target the BTB domain and CNC homolog-2 (BACH2) loci (6q15). Methylation increased up to 60% CpG at the BACH2 locus	[60]
dCas9-DNMT3A-DNMT3L	Increased DNA methylation and inhibited efficient gene transcription	Stepper et al. fused DNMT3A-DNMT3L and dCas9 to target epithelial cell adhesion molecule (EpCAM) [2p21], C-X-C motif chemokine receptor 4 (CXCR4) [2q22.1] and transferrin receptor (TFRC) [3q29] gene promoters. Findings from that study exhibited a greater percentage of induced methylation as compared with that of dCas9-DNMT3ACD	[61]
dCas9-DNMT3A-DNMT3L-KRAB	Increased DNA methylation and efficiently repressed genes	Amabile et al. reported that dCas-DNMT3A-DNMT3L-KRAB could more effectively methylate the target gene	[62]
dCas9-TET1	Decreased DNA methylation and increased gene transcription	Liua et al. fused dCas9-TET1 in Bombyx mori cells (a kind of insect). They chose three endogenous genes (BGIBMGA004109, BGIBMGA002379 and BGIBMGA001471) that have methylation fragments in introns or exons. dCas9-TET1 successfully removed methyl groups near the targeting region, resulting in decreased methylation levels and increased mRNA transcription levels. Choudhury et al. used the dCas9-TET1 system to target breast cancer antigen 1 (BRCA1) [17q21.31] promoter, resulting in the induced gene expression	[63,64]
dCas9-MS2-TET1	Increased gene transcription	Xu et al. inserted bacteriophage MS2 RNA into the conventional sgRNA. This caused direct tethering of MS2-fused Tet1CD proteins and increased gene transcription	[65]
dCas9-MS2-HP1	Increased gene repression	Braun et al. used the dCas9 system to target the CXCR4 gene. Their results showed decreased CXCR4 mRNA levels and induced gene silencing. This system caused more potent recruitment and histone modifications	[66]
dCas9-MS2-BAF	Increased gene activation	Braun et al. used dCas9-MS2-BAF to target four genes including GATA binding protein 4 (GATA4) [8p23.1]. Their results revealed increased gene expression	[66]
dCas9-SunTag-TET1CD	Amplified gene transcription	Morita et al. reported that dCas9-SunTag-TET1CD improves demethylation efficiency	[67]
dCas9-TDG	Increased gene expression	Gregory et al. showed that targeted DNA demethylation using TDG could decrease methylation and increase gene expression	[68]
dCas9-p300	Transcription activation	Hilton et al. used dCas9-p300 to target the myogenic differentiation 1 (Myod) [11p15.1] gene, resulting in induced transcription in adjacent areas	[69]
dCas9-HDAC3	Increased deacethylation and inhibited transcription	Kwon et al. used dCas9-HDAC3 to target the promoter of survival of motor neuron 1 (SMN1) [5q13.2] gene. They found that dCas9-HDAC3 could regulate SMN1 transcription	[70]
EZH2-dCas9	Induced histone methylation and inhibited transcription	O'Geen et al. used EZH2-dCas9 to target erb-b2 receptor tyrosine kinase 2 (HER2) [17q12] gene promoter. Their results showed long-term induced HER2 repression, increased H3K27 trimethylation and potent HER2 hypermethylation	[71]
dCas9-KRAB-MeCP2	Transcription repression	Yeo et al. used dCas9-KRAB-MeCP2 and could repress the transcription of multiple genes	[72]
dCas9-LSD1	Demethylation of histones	Kearns et al. set the dCas9-LSD1 complex to target T-box transcription factor 3 (Tbx3) [12q24.21]. Their results showed loss of H3K27Ac at the enhancer, downregulation of Tbx3 and silenced Tbx2 gene in embryonic stem cells	[73]
dCas9- ROS1	Increased transcription	Parrilla-Doblas et al. used dCas9-ROS1-5mC to target DNA glycosylase (ROS1CD). The results showed a decrease in methylation of targeted promoters, resulting the increased transcription	[74]
dCas9-KRAB	Gene repression	Amabile et al. used dCas9-KRAB to edit enhancer regions by changing the methylation status at the target site, thereby suppressing gene transcription	[62]
dCas9-VPR dCas9-VP64	Gene activation	Blanas et al. induced fucosyltransferase 4 (FUT4) [11q21] and FUT9 genes in the colorectal cancer cell (MC38) using dCas9-VPR fusion. Their results showed the transcriptional activation of FUT genes and specific neoexpression	[75]
dCas9-SunTag	Increased efficiency of EpiEffectors	Tanenbaum et al. reported that dCas9-SunTag could add multiple copies of the fusion protein at the target locus	[76]
dCas9-SunTag-DNMT3A	Transcription repression	Huang et al. used dCas9-SunTag-DNMT3A to target the Homeobox protein Hox A (HOXA) [7p15.2] genomic locus. They reported the ability of this system to recruit multiple copies of DNMT3A, causing more efficient methylation	[77]
dCas9-SunTag-VP64	Activated transcriptional modulators	Tanenbaum et al. used this system to recruit multiple copies of fusion proteins to achieve more efficacy in epigenetic editing	[76]
dCas9-MQ1	Increased methylation	Lei et al. used prokaryotic DNA methyltransferase MQ1 to generate genome-wide hypermethylation in wild-type mouse embryonic stem cells	[78]
Split dCas9-DNMT	Increased methylation with high specificity	Xiong et al. used the split dCas9 for higher specificity	[79]

ABA: Abscisic acid.

CRISPR-dCas9 System	Function	Example	Ref.
CRISPR-dCas9-R2	Blocked methylation	Lu *et al.* developed a novel CRISPR-dCas9-R2 system able to block the *DNMT1* activity with a R2-stem loop in the targeted loci, leading to decreased DNA methylation levels. Therefore, methylation of the targeted DNA loci was blocked	[80]
dCas9-CLOUD	Chromatin remodeling	dCas9-CLOUD consists of dCas9 proteins fused to a unique, reversible chemically-induced proximity system such as ABA. CLOUD9 could not only reversibly modulate chromatin contacts but also stimulate corresponding alterations in gene expression	[81]
CRISPR-genome organization	Modulated gene expression	CRISPR-genome organization regulates gene expression through chemical mediators. Findings from that study showed that this system could reversibly change the 3D location of gRNA in targeted loci. *In vitro* silencing of *CXCR4* was achieved through altered positioning of loci near nuclear lamina	[82]

Table 2. CRISPR-dCas9-X systems with their functions and examples for cancer treatment (cont.).

ABA: Abscisic acid.

also be recruited in newly-introduced methods through the sgRNA scaffold (scRNA) engineered to RNA modules such as MS2, com, PP7, etc. MS2, a hairpin RNA aptamer, has the ability to bind to particular RNA-binding proteins including bacteriophage MS2-coat protein (MCP). Therefore, effectors, such as transactivation complexes i.e. VP64 and P65-HSF1 (heat shock transcription activators), can fuse to the sgRNA-MS2 scaffold with the mediator of the MCP to activate gene expression. Synergistic activation mediator (SAM) includes the dCas9-VP64 fusion complex and MCP-fused P65-HSF1, exhibiting higher potency for gene expression activation [86]. SunTag is another novel strategy that uses a repeating peptide array such as GCN4 peptide repeats in dCas9 to attract single-chain variable fragment-linked effectors (VP64, p65-HSF1, p300 and others) [87]. This TREE system contains a combination of SunTag and Scaffold, containing up to 32 molecules of VP64 or p65-HSF1 [88].

The third generation of CRISPR was developed to establish more potent CRISPRi/a approaches for the temporal and spatial control of gene function. There are two leading strategies to produce input/output dCas9 molecular devices, including optogenetic or chemical sensing domain-coupled dCas9 and dCas9 coupled to ligand-sensing receptor domains. The former has optogenetically-inducible dimerizing domains (OIDs) or chemical-induced dimerizing domains (CIDs), each containing two separate parts, with the ability to fuse to dCas9 and EpiEffector. The existence of chemical or light ligands with a particular wavelength is able to prompt dimerization parts of OIDs or CIDs, allowing the ability to activate EpiEffectors for gene modulating. There are different types of CIDs or OIDs, including ABA-inducible ABI–PYL1 [89] or blue light-inducible CRY2-CIB1 [90]. Another dimerization system, which controls gene expression through the ligand-inducible control of dCas9, is split dCas9 molecules engendered with the ligand-binding domain such as estrogen receptor. This domain interacts with the cytosolic chaperone Hsp90; when the split dCas9 enters the cytoplasm, the addition of the ligand 4-hydroxytamoxifen disrupts the interaction between estrogen receptor and Hsp90, resulting in activation of dCas9 for gene regulation [91]. In the second strategy, known as the receptor-coupled system for the control of endogenous genes, cellular transmembrane receptors are coupled to the dCas9 system. These receptors, when interacting with their ligands, induce conformational changes in the receptors, resulting in the trigger of signaling in cells. There are several types of such systems, including G protein-coupled receptors, MESA and synthetic receptor tyrosine kinases, each of which has a special mechanism. The MESA system includes fusing dCas9 to the dimerizing target chain through fusing the TEV (tobacco etch virus) protease and cleavable linker to another protease chain [92]. More recently, studies have revealed that induction of long-range hypermethylation or targeted hypermethylation at key components including CTCF, which is capable of altering chromatin folding, may be more efficient as compared with local CpG methylation [93].

In the following, we explain some CRISPR-dCas9 clinical applications for therapeutic targets, which show the importance and potential of such epigenome editing methods. The application of dCas9-activating systems can promote and stabilize the expression of certain genes for different targets; for example, increased *FOXP3* expression by CRISPR/dCas9 in primary T cells could induce regulatory T cell differentiation, which can be used in the modulation of the immune system in autoimmune diseases [94]. In cancers, common tumor suppressor genes, such as *p53*, *PTEN* and others, have low expression that is mediated by tumor regulatory mechanisms [95–97]. Application of the activator dCas9 can modulate either these critical genes or the expression of some certain genes involved in heritable or acquisitive diseases. dCas9 can be used for activating latent viruses, such as HIV, to induce the immune system, or inactivating the virus genome by dCas9 blocker systems [98].
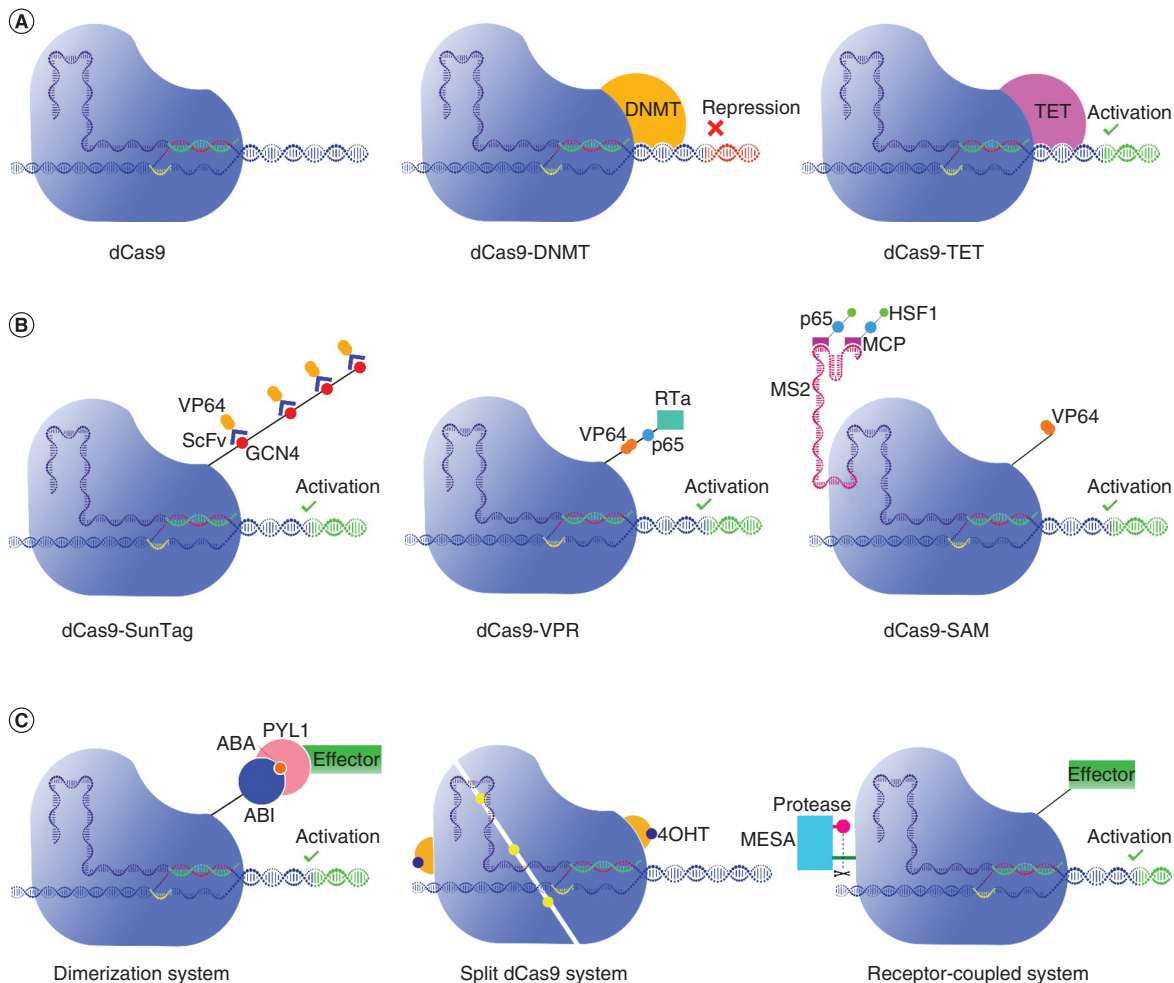
Figure 3.   Generations of dCas tools. (A) The first generation includes an EpiEffector coupled with dCas9 (CRISPRa/i) to alter gene transcription. For example, dCas9-DNMT has the ability to hypermethylate the target sequence, causing gene repression; however, dCas9-TET has the ability to remove methyl groups, resulting in gene transcription activation. **(B)** The second generation is designed to fuse multiple copies of EppiEffectors to dCas9 in CRISPRa to amplify them. The dCas9-SUNTag system uses repeating peptides such as GCN4 fused to dCas9 and multiple copies of effectors such as VP64 linked to the scFv, which can connect GCN4 and dCas9, resulting in potent gene activation. dCas9-VPR contains dCas9 fused to a tripartite transactivation complex, including VP64, P65 and Rta to strongly induce gene activation. dCas9-SAM includes a dCas9-VP64 fusion complex and MCP-fused P65-HSF1 through the MS2 scRNA, showing a higher potency for gene expression activation. **(C)** The third generation includes three systems: dimerization systems that have two separate parts as receptor; for example, ABI-PYL1 dimer (one of them [e.g., ABI] fuses with dCas9 while another part [e.g., PYL1] fuses with EpiEffector) uses chemical or light factors (e.g., ABA) as a ligand to induce dimerization parts and activate EpiEffectors to gene modulating. The split dCas9 system exerts split dCas9 molecules with the receptor such as ERT; the addition of the ligand such as 4OHT activates dCas9 for gene regulation. Receptor-coupled systems, such as MESA, consist of dCas9, a cleavable linker and a protease able to trigger signaling in cells, leading to gene regulation.
ABA: Abscisic acid; ERT: Estrogen receptor; MESA: Modular extracellular sensor architecture; scFv: Single-chain variable fragments.

Limitations of CRISPR-Cas9

CRISPR-Cas is a central part of gene editing techniques through potent activity, easy design, high velocity and capacity to target any DNA or RNA site. In addition to its advantages and extensive potentials, The CRISPR-Cas system poses numerous unsolved challenges for clinical applications [99] that can affect its specificity and efficiency such as target specificity, editing efficiency, delivery methods and off-target effects [100,101]. CRISPR-Cas9 suffers from off-target effects because of the fact that the recognition sequence of Cas9 is smaller than 20 base-pairs. More recently, tremendous attempts have been made to diminish off-target effects, which resulted in introduction

of sgRNA with two further guanine nucleotides at the 5′end or by the application of Cas9 paired nickases [102]. The nickase enzyme acts via induction of DSBs in the target DNA and production of a single nick in off-target locations, leading to decreased off-target mutations [103]. There are also other approaches to lessen off-targets, such as dCas9 [104], SpCas9 and fCas9 (Cas9 fused with the FokI nuclease domain). These catalytically inactive enzymes cleave target DNA sites with more than 100-fold specificity as compared with wild-type Cas9 [105]. Cas9.Cpf1 (a single RNA) is another type of endonuclease that requires no tracrRNA for DNA cleavage to insert DNA into the target site, and utilizes a T-rich PAM on the 5′side of the crRNA [106]. Another strategy is designing a synthetic switch to develop self-regulated Cas9 expression in both transcription and translation steps [107]. Another strategy is promoting HDR activity through decreasing or blocking the NHEJ pathway [108] and delivering HDR templates by using vectors, followed by a selection of special sequences to minimize matched off-target sites [101]. Tremendous efforts in the discovery of other types of the CRISPR system and Cas led to improvement in specificity and efficacy; for example, the introduction of RNA-targeting Cas13 suggested an interesting avenue to target the dynamic of endogenous RNA transcripts. dCas13, similar to dCas9, can directly edit RNA at endogenous RNA sites. Systems based on Cas13 can function as a valuable platform to investigate the regulation of endogenous RNAs [109]. Cellular delivery of CRISPR-Cas9 is another issue [110], which affects CRISPR efficacy. A variety of *ex vivo* strategies were used for the delivery of Cas9 and its derivatives, such as liposomes, plasmid DNA encoding Cas9 as well as sgRNAs [111] including direct injection of Cas9 mRNA and sgRNA [112], viral delivery such as the use of safe and nonpathogenic adeno-associated viruses and other viruses that have serotype-associated target cell specificity and low immunogenicity [113], nanoparticle delivery that leads to decreased nuclease expression, off-targets and side effects such as tumorigenesis [114], electroporation or nucleofection, as well as cationic peptides. However, *ex vivo* delivery conditions are a challenging issue for hematopoietic stem cells and some primary hematopoietic cells, such as T and B cells [115,116]. Although engineered viral variants deliver foreign DNA into different cell and tissue types, the size of the foreign DNA molecule and the immune system of the host are the main issues [117].

Conclusion

Gene editing has been revolutionized by the introduction of the CRISPR-Cas9 system. Beyond editing, dCas9 not only can be used for the regulation of gene expression, but also holds great potential for the treatment of human diseases such as cancer. Despite many advances in clinical applications of CRISPR-Cas9, there is still a long road for CRISPR-Cas9 to be used in *in vivo* genome editing.

Future perspective

In the near future, gene editing therapy is expected to be the first-line treatment option for cancer. This is realized by technology progression and overcoming the challenges by further research, such as improved recognition of genetic, epigenetic and various cancer mechanisms, delivery approaches, editing efficiency and target gene specificity, as well as decreased off-target effects and side effects. Consequently, the CRISPR-Cas9 system can be used as a safe, effective, everlasting therapeutic strategy to treat patients with cancer.

Executive summary

- Cancer is one of the most common diseases around the world and causes many deaths worldwide. Cancers are developed with both genetic and epigenetic abnormalities. More importantly, epigenetic abnormalities are even more frequent in most human cancers. DNA methylation, as one of the major mechanisms of epigenetic regulation, not only can control gene expression but also plays a well-established role in the pathogenesis of many cancers.

DNA methylation EpiEffectors
- Structure and function of the epigenome are controlled by a huge collection called EpiEffectors that are used as targets in epigenetic therapy or in the CRISPR-Cas9 system.

The role of DNA methylation in cancer development
- Aberrant DNA methylation is commonly found in tumors and marks the early stages of cancer development.
- EpiEffectors play highly important roles in gene expression and cellular processes, whose dysfunctions lead to cancer development.
- In epigenetic therapy, all efforts are made to modulate gene expression to the normal status through several ways. Of great note, CRISPR is a novel way to modulate gene expression.

Workmanship & ingredients of the CRISPR-Cas9 system as a gene editing tool
- CRISPR-Cas9 systems are genome editing tools, functioning by targeting and altering almost any sequence in the genome of cultured cells or whole organisms.
- In epigenetic editing, it is important to limit the nucleolytic activity of the CRISPR-Cas9 system.

Epigenome editing by CRISPR-dCas9
- EpiEffectors fused to catalytic-dCas9 by linkers in the CRISPR system. After recognizing and matching sgRNA and the complementary target sequence, the EpiEffector fulfills its duty at the target region and alters the gene expression profile.
- To date, three generations of dCas9 tools have been introduced.
- Some CRISPR-dCas9 clinical applications explained for therapeutic targets, which show the importance and potential of such epigenome editing methods.

Limitations of CRISPR-Cas9
- CRISPR-Cas is a central part of gene editing techniques through potent activity, easy design, high velocity and capacity to target any DNA or RNA site.
- In addition to its advantages and extensive potentials, there are numerous unsolved challenges for clinical applications, which can affect their specificity and efficiency such as target specificity, editing efficiency, delivery methods and off-target effects.

Future perspective
- In the near future, gene editing therapy is expected to be the first-line treatment option for cancer.

References

Papers of special note have been highlighted as: • of interest; •• of considerable interest

1. Abdollahpour-Alitappeh M, Hashemi Karouei SM, Lotfinia M, Amanzadeh A, Habibi-Anbouhi M. A developed antibody-drug conjugate rituximab-vcMMAE shows a potent cytotoxic activity against CD20-positive cell line. *Artif. Cells. Nanomed. Biotechnol.* 46(Suppl. 2), 1–8 (2018).

2. Azad M, Kaviani S, Noruzinia M *et al.* Gene expression status and methylation pattern in promoter of P15INK4b and P16INK4a in cord blood CD34+ stem cells. *IJBC* 16(7), 822 (2013).

3. Vogelstein B, Papadopoulos N, Velculescu VE, Zhou S, Diaz LA, Kinzler KW. Cancer genome landscapes. *Science* 339(6127), 1546–1558 (2013).

4. Jones PA, Issa J, Baylin S. Targeting the cancer epigenome for therapy. *Nat. Rev. Genet.* 17(10), 630–641 (2016).

5. Zhang Z-M, Lu R, Wang P *et al.* Structural basis for DNMT3A-mediated de novo DNA methylation. *Nature* 554(7692), 387–391 (2018).

6. Ho L, Jothi R, Ronan J, Cui K, Zhao K, Crabtree G. An embryonic stem cell chromatin remodeling complex, esBAF, is an essential component of the core pluripotency transcriptional network. *Proc. Natl. Acad. Sci. U. S. A.* 106(13), 5187–5191 (2009).

7.   Zeng W, Ball AR Jr, Yokomori K. HP1: Heterochromatin binding proteins working the genome. *Epigenetics* 5(4), 287–292 (2010).

8.   Wakefield R, Smith B, Nan X *et al.* The solution structure of the domain from MeCP2 that binds to methylated DNA. *J. Mol. Biol.* 291(5), 1055–1065 (1999).

9.   Chetverina D, Fujioka M, Erokhin M, Georgiev P, Jaynes JB, Schedl P. Boundaries of loop domains (insulators): determinants of chromosome form and function in multicellular eukaryotes. *Bioessays* 39(3), 1600233 (2017).

10. Hanssen LL, Kassouf MT, Oudelaar AM *et al.* Tissue-specific CTCF-cohesin-mediated chromatin architecture delimits enhancer interactions and function *in vivo*. *Nat. Cell Biol.* 19(8), 952–961 (2017).

11. Viré E, Brenner C, Deplus R *et al.* The Polycomb group protein EZH2 directly controls DNA methylation. *Nature* 439(7078), 871–874 (2006).

12. Ito S, Li S, Dai Q *et al.* Tet Proteins Can Convert 5Methylcytosine to 5-Formylcytosine and 5-Carboxylcytosine. *Science* 333(6047), 1300–1303 (2011).

13. Gagné ML, Boulay K, Topisirovic I, Huot MÉ, Mallette FA. Oncogenic activities of IDH1/2 mutations: from epigenetics to cellular signaling. *Trends Cell. Biol.* 27(10), 738–752 (2017).

14. Zhou X, Zhuang Z, Wang W *et al.* OGG1 is essential in oxidative stress induced DNA demethylation. *Cell. Signal* 28(9), 1163–1171 (2016).

15. He Y, Li B, Li Z *et al.* TetMediated formation of 5carboxylcytosine and its excision by TDG in mammalian DNA. *Science* 333(6047), 1303–1307 (2011).

16. Conticello SG, Thomas CJ, Petersen-Mahrt SK, Neuberger MS. Evolution of the AID/APOBEC family of polynucleotide (deoxy)cytidine deaminases. *Mol. Biol. Evol.* 22(2), 367–377 (2005).

17. Ghorban K, Shanaki M, Mobarra N *et al.* Apolipoproteins A1, B, and other prognostic biochemical cardiovascular risk factors in patients with beta-thalassemia major. *Hematology* 21(2), 113–120 (2016).

18. Shi Y, Whetstine J. Dynamic regulation of histone lysine methylation by demethylases. *Mol. Cell.* 1–14 (2007).

19. Ciccone D. KDM1B is a histone H3K4 demethylase required to establish maternal genomic imprints. *Nature* 461(7262), 415–418 (2009).

20. Wissmann M. Cooperative demethylation by JMJD2C and LSD1 promotes androgen receptordependent gene expression. *Nat. Cell Biol.* 9(3), 347–353 (2007).

21. Sun XJ, Man N, Tan Y, Nimer SD, Wang L. The role of histone acetyltransferases in normal and malignant hematopoiesis. *Front. Oncol.* 5, 108 (2015).

22. Sanchez R, Zhou M. The role of human bromodomains in chromatin biology and gene transcription. *Curr. Opin. Drug Discov Devel.* 12(5), 659–665 (2009).

23. Seto E, Yoshida M. Erasers of histone acetylation: the histone deacetylase enzymes. *Cold Spring Harb. Perspect. Biol.* 6(4), a018713 (2014).

24. Marot D, Opolon P, Brailly-Tabard S *et al.* The tumor suppressor activity induced by adenovirus-mediated BRCA1 overexpression is not restricted to breast cancers. *Gene. Ther.* 13(3), 235–244 (2006).

25. Esteller M. *Epigenetics in Biology and Medicine*. CRC press FL, USA (2008).

26. Hoseini M, Sahmani M, Foroughi F, Khazaei Monfared Y, Azad M. Evaluating the role of PTEN promoter methylation in patients predisposed to hypercoagulable states via methylation specific PCR. *Rep. Biochem. Mol. Biol.* 7(2), 223–229 (2019).

27. Esteller M. Cancer epigenomics: DNA methylomes and histone-modification maps. *Nature* 8(4), 286–298 (2007).

28. Hanada M, Delia D, Aiello A, Stadtmauer E, Reed JC. bcl-2 Gene hypomethylation and high-level expression in B-cell chronic lymphocytic leukemia. *Blood* 82(6), 1820–1828 (1993).

29. Nishigaki M, Aoyagi K, Danjoh I *et al.* Discovery of aberrant expression of R-RAS by cancer-linked DNA hypomethylation in gastric cancer using microarrays. *Cancer Res.* 65(6), 2115–2124 (2005).

30. Hou HA, Kuo YY, Liu CY *et al.* DNMT3A mutations in acute myeloid leukemia: stability during disease evolution and clinical implications. *Blood* 119(2), 559–568 (2012).

31. Yamashita Y, Yuan J, Suetake I *et al.* Array-based genomic resequencing of human leukemia. *Oncogene* 29(25), 3723–3731 (2010).

32. Steensma DP, Bejar R, Jaiswal S *et al.* Clonal hematopoiesis of indeterminate potential and its distinction from myelodysplastic syndromes. *Blood* 126(1), 9–16 (2015).

33. Rahmani T, Azad M, Chahardouli B, Nasiri H, Vatanmakanian M, Kaviani S. Patterns of DNMT1 promoter methylation in patients with acute lymphoblastic leukemia. *Int. J. Hematol. Oncol. Stem Cell. Res.* 11(3), 172–177 (2017).

34. Marcais A, Waast L, Bruneau J *et al.* Adult T cell leukemia aggressivenness correlates with loss of both 5-hydroxymethylcytosine and TET2 expression. *Oncotarget* 8(32), 52256–52268 (2017).

35. Bodor C, Grossmann V, Popov N *et al.* EZH2 mutations are frequent and represent an early event in follicular lymphoma. *blood* 122(18), 3165–3168 (2013).

36. Dang L, Jin S, Su S. IDH mutations in glioma and acute myeloid leukemia. *Trends Mol. Med.* 16(9), 387–397 (2010).

37. Ghiam A, Cairns R, Thoms J *et al.* IDH mutation status in prostate cancer. *Oncogene* 31(33), 3826 (2011).

38. Kipp B, Voss J, Kerr S *et al.* Isocitrate dehydrogenase 1 and 2 mutations in cholangiocarcinoma. *Hum. Pathol.* 43(10), 1552–1558 (2012).

39. Ropero S, Esteller M. The role of histone deacetylases (HDACs) in human cancer. *Mol. Oncol.* 1(1), 19–25 (2007).

40. Jiang Y, Ortega-Molina A, Geng H *et al.* CREBBP inactivation promotes the development of HDAC3-dependent lymphomas. *Cancer Disc.* 7(1), 38–53 (2016).

41. Shain A, Pollack J. The spectrum of SWI/SNF mutations, ubiquitous in human cancers. *PLoS One.* 8(1), e55119 (2013).

42. Kadoch C, Hargreaves D, Hodges C *et al.* Proteomic and bioinformatic analysis of mammalian SWI/SNF complexes identifies extensive roles in human malignancy. *Nat. Genet.* 45, 592–601 (2013).

43. Rebhandl S, Huemer M, Greil R, Geisberger R. AID/APOBEC deaminases and cancer. *Oncoscience* 2(4), 320–333 (2015).

44. Sahmani M, Vatanmakanian M, Goudarzi M, Mobarra N, Azad M. Microchips and their significance in isolation of circulating tumor cells and monitoring of cancers. *Asian. Pac. J. Cancer Prev.* 17(3), 879–894 (2016).

45. Yaghoubi S, Karimi MH, Lotfinia M *et al.* Potential drugs used in the antibody-drug conjugate (ADC) architecture for cancer therapy. *J. Cell. Physiol.* 235(1), 31–64 (2020).

46. Yaghoubi S, Najminejad H, Dabaghian M *et al.* How hypoxia regulate exosomes in ischemic diseases and cancer microenvironment? *IUBMB Life* 72(7), 1286–1305 (2020).

47. Xiong X, Chen M, Lim WA, Zhao D, Qi LS. CRISPR/Cas9 for human genome engineering and disease research. *Annu. Rev. Genomics Hum. Genet.* 17, 131–154 (2016).

48. Fu Y, Sander JD, Reyon D, Cascio VM, Joung JK. Improving CRISPR-Cas nuclease specificity using truncated guide RNAs. *Nat. Biotechnol.* 32(3), 279–284 (2014).

49. Barrangou R, Fremaux C, Deveau H *et al.* CRISPR provides acquired resistance against viruses in prokaryotes. *Science* 315(5819), 1709–1712 (2007).

50. Komor AC, Badran AH, Liu DR. CRISPR-based technologies for the manipulation of eukaryotic genomes. *Cell* 168(1–2), 20–36 (2017).

51. Gasiunas G, Barrangou R, Horvath P, Siksnys V. Cas9-crRNA ribonucleoprotein complex mediates specific DNA cleavage for adaptive immunity in bacteria. *Proc. Natl Acad. Sci.* 109(39), 2579–2586 (2012).

52. Bibikova M, Carroll D, Segal DJ *et al.* Stimulation of homologous recombination through targeted cleavage by chimeric nucleases. *Mol. Cell. Biol.* 21(1), 289–297 (2001).

53. Cong L, Ran FA, Cox D *et al.* Multiplex genome engineering using CRISPR/Cas systems. *Science* 339(6121), 819–823 (2013).

54. Makarova KS, Haft DH, Barrangou R *et al.* Evolution and classification of the CRISPR-Cas systems. *Nat. Rev. Microbiol.* 9(6), 467–477 (2011).

55. Konermann S, Brigham MD, Trevino AE *et al.* Genome-scale transcriptional activation by an engineered CRISPR-Cas9 complex. *Nature* 517(7536), 583–588 (2015).

56. Kampmann M. CRISPRi and CRISPRa screens in mammalian cells for precision biology and medicine. *ACS Chem. Biol.* 13(2), 406–416 (2017).

57. He ZY, Zhang YG, Yang YH *et al.* *In vivo* ovarian cancer gene therapy using CRISPR-Cas9. *Hum. Gene Ther.* 29(2), 223–233 (2018).

58. Xiaoshu X, Lei SQ. A CRISPR-dCas9 toolbox for genetic engineering and synthetic biology. *J. Mol. Biol.* 431(1), 34–47 (2019).

59. Mcdonald JI, Celik H, Rois LE *et al.* Reprogrammable CRISPR/Cas9-based system for inducing site specific DNA methylation. *Biology* 5(6), 866–874 (2016).

60. Vojta A, Dobrinic P, Tadic V *et al.* Repurposing the CRISPR-Cas9 system for targeted DNA methylation. *Nucleic Acids Res.* 44(12), 5615–5628 (2016).

•   The enrolling of dcas9-DNMT3A to decreased gene expression.

61. Stepper P, Kungulovski G, Jurkowska RZ *et al.* Efficient targeted DNA methylation with chimeric dCas9-Dnmt3a-Dnmt3L methyltransferase. *Nucleic Acids Res.* 45(4), 1703–1713 (2017).

62. Amabile A, Migliara A, Capasso P *et al.* Inheritable silencing of endogenous genes by hit-and-run targeted epigenetic editing. *Cell* 167(1), 219–232 (2016).

63. Liua Y, Maa S, Changa J *et al.* Programmable targeted epigenetic editing using CRISPR system in Bombyx mori. *Insect Biochem. Mol. Biol.* 110, 105–111 (2019).

64. Choudhury SR, Cui Y, Lubecka K, Stefanska B, Irudayaraj J. CRISPR-dCas9 mediated TET1 targeting for selective DNA demethylation at BRCA1 promoter. *Oncotarget* 7(29), 46545–46556 (2016).

65. Xu X, Tao Y, Gao X *et al.* CRISPR-based approach for targeted DNA demethylation. *Cell Discov.* 2, 16009 (2016).

66. Braun S, Kirkland J, Chory E, Husmann D, Calarco J, Crabtree G. Rapid and reversible epigenome editing by endogenous chromatin regulators. *Nat. Commun.* 8(1), 1–8 (2017).

67. Morita S, Noguchi H, Horii T *et al.* Targeted DNA demethylation in vivo using dCas9-peptide repeat and scFv-TET1 catalytic domain fusions. *Nat. Biotechnol.* 34(10), 1060–1065 (2016).

68. Gregory DJ, Zhang Y, Kobzik L, Fedulov AV. Specific transcriptional enhancement of inducible nitric oxide synthase by targeted promoter demethylation. *Epigenetics* 8(11), 1205–1212 (2013).

69. Hilton IB, D'ippolito AM, Vockley CM *et al.* Epigenome editing by a CRISPR-Cas9-based acetyltransferase activates genes from promoters and enhancers. *Nat. Biotechnol.* 33(5), 510–517 (2015).

• The dCas9-P300 activated transcription of target gene.

70. Kwon DY, Zhao Y-T, Lamonica JM, Zhou Z. Locus-specific histone deacetylation using a synthetic CRISPR-Cas9-based HDAC. *Nature* 8(1), 1–8 (2017).

71. O'geen H, Bates SL, Carter SS *et al.* Ezh2-dCas9 and KRAB-dCas9 enable engineering of epigenetic memory in a context-dependent manner. *Epigenetics Chromatin* 12(1), 26 (2019).

72. Yeo N, Chavez A, Lance-Byrne A *et al.* An enhanced CRISPR repressor for targeted mammalian gene regulation. *Nat. Methods* 15(8), 611–616 (2018).

• The Dcas9-KRAB-MeCP2 could effectively repress the target genes.

73. Kearns NA, Pham H, Tabaketal B. Functional annotation of native enhancers with a Cas9–histone demethylase fusion. *Nat. Methods* 12(5), 401–403 (2015).

74. Parrilla-Doblas JT, Ariza RR, Roldán-Arjona T. Targeted DNA demethylation in human cells by fusion of a plant 5-methylcytosine DNA glycosylase to a sequence-specific DNA binding domain. *Epigenetics* 12(4), 296–303 (2017).

75. Blanas A, Cornelissen LaM, Kotsias M *et al.* Transcriptional activation of fucosyltransferase (FUT) genes using the CRISPR-dCas9-VPR technology reveals potent N-glycome alterations in colorectal cancer cells. *Glycobiology* 29(2), 137–150 (2019).

76. Tanenbaum ME, Gilbert LA, Qi LS, Weissman JS, RD V. A protein-tagging system for signal amplification in gene expression and fluorescence imaging. *Cell* 159(3), 635–646 (2014).

77. Huang YH, Su J, Lei Y *et al.* DNA epigenome editing using CRISPR-Cas SunTag-directed DNMT3A. *Genome Biol.* 18(1), 176 (2017).

78. Lei Y, Zhang X, Su J *et al.* Targeted DNA methylation in vivo using an engineered dCas9-MQ1 fusion protein. *Nat. Commun.* 8(1), 1–10 (2017).

79. Xiong T, Meister GE, Workman RE *et al.* Targeted DNA methylation in human cells using engineered dCas9-methyltransferases. *Sci. Rep.* 7(1), 1–14 (2017).

80. Lu A, Wang J, Sun W *et al.* Reprogrammable CRISPR/dCas9-based recruitmentof DNMT1for site-specificDNA demethylation and gene regulation. *Cell Discov.* 5(1), 1–4 (2019).

81. Morgan SL, Mariano NCA, Bermudez B *et al.* Manipulation of nuclear architecture through CRISPR-mediated chromosomal looping. *Nat. Commun.* 8(1), 1–9 (2017).

82. Wang H, Xu X, Nguyen CM, Kipniss NH, Russa ML, Qi LS. CRISPR-mediated programmable 3D genome positioning and nuclear organization. *Cell* 175, 1405–1417 (2018).

83. Qi LS, Larson MH, Gilbert LA *et al.* Repurposing CRISPR as an RNA-guided platform for sequence-specific control of gene expression. *Cell* 152(5), 1173–1183 (2013).

84. Gilbert LA, Larson MH, Morsut L *et al.* CRISPR-mediated modular RNA-guided regulation of transcription in eukaryotes. *Cell* 154(2), 442–451 (2013).

85. Chavez A, Scheiman J, Vora S *et al.* Highly efficient Cas9-mediated transcriptional programming. *Nat. Methods* 12(4), 326–328 (2015).

86. Konermann S, Al E. Genome-scale transcriptional activation by an engineered CRISPR-Cas9 complex. *Nature* 517(7536), 583–588 (2015).

87. Xu X, Qi LS. A CRISPR–dCas Toolbox for genetic engineering and synthetic biology. *J. Mol. Biol.* 431(1), 34–47 (2018).

88. Kunii A, Hara Y, Takenaga M *et al.* Three-component repurposed technology for enhanced expression: highly accumulable transcriptional activators via branched tag arrays. *CRISPR J.* 1(5), 337–347 (2018).

•• The current applications of the dCas9 tools and their advantages.

89. Chen T, Gao D, Zhang R *et al.* Chemically controlled epigenome editing through an inducible dCas9 system. *J. Am. Chem. Soc.* 139(33), 11337–11340 (2017).

90. Nihongaki Y, Yamamoto S, Kawano F, Suzuki H, Sato M. CRISPR-Cas9-based photoactivatable transcription system. *Chem. Biol.* 22(2), 169–174 (2015).

91. Nguyen DP, Miyaoka Y, Gilbert LA *et al.* Ligand-binding domains of nuclear receptors facilitate tight control of split CRISPR activity. *Nat. Commun.* 7(1), 1–10 (2016).

92. Schwarz KA, Daringer NM, Dolberg TB, Leonard JN. Rewiring human cellular input–output using modular extracellular sensors. *Nat. Chem. Biol.* 13(2), 202–209 (2017).

93. Guo Y, Xu Q, Canzio D *et al.* CRISPR inversion of CTCF Sites alters genome topology and enhancer/promoter function. *Cell* 162(4), 900–910 (2015).

94. Okada M, Kanamori M, Someya K, Nakatsukasa H, Yoshimura A. Stabilization of Foxp3 expression by CRISPR-dCas9-based epigenome editing in mouse primary T cells. *Epigenetics Chromatin* 10(1), 24 (2017).

95. Moses C, Nugent F, Waryah CB, Garcia-Bloj B, Harvey AR, Blancafort P. Activating PTEN tumor suppressor expression with the CRISPR/dCas9 system. *Mol. Ther. Nucleic Acids.* 14, 287–300 (2019).

••   The CRISPR-dCas9 activator systems promoted FOXP3 expression and induced differentiation of regulatory T cells.

96. Wu J, He K, Zhang Y *et al.* Inactivation of SMARCA2 by promoter hypermethylation drives lung cancer development. *Gene* 687, 193–199 (2019).

••   The dCas9-VPR activated PTEN (as a tumor suppressor gene) expression.

97. Dehghanifard A, Kaviani S, Abroun S *et al.* Various signaling pathways in multiple myeloma cells and effects of treatment on these pathways. *Clin. Lymphoma. Myeloma. Leuk.* 18(5), 311–320 (2018).

98. Kim V, Mears BM, Powell BH, Witwer KW. Mutant Cas9-transcriptional activator activates HIV-1 in U1 cells in the presence and absence of LTR-specific guide RNAs. *Matters (Zur)*doi:10.19185/matters.201611000027 (2017).

99. Roy B, Zhao J, Yang C *et al.* CRISPR/cascade9-mediated genome editing challenges and opportunities. *Front. Genet.* 9, 240 (2018).

100. Lee CM, Cradick TJ, Fine EJ, Bao G. Nuclease target site selection for maximizing on-target activity and minimizing off-target effects in genome editing. *Mol. Ther.* 24(3), 475–487 (2016).

•   The CRISPR-Cas9 functional approaches and future challenges.

101. Zischewski J, Fischer R, Bortesi L. Detectionofon-target and off target mutations generated by CRISPR/Cas9 and other sequence-specific nucleases. *Biotechnol. Adv.* 35(1), 95–104 (2017).

102. Gupta RM, Musunuru K. Expanding the genetic editing tool kit: ZFNs, TALENs, and CRISPR-Cas9. *J. Clin. Invest.* 124(10), 4154–4161 (2014).

103. Ran FA, Hsu PD, Lin CY *et al.* Double nicking by RNA guided CRISPR cas9 for enhanced genome editing specificity. *Cell* 154(6), 1380–1389 (2013).

104. Kleinstiver BP, Pattanayak V, Prew MS *et al.* High-fidelity CRISPR-Cas9 nucleases with no detectable genome-wide off-target effects. *Nature* 529(7587), 490–495 (2016).

105. Tsai SQ, Wyvekens N, Khayter C *et al.* Dimeric CRISPR RNA-guided FokI nucleases for highly specific genome editing. *Nat. Biotechnol.* 32(6), 569–576 (2014).

106. Zetsche B, Gootenberg JS, Abudayyeh OO *et al.* Cpf1 is a single RNA-guided endonuclease of a class 2 CRISPR-Cas system. *Cell* 163(3), 759–771 (2015).

107. Shen CC, Hsu MN, Chang CW *et al.* Synthetic switch to minimize CRISPR off-target effects by self-restricting Cas9 transcription and translation. *Nucleic Acids Res.* 47(3), e13 (2018).

108. Maruyama T, Dougan SK, Truttmann MC, Bilate AM, Ingram JR, Ploegh HL. Increasing the efficiency of precise genome editing with CRISPR-Cas9 by inhibition of nonhomologous end joining. *Nat. Biotechnol.* 33(5), 538–542 (2015).

109. Cox DBT, Gootenberg JS, Abudayyeh OO *et al.* RNA editing with CRISPR-Cas13. *Science* 358(6366), 1019–1027 (2017).

110. Liu C, Zhang L, Liu H, Cheng K. Delivery strategies of the CRISPR-Cas9 gene editing system for therapeutic applications. *J. Control.Release* 266, 17–26 (2017).

111. Ran FA, Cong L, Yan WX *et al.* In vivo genome editing using Staphylococcus aureus Cas9. *Nature* 520(7546), 186–191 (2015).

112. Xue W, Chen S, Yin H *et al.* CRISPR-mediated direct mutation of cancer genes in the mouse liver. *Nature* 514(7522), 380–384 (2014).

113. Kotterman MA, Schaffer DV. Engineering adeno-associated viruses for clinical gene therapy. *Nat. Rev. Genet.* 15(7), 445–451 (2014).

114. Yin H, Song CQ, Dorkin JR *et al.* Therapeutic genome editing by combined viral and non-viral delivery of CRISPR system components in vivo. *Nat. Biotechnol.* 34(3), 328–333 (2016).

115. Lombardo A, Genovese P, Beausejour CM *et al.* Gene editing in human stem cells using zinc finger nucleases and integrase-defective lentiviral vector delivery. *Nat. Biotechnol.* 25(11), 1298–1306 (2007).

116. Maali A, Atashi A, Ghaffari S, Kouchaki R, Abdolmaleki F, Azad M. A review on leukemia and iPSC Technology: application in novel treatment and future. *Curr. Stem Cell Res. Ther.* 13(8), 665–675 (2018).

117. Swiech L, Heidenreich M, Banerjee A *et al.* In vivo interrogation of gene function in the mammalian brain using CRISPR Cas9. *Nat. Biotechnol.* 33(1), 102–106 (2015).

Benchmark

Evaluation protocol for CRISPR/Cas9-mediated CD19 knockout GM24385 cells by flow cytometry and Sanger sequencing

Sarah L Inwood*,[1] [ID], **Linhua Tian[1]** [ID], **Kirsten Parratt[1]** [ID], **Samantha Maragh[1]** [ID] **& Lili Wang**,[1]** [ID]

[1]*Biosystems and Biomaterials Division, National Institute of Standards and Technology, Gaithersburg, MD 20899, USA; *Author for correspondence: sarah.inwood@gmail.com; **Author for correspondence: lili.wang@nist.gov*

ABSTRACT

Although several genome editing options are available, CRISPR/Cas9 is one of the most commonly used systems for protein and advanced therapies. There are some long-term data regarding genomic and phenotypic stability, however, information is sparse. Flow cytometry can offer a method to characterize these edited cells for longitudinal studies. The objective of this work is to describe a protocol for using flow cytometry to measure the edits from CRISPR/Cas9 on a well-characterized B-lymphoblast cell line, GM24385, with the goal of supporting safe and effective CRISPR/Cas9-engineered therapies.

METHOD SUMMARY

The objective of this work is to describe a protocol for using flow cytometry to measure the edits from CRISPR/Cas9 on a well-characterized B-lymphoblast cell line, GM24385, with the goal of longitudinal monitoring to support safe and effective CRISPR/Cas9-engineered therapies. The protocol methods include cell culture, flow cytometry, CRISPR/Cas9 editing and Sanger sequencing.

KEYWORDS:

CD19 ● CRISPR/Cas9 ● flow cytometry ● genome editing ● GM24385 cell line

The CRISPR/Cas9 system is naturally found in bacterial and archaeal immune systems [1]; however, it has been adapted for use in eukaryotes as a Nobel prize-winning genome editing system [2,3]. The CRISPR/Cas9 system uses gRNA to direct the Cas9 nuclease to a specific target near an NGG protospacer adjacent motif sequence. The Cas9 then cleaves the DNA and the cell's native DNA damage repair machinery repairs the double-strand break.

The two main repair pathways leveraged for knockout and modification of target genes during CRISPR/Cas9 editing are the non-homologous end joining (NHEJ) and homology-directed repair pathways. NHEJ is the primary choice for repairing double-strand breaks when the donor DNA template is not available, making it a good option for CRIPSR/Cas9 knockout experiments. Loss and gain of nucleotides are common occurrences during NHEJ-mediated repair, and a knockout comes from a shift in the coding sequence. Homology-directed repair is based on availability of the donor DNA template and is mainly used for custom gene modifications in coding or non-coding sequences [4,5].

The CRISPR/Cas9 system is being used more and more often for advanced therapies, including cell and gene therapies, with great promise (e.g., CRISPR test for treating sickle cell disease) [6,7]. Many commercial products for enabling CRISPR/Cas9 nuclease RNA-guided genome editing are available in a variety of delivery methods. These products include DNA encoded in viruses, plasmids, mRNA and RNPs. Additionally, CRISPR gRNA can be delivered in two parts, crRNA and tracrRNA, or as an sgRNA. Multiple bacterial species offer CAS protein options; a commonly used one is *Streptococcus pyogenes* Cas9. Similarly, there are many options for how these molecules can be delivered into cells, including viral vectors, such as lentiviral and adeno-associated viral vectors, and chemical methods, such as lipids, injection and electroporation [8,9]. Although CRISPR/Cas9 is an exciting genome editing tool, there are limited longitudinal data on genomic and phenotypic stability after using CRISPR/Cas9 to edit cells. There are now several reports providing evidence that there is also the potential for additional unintended long-term changes [10–12] associated with CRISPR/Cas9 editing. In addition, genetic bottlenecks can arise during selection of edited cell subpopulations. Hence, it is essential to characterize the edited cells intended for use in advanced therapies such as cell and gene therapies, where the therapy often involves administering populations of edited cells to the patient [13].

Table 1. Flow cytometry reagents used for cell analysis.

Marker	Clone	Fluorophore	Company	Product no.	Dilution volume per 0.5⁶ cells, µl	B-cell subtype expression indicator
B-cell panel						
Live/Dead		Aqua	Thermo Fisher Scientific	L34957	0.5	Dead cells
CD19	J3-119	PE	Beckman Coulter	IM1285U	0.5	All B-cell lineages
CD27	1A4CD27	PE-Cy7	Beckman Coulter	A54823	7.5	Memory B cells and short-lived plasma cells
CD20	B9E9 (HRC20)	Pacific Blue	Beckman Coulter	A74777	7.5	Mature B cells and memory B cells
CD24	ALB9	APC	Beckman Coulter	A87785	7.5	All B cells
CD38	LS198.4.3	APC-AF700	Beckman Coulter	B23489	7.5	Regulatory B cells
IgD	IA6-2	FITC	Beckman Coulter	B306527	30	Naive B cells
CD138	MI14	BV711	BD Biosciences	563184	7.5	Bright plasma B cells
Compensation					Dilution volume per 0.5⁶ cells, µl	
CD19	SJ24C1	PE-Cy7	BD Biosciences	557835	5	
CD19	HIB19	APC	BioLegend	302212	5	
CD19	J3-119	APC-AF700	Beckman Coulter	A78837	5	
CD19	HIB19	FITC	BioLegend	302206	5	
CD19	SJ25C1	BV711	BD Biosciences	563036	5	
Intracellular					Dilution volume per 0.5⁶ cells, µl	
GAPDH	14C10	AF647	Cell Signaling Technology	3907S	5	

AF647: Alexa Fluor 647; APC: Allophycocyanin; APC-AF700: Allophycocyanin−Alexa Fluor 700; BV711: Brilliant Violet 711; FITC: Fluorescein isothiocyanate; PE: Phycoerythrin; PE-Cy7: Phycoerythrin−Cyanine7.

In biomanufacturing, mammalian cells are often engineered to produce protein products. Common mammalian cell lines for protein expression include Chinese hamster ovary, mouse myeloma (NS0) and human embryonic kidney 293 cells [14,15]. However, for cell and gene therapies, a variety of primary human cell types, including B cells and fibroblast cells, are modified [16,17].

In cell therapies, the final therapeutic edited cell product may be a pool of cells or cells that have been sorted for specific characteristics. Since the therapeutic value is often reliant on DNA sequence changes, it is imperative to determine if the edits are persistent [17]. Although it is expected that different cell types may have varying responses to CRISPR/Cas9 editing, there may also be some similar underlying long-term trends that have yet to be elucidated.

The Genome in a Bottle Consortium has put forth a significant amount of effort in characterizing and developing National Institute of Standards and Technology reference materials for the genomes of several cell lines [18]. For this reason, one of the Genome in a Bottle B-lymphoblast cell lines, GM24385, has become a good candidate for characterizing the products of genome editing. A well-known B-lymphocyte antigen, CD19, is expressed on the surface of human B cells [19] from early stages to terminally differentiated plasma cells, making it a good target for editing a B-lymphoblast cell line.

The objective of this protocol is to enable study of the longitudinal genotypic and phenotypic stability of CRISPR/Cas9 using genomics and flow cytometry. By evaluating the stability of CRISPR/Cas9 genome editing, we will have a better understanding of its long-term effects on the cell. This will help to further characterize the safety and effectiveness of therapies produced using the CRISPR/Cas9 system.

Protocol

Cells & media

The authors used the GM24385 B-lymphoblast cell line (Coriell Institute for Medical Research, NJ, USA), Roswell Park Memorial Institute (RPMI) 1640 medium with 2 mM L-glutamine (30-2001; American Type Culture Collection, VA, USA), fetal bovine serum (FBS) (16140071; Thermo Fisher Scientific, MA, USA) and T flasks or cell culture plates.

Flow cytometry

The authors used an Attune NxT flow cytometer (A24858; Thermo Fisher Scientific), antibodies for B-cell panel (Table 1), phosphate-buffered saline (PBS) (10010049; Thermo Fisher Scientific), FBS, FIX & PERM Cell Fixation and Cell Permeabilization Kit (GAS003; Thermo Fisher Scientific), Attune performance check beads (4449754; Thermo Fisher Scientific), Attune focusing fluid (100085929CST; Thermo Fisher Scientific), centrifuge and tubes (1.5, 5 and 15 ml).

Table 2. gRNAs for CD19 knockout.				
Guide	Sequence	Cut site, hg19	Exon	Binds to
1	CGCUGUGCUGCAGUGCCUCA	28,932,373	2	Sense
2	GCUGUGCUGCAGUGCCUCAA	28,932,374	2	Sense
3	UUCCCAGGCCUGGCAGCCCC	28,932,458	2	Antisense
4	UUCAACGUCUCUCAACAGAU	28,932,527	2	Sense

Table 3. Primers for PCR amplification of CD19-edited section.	
Direction	Sequence
Forward	GGGTGTCCTTGGCTGAGTAA
Reverse	CCTCTCTCCAGCTCCATTGT

Transfection reagents & instrumentation
The authors used 4D-Nucleofector (AAF-1003B; Lonza, NJ, USA), SF Cell Line Kit (V4XC-2032 or V4XC-2012; Lonza), sgRNA designed to target (Synthego, CA, USA) (Table 2), *S. pyogenes* Cas9 (9212-5MG; Aldevron, ND, USA) and tissue culture plates.

Sanger sequencing
The authors used a Veriti thermocycler (A48141; Thermo Fisher Scientific), NanoDrop (ND-ONE-W; Thermo Fisher Scientific), Quick-DNA Miniprep Plus Kit (D4069; Zymo Research Corporation, CA, USA), Q5 Hot Start High-Fidelity 2× Master Mix (M0494L; New England Biolabs, MA, USA), PCR primers (Table 3) and DNA Clean & Concentrator kit (D4014; Zymo Research Corporation).

Data analysis
The authors used FlowJo (Becton, Dickinson and Company, NJ, USA) and the inference of CRISPR Edits analysis tool (Synthego) for statistical analysis (alternative instruments, kits and software may have similar results).

Methods
Cell culture
The Genome in a Bottle B-lymphoblast cell line, GM24385, was selected as the cell line of choice as a result of its extensive use in genome sequencing [20]. GM24385 cells are anchorage-dependent cells and loosely aggregated when cultured in upright T flasks or plates. Low passage cells are recommended because growth rate decreases after a number of passages [21]. It should be noted that one should always be extremely careful to avoid contamination.

The authors maintained cells in RPMI 1640 medium supplemented with 15% FBS. Cells were cultured in a humidified incubator set at 5% CO_2 and 37°C. Cells were passaged when the density reached approximately 1×10^6 cells/ml (a split ratio of 1:4 is recommended). Prior to passage, cells were dissociated by pipetting. If cells had not reached the splitable density in 3−4 days, the medium was changed by centrifuging cells ($200 \times$ g for 10 min at 25°C), gently aspirating the supernatant and resuspending cells in prewarmed fresh medium.

CRISPR/Cas9 editing for CD19 knockout
CRISPR/Cas9 is a popular method for creating a DNA double-strand break. When a repair template is unavailable, the cell repairs double-strand breaks using the NHEJ pathway, during which several nucleotides may be lost at the repair sites, leading to knockout of gene expression. Of the many delivery methods available, transfection of an RNP complex by electroporation is popular because of its transient nature, which works for many cell types [22]. In this experiment, because of the possibility of different guide efficiencies, four gRNAs were tested. To knock out CD19, four gRNAs targeting human *CD19* (Table 2) were purchased as modified sgRNAs in a Synthego gene knockout kit. sgRNAs were selected based on location in the coding region of the gene, location in an exon found in most transcripts, activity score and base mismatches. sgRNAs were used following the manufacturer's instructions with the kit-supplied *S. pyogenes* Cas9 2NLS nuclease and transfected using 4D-Nucleofector and an SF Cell Line Kit. Prior to scaling up to cuvettes, samples were tested in nucleofection strips.

When designing transfection experiments, the authors recommend controls such as electroporation only, Cas9 and electroporation with no gRNA as well as a positive control such as a gRNA targeting the *RELA* gene with a known knockout effect. Because of the nature of nucleofection, many cells die during this step, and it takes time for the surviving cells to stabilize and replicate to a sufficient quantity to analyze. It is important to begin with healthy cells and handle them gently to minimize cell death.

The authors resuspended gRNA sterile nuclease-free water to make a 30-μM stock solution, used the stock solution to form RNP complexes with 20 μM of Cas9 and nucleofector reagent at a ratio of 9:1 for sgRNA and Cas9 and incubated for 10 min at room temperature. Depending on the size of the cuvette to be used, 1×10^6 cells per cuvette or 2×10^5 cells per well of a 16-well strip cuvette needed to be prepared. Cells were centrifuged at $100 \times$ g for 10 min at 25°C and then resuspended in nucleofector reagent to the appropriate

Table 4. Laser and antibody matrix for flow cytometry analysis.

Attune channel	440/50	512/25	710/50	530/30	585/30	780/60	670/14	720/30
Channel label	VL1	VL2	VL4	BL1	YL1	YL5	RL1	RL2
Fluorophore	Pacific Blue	Aqua	BV711	FITC	PE	PE-Cy7	APC	APC-AF700
Comp_unstained								
Comp_Pac Blue	CD20							
Comp_Aqua		Live/Dead						
Comp_BV711			CD19					
Comp_FITC				CD19				
Comp_PE					CD19			
Comp_PC7						CD19		
Comp_APC							CD19	
Comp_APC-AF700								CD19
FMO1		Live/Dead			CD19			
FMO2	CD20	Live/Dead	CD138	IgD	CD19		CD24	
FMO3	CD20	Live/Dead			CD19	CD27		CD38
Samples	CD20	Live/Dead	CD138	IgD	CD19	CD138	CD27	CD24

APC: Allophycocyanin; APC-AF700: Allophycocyanin−Alexa Fluor 700; BV711: Brilliant Violet 711; Comp: Compensation; FITC: Fluorescein isothiocyanate; FMO: Fluorescence minus one; Pac Blue: Pacific Blue; PC7: Phycoerythrin−Cyanine7; PE: Phycoerythrin; PE-Cy7: Phycoerythrin−Cyanine7.

Figure 1. Example compensation matrix for flow cytometry analysis. A compensation matrix was used to ensure proper separation of the fluorescence signals for cell marker staining.

volume (5 μl of cells at 3×10^4 cells/ml per well). Cells were then transferred to a nucleofector cuvette, with RNP complexes or controls added to the cells in the cuvettes and wells to a total of 100 μl per cuvette or 30 μl per well of solution. Next, cells were nucleofected using the SF Cell Line and DN-100 in 4D-Nucleofector. Prewarmed medium was then added to the cuvettes and wells and incubated at 37°C for 30 min. Finally, cells were transferred to a prewarmed six-well plate and incubated at 37°C for 72 h until harvesting.

B-cell panel with flow cytometry

To measure the phenotypic effect of knocking out CD19, the authors established a panel for measuring differences and a baseline phenotype. B lymphoblasts that are immortalized with Epstein−Barr virus express CD19 on the cell surface, so this was used as the test marker for knockout [23−25]. A panel containing several surface markers common to B cells and a viability marker was designed based on the expression levels of surface markers and availability of lasers and fluorescence channels (Tables 1 & 4). This panel was initially measured to create a baseline from the parent GM24385 cells. The panel was used with the parent GM24385 cells to set the gates (Figures 1 & 2) [26]. The steps for performing the flow cytometry analysis are discussed in the following sections. This analysis was periodically applied to the edited cells.
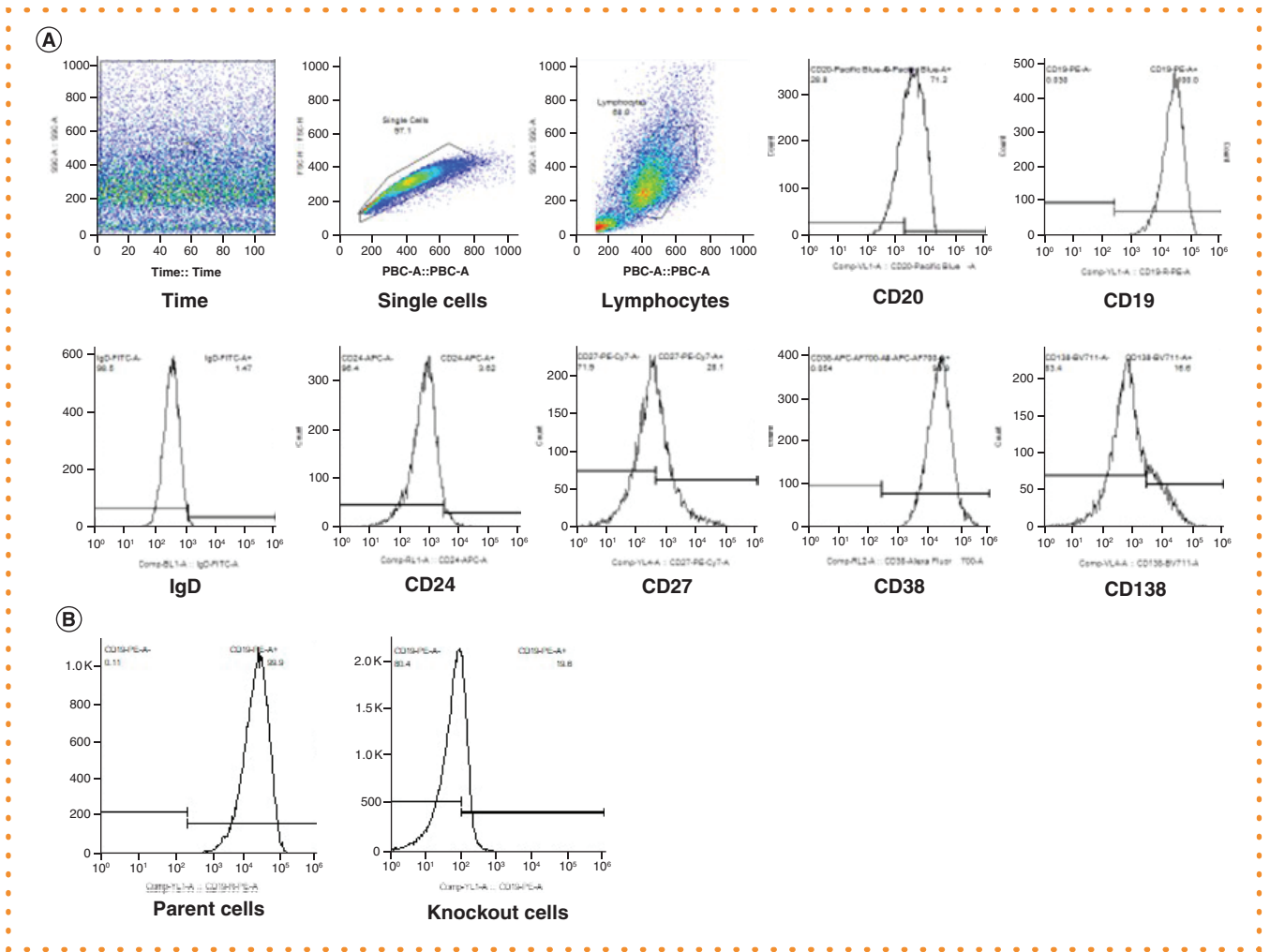
Figure 2. Representative gating strategy for flow cytometry analysis. (A) Representative gating strategy for flow cytometry analysis based on gates set using FMO controls. Time versus SSC was used to gate the steady-state population. Single cells were then gated using the FSC-A versus FSC-H plot. A lymphocyte gate was created using the FSC versus SSC plot. The remaining plots are histograms of the respective markers (CD20, CD19, IgD, CD24, CD27, CD38 and CD138). **(B)** Example CD19 histogram plot comparing parent cells with knockout cells demonstrating a count of CD19+ cells in the knockout group.
FMO: Fluorescence minus one; FSC: Forward scatter; FSC-A: Forward scatter area; FSC-H: Forward scatter height; SSC: Side scatter.

Because of the influence of cell passaging time in cell culture, it is important to be consistent with timing of the sample collection between experiments (e.g., collecting cells of the same passage). Therefore, to minimize variations due to sample preparation and cell behavior, measurements should be made at the same time point.

For cell sample preparation, cells were divided into three groups: live/dead compensation samples; single fluorophore-conjugated antibody-stained samples for compensation; and sample cells, including the controls. Additionally, an intracellular staining process was used with CD19 antibody to determine whether any CD19 proteins were expressed but not translocated on the cell surface. Three groups of samples were stained in parallel. Approximately 5×10^5 cells were needed for each sample, and this was determined using the flow cytometry analysis laser and antibody matrix as a guideline for staining (Table 4). It should be noted that the parent cells were used for compensation and fluorescence minus one controls. Compensation beads can alternatively be used, but they are not the same size as stained cells. Compensation is a technique used in multifluorophore panels to correct for fluorescence spillover between detectors. Fluorescence minus one controls are used to identify positive and negative cells to appropriately place gates for marker identification.

With regard to staining cell samples, the aqua compensation tube should possess dead cells to stain for compensation. To obtain dead cells, cells were placed in a tube and heated to 60°C for 20 min. Cells were stained with the Live/Dead stain after washing with PBS or alternatively stained with the compensation stain using PBS containing 2% FBS. The authors added 1 ml of PBS containing Live/Dead stain and incubated in the dark at room temperature for 30 min. To obtain a compensation matrix, the authors stained one tube for each
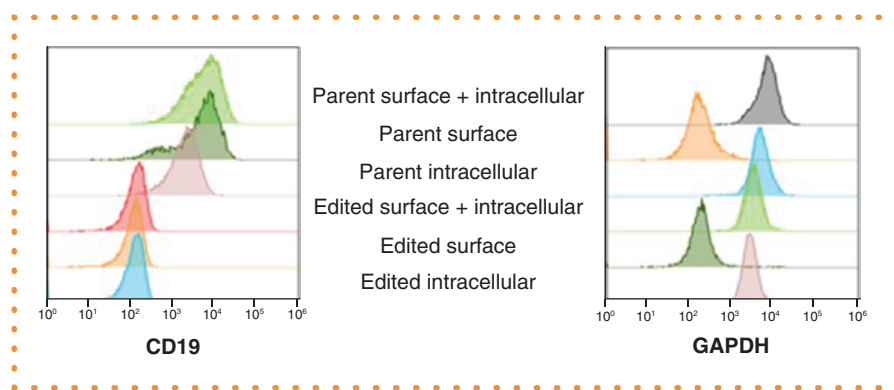
Figure 3. Sample histograms from intracellular staining. An overlay plot of CD19 histograms comparing the knockout and parental cell lines with surface staining only, internal staining only and both surface and internal staining shows less CD19 in the knockout cell lines. Using GAPDH as a control for the staining protocol shows a lack of GAPDH in the surface staining-only cell lines.

of the fluorophores used (in this case with CD19 to get a sharp peak). After coating the tube with PBS containing FBS, the stain was added to the cells and incubated for 30 min at room temperature.

To remove extra fluorophores, the authors washed cells with PBS containing 2% FBS and then placed the compensation tubes in a refrigerator until use. Next, antibodies were added for additional markers and incubated for 30 min at room temperature. For intracellular staining, cells were split into three groups: cells that were stained with both surface and intracellular antibodies, cells that were stained with only surface antibodies and cells that were stained with only intracellular antibodies (Figure 3). Cells were then washed with PBS and stained with Live/Dead as previously described. Next, cells were washed with PBS containing 2% FBS and stained with a cocktail of CD19 antibodies and GAPDH antibodies as a control for 30 min at 4°C. Finally, cells were washed with PBS with 2% FBS.

The authors fixed and permeabilized the cells using the FIX & PERM Cell Fixation and Cell Permeabilization Kit following the manufacturer's instructions. Briefly, FIX & PERM buffer A was added to the cells and incubated at room temperature for 15 min. Cells were washed with PBS containing 5% FBS and 0.1% sodium azide. FIX & PERM buffer B was added to cells with intracellular antibodies, CD19 and GAPDH and incubated at room temperature for 15 min. Excess fluorophores were washed and all cells were then resuspended in PBS containing 2% FBS.

To measure samples, the authors used a panel designed for the Attune NxT flow cytometer. The steps used included checking performance and generating a compensation matrix and then measuring the samples. First, a startup and performance check was done. Following the manufacturer's instructions, the authors started the instrument, computer and software. Next, three drops of performance beads were added to 2 ml of PBS, vortexing before and after, and a performance check was run.

For compensation samples, the lasers to be used were selected in the compensation window (Table 4). Using a small sample size and slow rate, a small amount of each compensation sample was sampled to make sure the voltages were correct (highest peaks for the positive sample with good separation of positive and negative peaks). After voltages were set, compensation samples were measured at a sample rate of 100 μl/min, and the authors collected 100,000 lymphocyte events. Finally, a compensation matrix was applied (Figure 1). With regard to samples, the authors set up plots for single cell, live/dead and lymphocyte (one for the knockout marker is also recommended). Samples were measured at a sample rate of 200 μl/min, and 200,000 lymphocyte events were collected.

Although several data analysis options are available for flow cytometry data, the authors used FlowJo software. The authors created a group for compensation and a group for the samples and added the respective flow cytometry standard files. The authors used the compensation wizard to create a compensation matrix and applied it to the samples. The authors then set up the gates for the samples using the fluorescence minus one control samples (Figure 2) and used the layout and table editors to generate plots and tables for the samples.

DNA sequencing

To determine the effect of CRISPR/Cas9 editing on the genome, sequencing analysis of the target site was performed after 72 h and then at periodic time points after cell harvest. Cells were harvested by collecting up to 1.5 ml of cell culture by centrifuging at 100 × g and washing cells with PBS. The remaining cells were maintained in the incubator for flow cytometry analysis as described earlier and for future sequencing. The authors extracted gDNA using a Quick-DNA Miniprep Plus Kit following the manufacturer's protocol and measured DNA concentration using a NanoDrop. The authors used PCR to amplify the CRISPR/Cas9-edited *CD19* locus using the primers listed in Table 3 and Q5 Hot Start High-Fidelity 2× Master Mix; the authors followed the manufacturer's instructions for preparing PCR reaction samples. A total of 500 ng of DNA, the Q5 Hot Start High-Fidelity 2× Master Mix, 10 μM of each primer and nuclease-free water were combined for a 50-ul reaction.
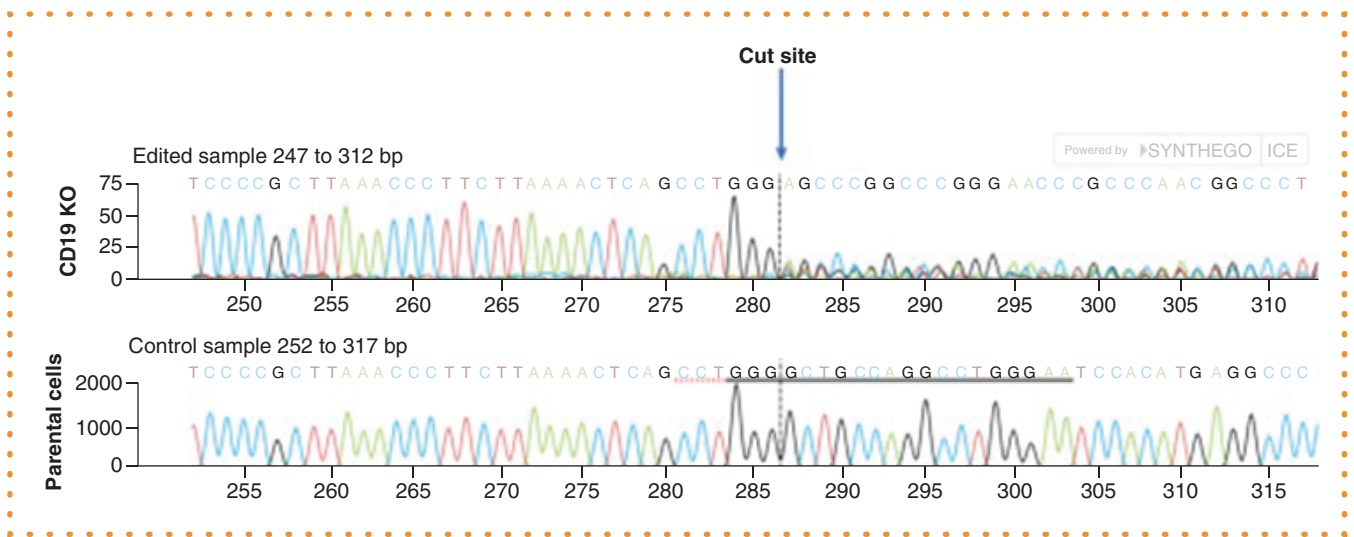
Figure 4. Example Inference of CRISPR Edits analysis result demonstrating edit near the cut site. The defined peaks prior to the targeted CRISPR/Cas9 DNA cut site in the knockout cell line match the parental cell line. At the cut site, the lower-amplitude peaks demonstrate a mixed population of edited cells.

The following conditions were used for PCR in a Veriti thermocycler: denaturation at 95°C for 30 s followed by 35 cycles at 95°C for 5 s, 67°C for 30 s and 72°C for 30 s and a final extension at 72°C for 2 min. The PCR products were cleaned using the DNA Clean & Concentrator kit according to the manufacturer's instructions and eluted into 25 μl of ultrapure water. The final PCR concentration was determined using a NanoDrop. Clean PCR products were submitted to Psomagen (MD, USA) for Sanger sequencing using their protocol for difficult-to-sequence DNA products. DNA sequences were returned as .ab1 files and analyzed using the Synthego Inference of CRISPR Edits tool to determine editing efficiency (Figure 4). The expected outcome for Sanger sequencing on a mixed population of edited cells is a lower-amplitude signal and mixed signal near the expected CRISPR/Cas9 DNA cut site. Analytics such as the Synthego Inference of CRISPR Edits tool may enable disambiguation of mixed Sanger sequence signal around the cut site.

Additional analysis

For long-term stability analysis, Sanger sequencing and flow cytometry are used at multiple time points following editing. To further analyze the effects of CRISPR/Cas9 editing, transcriptomics, next-generation DNA sequencing and single-cell sequencing should be considered as follow-ups for stability analysis. To ensure that the cell population contains a 100% knockout, cell sorting can be used to isolate knockout cells. Ideally, this would occur over a significant period of time, but culture limitations and cell exhaustion will likely impact this time frame.

Author contributions

S Inwood, with assistance from L Wang and S Maragh, formulated the idea and direction for the manuscript. L Tian and K Parratt worked with S Inwood to complete supporting experiments.

Disclaimer

To specify an experimental procedure as completely as possible, certain commercial materials, instruments and equipment are identified in this manuscript. In no case does identification of the manufacturer of particular equipment or materials imply a recommendation or endorsement by the National Institute of Standards and Technology, nor does it imply that the materials, instruments and equipment identified are necessarily the best available for the purpose.

Financial & competing interests disclosure

Open access

This work is licensed under the Attribution-NonCommercial-NoDerivatives 4.0 Unported License. To view a copy of this license, visit http://creativecommons.org/licenses/by-nc-nd/4.0/.

References

1. Horvath P, Barrangou R. CRISPR/Cas, the immune system of bacteria and archaea. *Science* 327(5962), 167–170 (2010).
2. Yang L, Yang JL, Byrne S, Pan J, Church GM. CRISPR/Cas9-directed genome editing of cultured cells. *Curr. Protoc. Mol. Biol.* 107, 31.1.1–31.1.17 (2014).
3. Mullard A. CRISPR pioneers win Nobel prize. *Nat. Rev. Drug Discov.* 19, 827 (2020).
4. Mei Y, Wang Y, Chen H, Sun ZS, Ju XD. Recent progress in CRISPR/Cas9 technology. *J. Genet. Genomics* 43, 63–75 (2016).
5. Cao JX, Wang YL, Wang ZX. Advances in precise regulation of CRI6PR/Cas9 gene editing technology. *Yi Chuan* 42, 1168–1177 (2020).
6. Leonova EI, Gainetdinov RR. CRISPR/Cas9 technology in translational biomedicine. *Cell Physiol. Biochem.* 54, 354–370 (2020).
7. Fernandes L. UC consortium launches first clinical trial using CRISPR to correct gene defect that causes sickle cell disease (2021). www.ucsf.edu/news/2021/03/420137/uc-consortium -launches-first-clinical-trial-using-crispr-correct-gene-defect
8. Tian X, Gu T, Patel S, Bode AM, Lee MH, Dong Z. CRISPR/Cas9 – an evolving biological tool kit for cancer biology and oncology. *NPJ Precis. Oncol.* 3, 8 (2019).
9. Li H, Yang Y, Hong W, Huang M, Wu M, Zhao X. Applications of genome editing technology in the targeted therapy of human diseases: mechanisms, advances and prospects. *Signal Transduct. Target. Ther.* 5, 1 (2020).
10. Liu Q, He D, Xie L. Prediction of off-target specificity and cell-specific fitness of CRISPR-Cas system using attention boosted deep learning and network-based gene feature. *PLoS Comput. Biol.* 15, e1007480 (2019).
11. Bae T, Kim H, Kim JH *et al.* Specificity assessment of CRISPR genome editing of oncogenic EGFR point mutation with single-base differences. *Molecules* 25(1), 52 (2019).
12. Peng R, Lin G, Li J. Potential pitfalls of CRISPR/Cas9-mediated genome editing. *FEBS J.* 283, 1218–1231 (2016).
13. Preece R, Georgiadis C. Emerging CRISPR/Cas9 applications for T-cell gene editing. *Emerg. Top. Life Sci.* 3, 261–275 (2019).
14. Dyson MR. Fundamentals of expression in mammalian cells. *Adv. Exp. Med. Biol.* 896, 217–224 (2016).
15. Dumont J, Euwart D, Mei B, Estes S, Kshirsagar R. Human cell lines for biopharmaceutical manufacturing: history, status, and future perspectives. *Crit. Rev. Biotechnol.* 36, 1110–1122 (2016).
16. Elverum K, Whitman M. Delivering cellular and gene therapies to patients: solutions for realizing the potential of the next generation of medicine. *Gene Ther.* 27, 537–544 (2020).
17. Anguela XM, High KA. Entering the modern era of gene therapy. *Annu. Rev. Med.* 70, 273–288 (2019).
18. Zook JM, Catoe D, McDaniel J *et al.* Extensive sequencing of seven human genomes to characterize benchmark reference materials. *Sci. Data* 3, 160025 (2016).
19. HUGO Gene Nomenclature Committee. CD19 CD19 molecule [Homo sapiens (human)] (2022). www.ncbi.nlm.nih.gov/gene/930
20. Church GM. The personal genome project. *Mol. Syst. Biol.* 1, (2005). https://www.embopress.org/action/showCitFormats?doi=10.1038%2Fmsb4100040
21. Coriell Institute for Medical Research. GM24385 LCL from B-lymphocyte (2021). www.coriell.org/0/Sections/Search/Sample_Detail.aspx?Ref=GM24385
22. Zeballos CM, Gaj T. Next-generation CRISPR technologies and their applications in gene and cell therapy. *Trends Biotechnol.* 39(7), 692–705 (2021).
23. Styles CT, Bazot Q, Parker GA, White RE, Paschos K, Allday MJ. EBV epigenetically suppresses the B cell-to-plasma cell differentiation pathway while establishing long-term latency. *PLoS Biol.* 15, e2001992 (2017).
24. Wang K, Wei G, Liu D. CD19: a biomarker for B cell development, lymphoma diagnosis and therapy. *Exp. Hematol. Oncol.* 1, 36 (2012).
25. LeBien TW, Tedder TF. B lymphocytes: how they develop and function. *Blood* 112, 1570–1580 (2008).
26. Beckman Coulter.White Paper: DuraClone reagents are a robust solution for standardizing multicolor flow cytometry applications (2014). https://www.beckman.com/gated-media?mediaId={447E1F9F-7DF8-49F6-AA15-7F9C5454F0A9}

New 4D-Nucleofector® Platform

Efficient and Reproducible Results for Your Transfection Applications
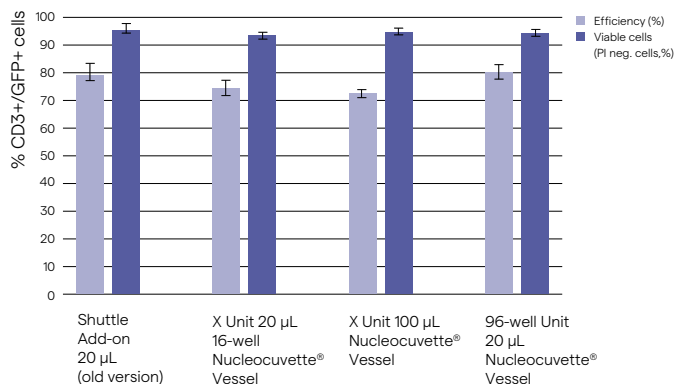
The modular design of the Nucleofector® Platform with units for small, medium or large scale, adherent cells or cells in suspension, allows you to configure the 4D-Nucleofector® System to fit your specific research needs. Up to 3 functional units can be added to the 4D-Nucleofector® Core Unit and each is suited for different applications:

X Unit: Nucleofection® of various cell numbers in different formats (16-well Nucleocuvette® Strips or 100 μL Nucleocuvette® Vessels)

Y Unit: Enabling adherent Nucleofection® in 24-well culture plates

LV Unit: Large-scale transfection of up to 1×10⁹ cells in a single run

96-well Unit: Higher throughput Nucleofection® Experiments in 96-well Nucleocuvette® Plates

Cell type-specific Optimized Protocols or recommendations are available in our Knowledge Center. In these Optimized Protocols we share our recommended Nucleofection® Conditions as well as our experience and knowledge for treatment of individual cell types.

lonza.com/New-4D-Nucleofector

Transferability of Nucleofection® Conditions Between Units and Vessels

Transfection of human T cells with plasmid DNA (pMax-GFP® Plasmid) Fresh PBMCs were transfected with pmaxGFP® Plasmid in a 100 μL Nucleocuvette® Vessel or a 20 μL Nucleocuvette® Vessel using the Next Generation 4D-Nucleofector® X Unit, the 96-well Unit or the Nucleofector® Shuttle® Add-on for reference. Transfection efficiency in CD3-positive T cells was analyzed 24 hours post Nucleofection® Procedure. Plasmid data represent the mean of various independent experiments. Live cell discrimination was done with Propidium Iodide.

RegMedNet

Contact us

Editorial Department

Editor
Megan Giboney
m.giboney@future-science-group.com

Business Development & Support

sales@future-science-group.com

@RegMedNet   @RegMedNet   RegMedNet

www.RegMedNet.com